3/3 AA

DATA REPORT #1

Large Scale Modelling of Soil/Pipe Interaction Under Moment Loading

Test GSC 01

Submitted to:

Terrain Sciences Division
Geological Survey of Canada
Ottawa, Ontario

Submitted by:

C-CORE
St. John's, Newfoundland

C-CORE Publication No. 98-C20
September, 1998

C-CORE
Memorial University of Newfoundland
St. John's, NF, A1B 3X5, Canada
Tel. (709) 737-8354 Fax. (709) 737-4706

The correct citation for this report is:

Hurley, S., Zhu, F., Phillips, R., and Paulin, M.J. (1998). "Large Scale Modelling of Soil/Pipe Interaction Under Moment Loading: Test GSC 01 Data Report". Contract Report for Terrain Sciences Division, Geological Survey of Canada, C-CORE Publication 98-C20.

TABLE OF CONTENTS

APPENDICES

1.0 GENERAL

1.1 Program Summary

This is the first data report associated with the "Large Scale Modelling of Soil/Pipe Interaction Under Moment Loading" project for the Geological Survey of Canada (GSC).

The objective of this project is to assess the flexural behaviour of a pipe buried in dense sand during bending induced by lateral loading up to a limit of 10% pipeline ovalization.

Pipeline bending strain limits have been established in part by considering the bending response of exposed pipelines. This response may be moderated in buried pipelines by the restraint of the surrounding soil. This project will compare the measured response and failure mode of buried pipelines subjected to bending to those previously determined from exposed pipelines.

During each test, the pipeline longitudinal profile, pipe ovalization, associated soil deformations and pipeline forces under the applied loads are measured.

Laboratory test results on the soil used during the program and specimens from the pipe will be reported in Data Report #3.

2.0 WORK ACTIVITY PROGRESS

2.1 Procurement and Modifications

As outlined under Task 1 in C-CORE proposal PCF-97-013, the test tank was reconfigured and the loading actuator systems were modified for this project.

Modification of the actuator systems consisted of relocating both actuators from the end wall to the side wall of the tank, cutting holes through the concrete side wall for passage of the actuator cables and reinforcing the side wall in the vicinity of the actuators with reinforced concrete and 3/4" steel plate to resist the anticipated loads.

Each end of the pipeline was loaded using 31 mm (1.25") diameter steel cable. The overall length of each steel cable is approximately 2.95 m. Each loading cable is equipped with 6 steel buttons which are crimped approximately 65 mm apart from one end of the cable as shown in Figure 1. There is another smaller button at the end of each cable which passes through the wall of the pipeline and is secured to a steel insert in the end of the pipe. This provides the rigid connection between the pipeline and the cables.

Each of the six buttons has an approximate diameter and length of 60 mm and 85 mm respectively. This type of mechanism to transfer load to the ends of the pipeline was required due to the fact that the travel limit on the actuators is 165 mm and the required total pull distance was anticipated to be greater then the travel limit. At the start of the test, a linkage was placed around the cable button and connected to the actuator. After pulling 150 mm (which equals the button length plus space to next button), another linkage was placed around the second button and the linkage/button was allowed to bear against the wall thereby maintaining the load in the cables. The first button was then cut off, the actuator connected to the second linkage, and the test proceeded.

Approximately 50 tons of sand was obtained locally from Concrete Products Ltd. for use in the tank. Details on laboratory testing of the sand will be forthcoming in Data Report #3. The pipeline section was obtained from TW Metals Ltd. in Atlanta, Georgia. The pipeline was instrumented with strain gauges, obtained from Measurements Group Ltd., to measure both axial and bending strains developed in the pipe during displacement. Some pipe specifications are given below:

Overall Length (mm)	5814
Nominal Outside Diameter	8" (203.2 mm)
Nominal Wall Thickness	1/8" (3.175 mm)
Material	1010 Carbon Steel
Bending Strain Gauge Model #	EA-06-250PD-350
Axial Strain Gauge Model #	CEA-06-125UT-350

2.2 Pipeline Sensor Array

A pipeline array was designed and manufactured to incorporate displacement transducers inside the pipe for measurement of pipeline curvature and ovalization during testing. A drawing of the pipeline array is given in Figure 2 while Figure 3 is a photograph of the array. In Figure 2(b), the bend sensor and strain gauge locations are shown relative to the pipe centerline. Also shown in Figure 2(b) are the locations of the three pipe displacement transducers. The pipeline array was constructed using 25 mm x 25 mm x 3 mm aluminum angle and 25 mm aluminum square blocks and was glued to the inside bottom surface of the pipe prior to placement of the pipe in the tank. There are 10 individual arms which make up the array and each arm has the ability to pivot with respect to its neighbours. A cantilever curvature sensor is located at one end of each arm and registers above the pivot point allowing measurement of the amount of rotation of one arm with respect to the adjacent arm of its neighbour. The bend sensors were initially biased to maximise their response range during the pipe flexure. Knowing the length of each arm, the amount of rotation in degrees (or radians) can be converted to an associated displacement in millimeters which can then be used to create a displaced pipeline profile. Figure 4 is a diagram of the curvature sensors used in test GSC 01.

Each bend sensor was calibrated individually by monitoring the output of the bend sensor while displacing the end of the corresponding arm a known distance, measured with a micrometer. In this manner, a relationship between bend sensor voltage output and arm displacement (rotation) was obtained.

To place the array inside the pipe, the array was pinned to and clamped between two aluminum channel sections to ensure that it was kept as straight as possible during placement. Glue was applied to the bottom of each square aluminum block and allowed to harden. The clamped array was then slowly inserted into the pipeline through the Master end. Once the array was in its final position, heat was applied to the underside of the pipe at the aluminum block positions using a propane torch. The glue on the blocks melted. Once the heat was removed, the glue hardened again and secured the pipeline array to the inside bottom surface of the pipeline. The two channel sections were then carefully removed. The pipeline strain gauges, bend sensors and ovalisation sensors were connected to a signal conditioning box which was located in the end of the pipe. Air was circulated through the pipe to prevent overheating of the electrical instrumentation and to reduce the possibility of condensation.

2.3 Test Results

2.3.1 Pipeline Placement

Figure 5 and 6 present plan and profile views of the test setup. The pipeline was removed during placement of a dense bedding layer approximately 260 mm thick. Upon completion of this layer, the pipeline and pull cables were lowered inside the tank and the cables were placed through the access holes in the tank wall and connected to the actuators. The pipeline was lowered onto the dense bedding layer and positioned so that it was an average of 396 mm away from the rear wall,

2368 mm away from the front wall and 178 mm away from both side walls. Once the pipeline was in the start position, jacking mechanisms were placed between the pipeline and the actuator wall at both the Master and Slave ends and any slack in the pull cables was removed by tensioning the pull cables. Elevation measurements taken after pipeline placement indicated that the base of the pipeline was at an average elevation of 268 mm above the base of the tank. Figure 7 is a photograph showing the pipe being prepared for placement onto the bedding layer.

2.3.2 Testbed Preparation

During testbed preparation, plywood sheets were placed on the prepared soil layers to minimize disturbance of the layers and to provide a platform from which to work. Sand was placed in the tank using 15 litre buckets and levelled using a hand trowel to the appropriate layer thickness of 100 mm. A manual tamper with a mass of 5 kg and a footprint of 127 x 300 mm was then used to compact the sand. After at least two passes with the manual tamper, four passes over the soil surface were made with a vibratory tamper. This process was repeated for each layer until the soil reached the final elevation of 1300 mm from the floor of the tank. The final elevation of the prepared surface appeared to be ± 5 mm with respect to the final grade. After preparing the surface of the testbed, a chalk line was used to place a grid on the soil surface as depicted in Figure 8. Grid point and grid square designations are indicated on the figure as is an outline of the pipeline position. The grid cell designation was made from the lower right corner as shown in the figure.

It was necessary to obtain several shipments of sand due to the large quantity necessary to fill the testbed. There were some slight variations in the characteristics (i.e. color, moisture content, gradation) of the sand but the results of the laboratory tests indicated that these variations had negligible effect on the test results.

A number of density checks were carried out during the preparation of the testbed to characterize the soil. Density pans (approximate inside diameter = 243 mm, approximate height = 50 mm) were placed at different positions within the testbed (Method #1) and removed after the test during testbed excavation. The results of these tests are summarized in Table 1. Another type of test (Method #2) was conducted during testbed preparation in which one of the pans was lowered by a harness, filled with compacted material, retrieved and weighed. Results are also presented in Table 1. The location of the test is presented by the approximate elevation and grid square in which the test was conducted. The Type #1 tests yielded densities ranging from 1730 kg/m^3 to 1939 kg/m^3 with an average density of 1796kg/m^3. The Type #2 tests yielded an average density of 1790 kg/m^3 with values ranging from 1749 to 1851 kg/m^3. Overall, the average density was 1792 kg/m^3. Table 1 also presents moisture content data determined from the density pan tests.

Figure 9 presents photographs of the testbed early in the preparation phase. Also shown in the photographs are the vibratory tamper and a density pan placed on the sand surface.

Following completion of the testbed, vertical deformation tubes were inserted into the testbed and the pre-test surface elevation was measured using a surveyors level and rod. Surface elevation data

are presented in Table 2 where the pre-test surface position has been established at an elevation of 1300 mm (rod reading = 336 mm). Surface settlement transducers were then placed on the testbed and an acoustic surface profiler was positioned over the testbed. These instrumentation are described further below.

Vertical Deformation Tubes

Figure 10 depicts the vertical deformation tube developed to measure deformation profiles within the testbed. Esentially, the deformation tubes consist of flexible tygon tubing connected to a metal tip. The overall length of these vertical deformation tubes was approximately 1400 mm. The tubes and attached tips were driven the complete depth of the testbed using a 0.25 inch metal rod which was inserted down the tubing and rested in a recess in the anchor. Prior to removal of the rod, the entry angle of the tube both parallel and perpendicular to the pipeline were measured and recorded (Table 3). The coordinates of the location where the tubing intersected the soil surface were then measured and recorded (Table 3).

Following the test, the position of the tubing/testbed intersection was recorded. The tubes were then filled with a fibreglass resin and allowed to cure overnight prior to beginning excavation. The excavation was conducted in stages and periodically the vertical tube above the excavation was fixed in position to a string suspended to the sides of the tank. Care was taken during the excavation process not to disturb the tubing and positions of the tubes were measured at 50 mm increments. These data are presented in Table 4. There is no data pertaining to tubes 4,5 and 6 because these tubes did not move during the test.

Figure 11 shows a profile view of the vertical deformation tubes used in Test GSC 01. Shown on the figure are the inferred pre-test centreline positions of the deformation tubes based on the entry angle measurement of the rod. As well, the pre-test centreline positions of the deformation tubes based on pre-test surface positions of the tubes and post-test locations (Table 4) of the tubes at an elevation of 50 mm are presented (it has been assumed that no deformation of the tubes occurred at that elevation during pipeline movement).

Acoustic Surface Profiler

Prior to testing, the acoustic surface profiler was set up over the testbed. The set up was such that the profile would be taken along the X = 1620 mm transect perpendicular to the central axis of the pipe. A complete description of the profiler system, its calibration, and proofing tests is available as an engineering student work term report (Bungay, 1996) on request.

Surface Settlement Transducers

The surface settlement transducers used in test GSC 01 consisted of four small weights (approximate mass = 500 g) which were placed on the sand surface along the X = 4550 mm transect. Each weight consisted of a 40 mm x 40 mm (approximate dimensions) steel plate furnished with a small hook

for attachment to each string potentiometer. An I-beam with four string potentiometers was placed directly over the weights and each potentiometer was attached to a particular weight. These transducers were used to record any movement of the sand surface during the test. The locations (post-test) of the surface settlement transducers are shown in Figure 5.

Test Conduct and Results

Testbed preparation took place from April 1 to June 6/1998. The surface profiler system was installed on June 7 and on the same day, the electrical instrumentation and data acquisition systems were powered up. The pipeline pull was started at 1014hrs on June 8 and pipeline displacement was completed by approximately 2100hrs on June 9. It was decided to stop the test at this time because the data indicated that the location of the plastic hinges in the pipe during the test were not sufficiently close to the instrumentation positions. The bend sensors indicated that buckling of the pipeline had occurred at approximately 1 m from each end.

Three displacement transducers were incorporated into the test to monitor pipeline movement; one was located to monitor the master pipeline end displacement, one was located to monitor the slave pipeline end displacement and the third was located to monitor movement at the center of the pipeline. Output from the displacement transducers at the pipe ends are presented in Figure 12. There was negligible movement recorded by the displacement transducer at the center of the pipeline. For this reason, output from this transducer is not presented.

There was a delayed response (lag) in the master displacement transducer. This lag can possibly be attributed to "slack" in the string between the displacement transducer and the pipe at the master end. The data in Figure 12 have been corrected for this slack. A displacement rate of 10.8 mm/hour has been calculated by taking the average of the master and slave displacement transducer outputs.

Processed data from the Master Load Cell (MLC) and Slave Load Cell (SLC) are presented in Figure 13 and Figure 14 as load-displacement curves. Figures 13(b) and 14(b) show load-displacement for the first 50 mm of pipe displacement. Measured response of the two actuators are compared in Figure 15. During conduct of the test, significant heave and cracking of the testbed surface was observed. This cracking was observed to begin near the ends of the pipeline and propagated inwards towards the pipe centreline as the test progressed. A video record of testing activities which shows the testbed surface in various stages of pipeline displacement is forthcoming. Subsequent observations and measurements are discussed in the following sections.

Data obtained using the acoustic surface profiler prior to the start of pipeline displacement are presented in Figure 16. Profiles taken during the test are presented in Appendix B. Figure 17 presents average post-test profiles after the release of pipeline load. The data suggest a maximum of 30 mm of testbed surface heave along the transect of the surface profiler during testing. "Spikes" in the post-test profile data are the result of sharp transitions in the testbed surface along the transect of the surface profiler.

Processed data from the surface settlement transducers are presented in Figure 18 as a function of pipeline displacement. Extension of the linear potentiometer is positive and conversely retraction is negative. The response of each linear potentiometer is the result of both horizontal and vertical movement of the soil surface. Maximum heave on the order of 25 mm was measured along the transect of the surface settlement transducers (X = 4550 mm).

Processed data from the pipeline bend sensors are presented in Figure 19 as a function of pipeline displacement. Curvature data ranged from a maximum of approximately 0.9 degrees (Sensor #9,10) to a minimum of approximately 0 (Sensor #6). Upon excavation of the pipeline, it was found that major buckles or hinges in the pipeline were located at 1300 mm from the Master end and 1160 mm from the Slave end of the pipe. The significant outputs from bend sensors 9 and 10 are consistent with the location of the buckle at the Master end of the pipe. The Master buckle occurred about 1600 mm from the pipe centreline which is 100 mm away from the location of bend sensor #9. Bend sensors 6 and 7 show very little output due to the fact that the centre portion of the pipeline was undeformed. Bend sensor #1, located at the Slave side of the pipe at the end of the array, also had a very low response because it was located approximately 550 mm away from the buckle location.

Figure 20 presents output from the pipeline strain gauges as a function of pipeline displacement. These data are corrected for a temporary change in bridge excitation voltage which occurred during the test. Maximum measured bending strains were apparently on the order of 1000 (microstrain) while maximum axial strains were apparently on the order of 3300 (microstrain). The strain gauge calibration factors were calculated using the formulas given below:

Bending: $E_o/E = F\epsilon \times 10^{-3}$

Axial: $E_o/E = F\epsilon(1+\nu) \times 10^{-3} / [2 + F\epsilon (1-\nu) \times 10^{-6}] \sim F\epsilon(1+\nu) \times 10^{-3} /2$

where E is the bridge excitation voltage in V (5 Volts), E_o is the bridge output in mV, F is the gauge factor (~2), ν is Poisson's ratio (~0.3 for this material) and strain in microstrain is ϵ.

Figure 21 depicts pipeline ovalization measurements as a function of pipeline displacement. The maximum change in pipeline diameter measured by the pipe ovalization sensors during the test was on the order of 0.6-0.7 mm or ~ 0.3 % ovalization. However much higher ovalizations were measured near the buckle locations using calipers after the pipe was excavated and these data are presented in Table 5. Maximum ovalizations are greater than 15%.

Post-Test Observations and Excavation

The post-test elevation of the testbed surface was measured using a surveyors level and rod. Post-test surface elevation data are presented in Table 2 where the datum has been established as an elevation of 1300 mm (rod reading = 248 mm). Significant heave (maximum 96 mm) of the testbed surface occurred near the ends of the pipe. There was minimal settlement (maximum 6 mm) of the soil surface due to pipeline displacement along the pipe centerline (Gridline K) and along the

actuator wall. Contours of elevation are presented in Figure 22. Note that the program used to generate this plot linearly interpolates to generate an equally spaced grid from unequally spaced points prior to contouring.

Prior to excavation, soil penetration tests were conducted at selected grid points using a Tecnotest probe. Data from the post-test testing are presented in Appendix C.

Pre-test positions of the vertical deformation tubes that were used during this test were presented in Figure 11. Figure 23 shows the pre-test positions of the vertical deformation tubes taken as the average of the two measurement methods presented in Figure 11. The initial position of the deformation tubes has been taken as the average position of the tubes based on the entry angle measurements as well as the post-test location of the tubes at elevation of 50 mm assuming no deformation of the tubes occurred at that elevation during pipeline movement. Also shown on Figure 23 are the post-test positions of the vertical deformation tubes based on the excavation measurements at 50 mm increments. Only post-test data from three vertical deformation tubes are presented because the positions of tubes four, five and six did not change during the test. Figure 24 is a photograph which shows tubes one, two and three following excavation.

Measurements were also taken to assess the post-test excavated pipeline profile. A drawing of the deformed shape of the pipe after excavation is presented as Figure 25 while measurements taken along the length of the pipe are presented in Table 5. It can be seen from Figure 25 that buckles occurred at 1300 mm and 1160 mm from the Master and Slave ends respectively. The post-test pipe elevation was also measured and pipe elevation data are also presented in Table 5. These data indicate that the ends of the pipe had risen about 37 mm during the test. There was no elevation change observed in the centre portion of the pipe. Figure 26 contains photographs of the deformed pipeline while Figures 27 and 28 are photographs of the buckles in the pipeline at the Master and Slave ends respectively.

Figure 29 presents pipeline profiles which have been determined from output of the pipeline bend sensors. Profiles are presented for pipeline displacements of 60 mm, 140 mm, 220 mm and 300 mm relative to the pipe centreline where it was assumed there was no movement. However, there had to be a small amount of movement in this location to mobilise sand resistance. Output from the displacement transducer at the centre of the pipe indicated that this movement was less than 1 mm. The post-test pipeline displacement profile is reasonably consistent with the bend sensor output. Bend sensors 9 and 10 displayed considerable output since they were located near the hinge location on the Master side. The output of the bend sensors located at or near the centre of the pipe was very small which is consistent with this section of the pipeline remaining relatively straight. At the slave end, there was not much change in the output of bend sensor 1 (at the end of the array) since this was located away from the hinge location.

3.0 FINITE ELEMENT ANALYSIS of GSC 01 PIPE

3.1 Introduction

A finite element (FE) analysis of the GSC 01 pipeline has been carried out using ABAQUS. The purpose of the FE analysis was to establish a FE model for laterally loaded pipelines that could be calibrated against the test results from the GSC 01 pipeline. This FE model will be used to guide the design of the GSC 02 pipeline test.

3.2 Material Properties

The GSC 01 pipe had an outside diameter of 203.2 mm and a wall thickness of 3.175 mm and was made from 1010 steel. The pipe material had a Young's modulus of 207 GPa and a Poisson's ratio of 0.3. These values were determined from available literature on this material. Tension tests of specimens cut from the post-test pipe were carried out and will be reported in detail in Data Report #3 which is forthcoming. The average stress-strain relationship of the pipe steel obtained from tension tests of three specimens is shown by the solid line in Figure 30. The yield strength of pipe steel is about 260 MPa, and the ultimate strength is about 370 MPa. In the finite element (FE) analysis, the measured stress-strain relationship is approximated by the dashed line shown in the figure. The stress-strain relationship used in the analysis is below.

Uniaxial tension stress, σ (MPa)	Tension strain ε
0	0.0
260	0.00126
288	0.003
339	0.040
370	0.10 or greater

The soil depth at the pipe springline was 932 mm. The sand had a unit weight of 17.3 kN/m^3. The lateral soil reaction load on the pipe was defined by a bilinear P-Y (load-displacement) relationship. The soil was assumed to fail at a displacement of Y_u, corresponding to the ultimate load capacity of P_u. P was assumed to increase linearly with Y when $Y \leq Y_u$; after that, P is equal to a constant value of P_u. The values of P_u and Y_u have been interpreted directly from data collected from full-scale lateral pipe/soil interaction tests in dense sand with a soil depth to springline also of 931mm (Paulin and Hurley, 1996). In both cases the burial depths were the same and the sands were dense but the pipe diameter, pipe coating, pipe flexibility and sand type were different. Because the spring elements for modelling soil reaction in ABAQUS cannot account for strain softening behaviour, a bilinear relationship with P_u = 96.4 kN/m and Y_u = 22.3 mm was used in the analysis.

3.3 Pipe Elements and Spring Elements

The pipe-soil system is simulated using a beam-spring model, as shown in Figure 31. The pipe was 5.8 m long. Taking advantage of symmetry, a half length of 2.9 m was analysed. The 2.9 m long half pipe was modelled by 29 PIPE21 pipe (beam) elements each 0.1 m long. These pipe elements are used for modelling hollow, thin-walled circular beam sections which do not distort in cross-section. These elements include a hoop stress consideration as both axial stress and hoop stress are considered in the Mises yield behaviour (Figure 32).

Lateral soil resistance is represented by spring elements, as shown in Figure 31. One end of each spring element is attached to the pipe element node; the other end is constrained in the lateral (Y) direction and is forced to move in the axial (X) direction in the same way as the pipe element node to which it is connected. The yield load of each spring is $P_u = 9.64$ kN at a displacement of $Y_u = 22.3$ mm; the load-displacement is linear until Y_u, after that the load is equal to a constant value of 9.64 kN.

Because the pipe is relatively short, the soil reaction load in the axial direction was not considered in the analysis.

The pipe was pulled laterally 0.3 m at a location 0.11 m from the end of the pipe. The number of loading (displacement) increments was 40. Because the pipe displacement is large, geometric nonlinearity was accounted for in the analysis. The computational results of pipe displacement, bending moment, stress, strain, and soil reaction loads are presented in the following sections.

3.4 Load-Displacement Relation

In the FE analysis, the pipe was pulled 0.3 m in the lateral direction at a location of 0.11 m from the pipe end. The displaced pipe is shown in Figure 33. Lateral displacement along the pipe length is shown in Figure 34. The plastic hinge develops about 1.2 m from the pipe end. The relationship between the load applied and the displacement of the loading location on the pipe is shown in Figure 35. At the beginning, the resistance load increases significantly with displacement; the relationship between the load and displacement is approximately linear. The failure load is about 107 kN, which occurs at a displacement of approximately 60 mm after which the slope of the curve becomes relatively constant. After the failure load, the load applied increases slightly with displacement. This is due to the strain hardening behaviour of the pipe material as presented in Figure 30. Because the FE model cannot account for pipe ovalization (pipe cross section is assumed not to change), the analysis is valid only to some limit of displacement.

3.5 Soil Reaction Load

The soil reaction load is applied to the pipe through the spring elements and is dependent on the lateral displacement of the pipe. The distribution of soil reaction loads is shown in Figure 36. From the pipe end to the hinge location at about 1.2 m from the pipe end, the soil reaction load is a

constant ultimate value of 96.4 kN/m, because the pipe displacement is larger than the soil yield displacement of 22.5 mm. Towards the centre, the soil reaction load decreases because of the smaller lateral displacement of the pipe; the direction of soil reaction load is in accordance with the predicted direction of pipe displacement.

3.6 Bending Moment, Strain and Stress of Pipe

As seen in Figure 37, the maximum bending moment at the end of the last load increment is 49 kN-m at a location about 1.2 m from the pipe end. This is the same location where the buckling occurred in the physical test. At the center of the pipe, the bending moment is reduced to 21 kN-m.

The axial (bending) strain along the pipe is shown in Figure 38. The maximum predicted strain of about 4.5% occurs at the hinge location of 1.2 m from the pipe end. Large plastic strains were developed to a distance of about 0.5 m on either side of the hinge location. The maximum strain is excessive and exceeds the limit at which a real pipe would have ovalised and buckled.

The axial stress along the pipe is shown in Figure 39. The maximum axial stress of 398 MPa occurs about 1.2 m from the pipe end. The hoop stress of the pipe is shown in Figure 40. The maximum hoop stress is 199 MPa. Because the hoop stress affects the yield behaviour of the pipe, the axial stress with a maximum value of 398 MPa could exceed the ultimate strength of 370 MPa obtained from uniaxial tension tests.

The development of the maximum fibre stress and strain at the hinge location with the lateral pulling displacement of the pipe at the location of 0.11 m from the end of the pipe are shown in Figure 41 and Figure 42 respectively. The initial yielding at the hinge location occurs at a displacement of about 30 mm. After that, the increase in stress becomes smaller but the strain continues to increase significantly with pipeline displacement.

3.7 Summary

The predicted displaced shape of the pipe and the load-displacement relationship obtained using the FE model established for laterally loaded pipeline are in accordance with the measured results of the GSC 01 pipeline test. The FE model can be used to predict soil reaction load, stress, strain and bending moment along the pipeline. However, this model cannot predict the actual ovalization of the pipe.

4.0 COMPARISON BETWEEN ACTUAL AND PREDICTED RESULTS

Actual experimental maximum loads were measured to be 99 kN at the Master end and 104 kN at the Slave end of the pipeline for an average maximum load of 102 kN. Displacements to maximum load were measured to be 34 mm and 27 mm at the Master and Slave ends respectively. After reaching maximum load, the load decreased slightly to some steady state value.

The FE model predicted a failure load of 102 kN with a corresponding displacement to failure load of 60 mm for each end of the pipe. However, initial yielding at the hinge location was predicted to occur at a displacement of 30 mm. The model also predicted that after the failure load, the load would continue to slightly increase with pipeline displacement due to the strain hardening behaviour of the pipeline material.

These values of maximum loads agree reasonably well with those predicted from the FE model. Measured displacements to maximum load are consistent with the predicted displacement to initial yielding.

The plastic hinge in the pipe was predicted to occur about 1.2 m from the pipe end. Following pipeline excavation, the actual location of the plastic hinges was observed to be 1.3 m from the Master end and 1.2 m from the Slave end.

Further data analysis and comparison will be made in the final report.

5.0 REFERENCES

Bungay, N. (1996). *Design, Construction, and Commissioning of the NOVA Ultrasonic Surface Profiler*. Engineering Work Term Report Prepared for NOVA, the National Energy Board, C-CORE, and the Faculty of Engineering and Applied Science, Memorial University of Newfoundland, April.

Hibbitt, H.D., Karlsson, B.I., and Sorenson, E.P. (1997) "User's Manual and Theory Manual." ABAQUS/Standard Version 5.7 Documentation, Hibbit, Karlsson & Sorenson Ltd., Providence, Rhode Island.

Paulin, M.J. and Hurley, S. (1996). "Full-Scale Pipe/Soil Interaction Study - Progress Report No. 3". C-CORE Progress Report to NOVA Gas Transmission Limited and National Energy Board, March.

Appendix A

Data Presentation, Tables and Figures

List of Tables

Table 1 - Density and Moisture Content Measurements - Test GSC 01

Test #	Test Type	Grid Location	Elevation (mm)	Moist Density (kg/m^3)	Dry Density (kg/m^3)	Moisture Content (%)
1	1	D7	100	1839	1752	4.7
2	2	L1	100	1794	1750	2.5
3	2	J10	200	1781	1750	1.7
4	2	K9	300	1851	N/A	N/A
5	2	E10	400	1809	1749	2.8
6	1	Q10	500	1939	1865	3.8
7	2	U6	500	1804	1728	4.3
8	2	K1	600	1766	1715	2.2
9	1	U3	700	1759	1713	2.6
10	2	A4	700	1813	1740	4.0
11	2	T2	800	1749	1711	2.2
12	1	I5	900	1751	1667	4.8
13	2	A7	900	1796	1702	5.2
14	2	P2	1000	1813	1706	5.9
15	1	J7	1100	1730	1692	2.2
16	2	H9	1100	1774	1706	3.8
17	1	O9	1200	1755	1721	2.0
18	2	K2	1200	1766	1685	3.9
19	2	M2	1300	1753	1685	3.9
			Average	1792	1724	3.5

Table 2 - Surface Elevation Measurements - Test GSC 01

Grid Point	X (mm)	Y (mm)	Pre Test Reading (mm)	Pre Test Elevation (mm)	Post Test Reading (mm)	Post Test Elevation (mm)	Elevation Difference (mm)
A0	0	0	337	–1	247	1	2
A1	250	0	337	–1	233	15	16
A2	550	0	338	–2	208	40	42
A3	850	0	333	3	172	76	73
A4	1150	0	332	4	171	77	73
A5	1450	0	335	1	214	34	33
A6	1750	0	331	5	241	7	2
A7	2050	0	335	1	248	0	–1
A8	2350	0	338	–2	250	–2	0
A9	2650	0	338.5	–2.5	251	–3	–0.5
A10	2950	0	332	4	246	2	–2
B0	0	170	337	–1	239	9	10
B1	250	170	337	–1	230	18	19
B2	550	170	337	–1	200	48	49
B3	850	170	333	3	173	75	72
B4	1150	170	333	3	160	88	85
B5	1450	170	336	0	205	43	43
B6	1750	170	333	3	243	5	2
B7	2050	170	337	–1	248	0	–1
B8	2350	170	336.5	–0.5	249	–1	–0.5
B9	2650	170	336	0	250	–2	–2
B10	2950	170	331	5	246	2	–3
C0	0	470	329	7	231	17	10
C1	250	470	334	2	224	24	22
C2	550	470	333.5	2.5	200	48	45.5
C3	850	470	335	1	174	74	73
C4	1150	470	332	4	148	100	96
C5	1450	470	331	5	182	66	61
C6	1750	470	332	4	234	14	10
C7	2050	470	335.5	0.5	247	1	0.5
C8	2350	470	336	0	248	0	0
C9	2650	470	331	5	244	4	–1
C10	2950	470	320	16	234	14	–2

Table 2, cont... - Surface Elevation Measurements - Test GSC 01

Grid Point	X (mm)	Y (mm)	Pre Test Reading (mm)	Pre Test Elevation (mm)	Post Test Reading (mm)	Post Test Elevation (mm)	Elevation Difference (mm)
D0	0	770	330	6	228	20	14
D1	250	770	336	0	224	24	24
D2	550	770	336	0	204	44	44
D3	850	770	334.5	1.5	177	71	69.5
D4	1150	770	332	4	156	92	88
D5	1450	770	329	7	186	62	55
D6	1750	770	331	5	235	13	8
D7	2050	770	332	4	245	3	−1
D8	2350	770	328	8	242	6	−2
D9	2650	770	328	8	242	6	−2
D10	2950	770	321	15	236	12	−3
E0	0	1070	329	7	231	17	10
E1	250	1070	332	4	212	36	32
E2	550	1070	333	3	208	40	37
E3	850	1070	330	6	184	64	58
E4	1150	1070	328	8	180	68	60
E5	1450	1070	324	12	205	43	31
E6	1750	1070	329	7	240	8	1
E7	2050	1070	329	7	242	6	−1
E8	2350	1070	326	10	240	8	−2
E9	2650	1070	328	8	242	6	−2
E10	2950	1070	327	9	242	6	−3
F0	0	1370	328.5	7.5	223	25	17.5
F1	250	1370	329	7	225	23	16
F2	550	1370	332	4	217	31	27
F3	850	1370	335.5	0.5	213	35	34.5
F4	1150	1370	329	7	212	36	29
F5	1450	1370	323	13	221	27	14
F6	1750	1370	323	13	235	13	0
F7	2050	1370	322	14	237	11	−3
F8	2350	1370	323	13	238	10	−3
F9	2650	1370	327	9	240	8	−1
F10	2950	1370	325	11	239	9	−2

Table 2, cont... - Surface Elevation Measurements - Test GSC 01

Grid Point	X (mm)	Y (mm)	Pre Test Reading (mm)	Pre Test Elevation (mm)	Post Test Reading (mm)	Post Test Elevation (mm)	Elevation Difference (mm)
G0	0	1670	335.5	0.5	249	−1	1.5
G1	250	1670	332	4	237	11	7
G2	550	1670	330	6	229	19	13
G3	850	1670	335	1	230	18	17
G4	1150	1670	327	9	228	20	11
G5	1450	1670	328	8	238	10	2
G6	1750	1670	324	12	237	11	−1
G7	2050	1670	325	11	240	8	−3
G8	2350	1670	326	10	241	7	−3
G9	2650	1670	326	10	242	6	−4
G10	2950	1670	330	6	248	0	−6
H0	0	1970	331	5	241	7	2
H1	250	1970	332	4	240	8	4
H2	550	1970	329	7	236	12	5
H3	850	1970	334	2	239	9	7
H4	1150	1970	330	6	239	9	3
H5	1450	1970	332	4	244	4	0
H6	1750	1970	334	2	246	2	0
H7	2050	1970	330	6	244	4	−2
H8	2350	1970	328	8	242	6	−2
H9	2650	1970	329	7	243	5	−2
H10	2950	1970	327	9	242	6	−3
I0	0	2270	327	9	240	8	−1
I1	250	2270	332	4	243	5	1
I2	550	2270	333	3	243	5	2
I3	850	2270	328	8	238	10	2
I4	1150	2270	334	2	245	3	1
I5	1450	2270	332.5	3.5	245	3	−0.5
I6	1750	2270	338	−2	251	−3	−1
I7	2050	2270	333	3	242	6	3
I8	2350	2270	328	8	242	6	−2
I9	2650	2270	330	6	245	3	−3
I10	2950	2270	327	9	241	7	−2

Table 2, cont... - Surface Elevation Measurements - Test GSC 01

Grid Point	X (mm)	Y (mm)	Pre Test Reading (mm)	Pre Test Elevation (mm)	Post Test Reading (mm)	Post Test Elevation (mm)	Elevation Difference (mm)
J0	0	2570	330	6	243	5	–1
J1	250	2570	336	0	248	0	0
J2	550	2570	339	–3	251	–3	0
J3	850	2570	336	0	248	0	0
J4	1150	2570	332	4	245	3	–1
J5	1450	2570	329	7	242	6	–1
J6	1750	2570	334	2	248	0	–2
J7	2050	2570	331	5	246	2	–3
J8	2350	2570	330	6	244	4	–2
J9	2650	2570	330	6	245	3	–3
J10	2950	2570	327	9	241	7	–2
K0	0	2870	336	0	250	–2	–2
K1	250	2870	340	–4	252	–4	0
K2	550	2870	339	–3	252	–4	–1
K3	850	2870	334.5	1.5	247	1	–0.5
K4	1150	2870	328	8	242	6	–2
K5	1450	2870	327	9	240	8	–1
K6	1750	2870	330	6	244	4	–2
K7	2050	2870	328	8	242	6	–2
K8	2350	2870	330	6	244	4	–2
K9	2650	2870	328	8	243	5	–3
K10	2950	2870	326	10	242	6	–4
L0	0	3170	335	1	247	1	0
L1	250	3170	338	–2	249	–1	1
L2	550	3170	339	–3	250	–2	1
L3	850	3170	332	4	246	2	–2
L4	1150	3170	330	6	243	5	–1
L5	1450	3170	327	9	241	7	–2
L6	1750	3170	327	9	243	5	–4
L7	2050	3170	325	11	240	8	–3
L8	2350	3170	330	6	246	2	–4
L9	2650	3170	330	6	245	3	–3
L10	2950	3170	331	5	247	1	–4

Table 2, cont... - Surface Elevation Measurements - Test GSC 01

Grid Point	X (mm)	Y (mm)	Pre Test Reading (mm)	Pre Test Elevation (mm)	Post Test Reading (mm)	Post Test Elevation (mm)	Elevation Difference (mm)
M0	0	3470	328	8	239	9	1
M1	250	3470	337	–1	246	2	3
M2	550	3470	337	–1	247	1	2
M3	850	3470	329	7	242	6	–1
M4	1150	3470	331	5	244	4	–1
M5	1450	3470	329	7	243	5	–2
M6	1750	3470	325	11	240	8	–3
M7	2050	3470	326	10	240	8	–2
M8	2350	3470	326	10	241	7	–3
M9	2650	3470	332	4	247	1	–3
M10	2950	3470	338	–2	244	4	6
N0	0	3770	326	10	237	11	1
N1	250	3770	338	–2	248	0	2
N2	550	3770	337	–1	246	2	3
N3	850	3770	326	10	239	9	–1
N4	1150	3770	330	6	243	5	–1
N5	1450	3770	328	8	243	5	–3
N6	1750	3770	327	9	242	6	–3
N7	2050	3770	325	11	240	8	–3
N8	2350	3770	322	14	238	10	–4
N9	2650	3770	331	5	246	2	–3
N10	2950	3770	328	8	244	4	–4
O0	0	4070	336	0	248	0	0
O1	250	4070	340	–4	249	–1	3
O2	550	4070	336	0	242	6	6
O3	850	4070	335	1	244	4	3
O4	1150	4070	330	6	241	7	1
O5	1450	4070	330	6	243	5	–1
O6	1750	4070	332	4	246	2	–2
O7	2050	4070	328	8	242	6	–2
O8	2350	4070	328	8	242	6	–2
O9	2650	4070	330	6	245	3	–3
O10	2950	4070	327	9	242	6	–3

Table 2, cont... - Surface Elevation Measurements - Test GSC 01

Grid Point	X (mm)	Y (mm)	Pre Test Reading (mm)	Pre Test Elevation (mm)	Post Test Reading (mm)	Post Test Elevation (mm)	Elevation Difference (mm)
P0	0	4370	328	8	239	9	1
P1	250	4370	335	1	241	7	6
P2	550	4370	328	8	229	19	11
P3	850	4370	332	4	233	15	11
P4	1150	4370	324	12	228	20	8
P5	1450	4370	331	5	242	6	1
P6	1750	4370	329	7	241	7	0
P7	2050	4370	331	5	244	4	−1
P8	2350	4370	328	8	242	6	−2
P9	2650	4370	328	8	241	7	−1
P10	2950	4370	326	10	240	8	−2
Q0	0	4670	327	9	234	14	5
Q1	250	4670	333	3	234	14	11
Q2	550	4670	326	10	216	32	22
Q3	850	4670	331	5	215	33	28
Q4	1150	4670	325	11	213	35	24
Q5	1450	4670	329	7	235	13	6
Q6	1750	4670	327	9	238	10	1
Q7	2050	4670	330	6	243	5	−1
Q8	2350	4670	327	9	240	8	−1
Q9	2650	4670	330	6	243	5	−1
Q10	2950	4670	328	8	242	6	−2
R0	0	4970	330	6	236	12	6
R1	250	4970	335	1	231	17	16
R2	550	4970	334	2	212	36	34
R3	850	4970	333	3	189	59	56
R4	1150	4970	330	6	185	63	57
R5	1450	4970	329	7	218	30	23
R6	1750	4970	330	6	239	9	3
R7	2050	4970	328	8	241	7	−1
R8	2350	4970	326	10	239	9	−1
R9	2650	4970	330	6	245	3	−3
R10	2950	4970	334	2	247	1	−1

Table 2, cont... - Surface Elevation Measurements - Test GSC 01

Grid Point	X (mm)	Y (mm)	Pre Test Reading (mm)	Pre Test Elevation (mm)	Post Test Reading (mm)	Post Test Elevation (mm)	Elevation Difference (mm)
S0	0	5270	331	5	235	9	4
S1	250	5270	336	0	229	19	19
S2	550	5270	333	3	206	42	39
S3	850	5270	333	3	180	68	65
S4	1150	5270	330	6	159	89	83
S5	1450	5270	329	7	184	64	57
S6	1750	5270	330	6	230	18	12
S7	2050	5270	328	6	239	9	3
S8	2350	5270	327	9	239	9	0
S9	2650	5270	335	1	249	–1	–2
S10	2950	5270	339	–3	252	–4	–1
T0	0	5570	330	6	232	16	10
T1	250	5570	339	–3	234	16	19
T2	550	5570	334	2	209	39	37
T3	850	5570	336.5	–0.5	185	63	63.5
T4	1150	5570	333	3	160	88	85
T5	1450	5570	332	4	171	77	73
T6	1750	5570	331	5	229	19	14
T7	2050	5570	330	6	244	4	–2
T8	2350	5570	328	8	241	7	–1
T9	2650	5570	334	2	249	–1	–3
T10	2950	5570	338	–2	253	5	7
U0	0	5870	331	5	237	11	6
U1	250	5870	336	0	230	18	18
U2	550	5870	333	3	210	38	35
U3	850	5870	338	–2	189	59	57
U4	1150	5870	336	0	165	63	63
U5	1450	5870	334.5	1.5	192	56	54.5
U6	1750	5870	335	1	235	13	12
U7	2050	5870	336	0	249	–1	–1
U8	2350	5870	334	2	249	–1	–3
U9	2650	5870	338	–2	252	–4	–2
U10	2950	5870	338	–2	252	–4	–2

Table 2, cont... - Surface Elevation Measurements - Test GSC 01

Grid Point	X (mm)	Y (mm)	Pre Test Reading (mm)	Pre Test Elevation (mm)	Post Test Reading (mm)	Post Test Elevation (mm)	Elevation Difference (mm)
V0	0	6170	330	6	244	4	–2
V1	250	6170	333	3	231	17	14
V2	550	6170	332	4	215	33	29
V3	850	6170	333	3	183	65	62
V4	1150	6170	334	2	180	68	66
V5	1450	6170	336	0	224	24	24
V6	1750	6170	335.5	0.5	248	0	.5
V7	2050	6170	338	–2	252	–4	–2
V8	2350	6170	338	–2	253	–5	–3
V9	2650	6170	338	–2	252	–4	–2
V10	2950	6170	337	–1	252	–4	–3

Table 3 – Pre-Test Vertical Deformation Tube Positions – Test GSC 01

Vertical Deformation Tube	Approximate Z (mm)	X (mm)	Y (mm)	Angle[1] Perpendicular To Pipe (Deg.)	Angle[2] Parallel To Pipe (Deg.)
1	1300	793	880	2.0	2.2
1[3]	50	825	974	----	----
2	1300	1015	889	-1.5	0.7
2[3]	50	967	913	----	----
3	1300	1210	891	-1.5	-0.1
3[3]	50	1171	881	----	----
4	1300	1238	2346	3.5	0.2
4[4]	50	1318	2351	----	----
5	1300	1010	2360	3.65	1.0
5[4]	50	1093	2383	----	----
6	1300	815	2365	2.7	0.35
6[4]	50	876	2373	----	----

Notes:
1. Top of Tube Inclined Towards Increasing X-direction - Angle is Negative.
2. Top of Tube Inclined Towards Increasing Y- direction - Angle is Negative.
3. Inferred from Post-Test Position.
4. Inferred from Pre-Test Angles.

Table 4 – Post-Test Vertical Deformation Tube Positions – Test GSC 01

	Tube 1		Tube 2		Tube 3	
Approximate Elevation Z (mm)	**X (mm)**	**Y (mm)**	**X (mm)**	**Y (mm)**	**X (mm)**	**Y (mm)**
Surface	775	890	990	890	1210	907
1250	782	890	991	888	1208	896
1200	789	891	996	885	1210	885
1150	797	890	1001	886	1210	880
1100	801	890	1003	883	1209	880
1050	803	888	1003	882	1207	881
1000	807	890	1006	882	1210	880
950	812	889	1010	881	1218	876
900	814	890	1009	877	1218	875
850	819	890	1010	873	1220	877
800	822	888	1013	872	1222	878
750	828	888	1020	872	1226	877
700	834	891	1030	881	1236	880
650	840	893	1030	881	1233	881
600	851	900	1035	886	1218	877
550	860	903	1039	887	1191	880
500	855	907	1038	897	1183	878
450	847	904	1020	902	1180	879
400	843	912	1011	900	1179	877
350	833	919	995	892	1177	881
300	822	935	977	895	1176	878
250	823	942	975	904	1175	878
200	819	952	973	907	1172	880
150	818	967	970	908	1771	880
100	822	994	970	909	1172	882
50	825	974	967	913	1171	881

Notes: 1) VDT Tubes 4, 5 & 6 showed no movement therefore their post-test positions have not been presented.

2) Surface elevations were approximated as follows: Tube 1, Z = 1229mm; Tube 2, Z = 1236mm; Tube 3, Z = 1265mm

Table 5(a) – Post-Test Pipe Location, Elevation, and Ovalization (Master Side) - Test GSC 01

Location[1] Along Pipe (mm)	Displacement From Pre-Test Position (mm)	Pipe Elevation[2]	D1[3]	D2[4]	% Ovalization
0	388	792	203	202.5	0.1
50	278	793	203	202.5	0.1
100	266	794	203	202.5	0.1
150	255	796	203	202.5	0.1
200	244	797	203	202.5	0.1
250	232	798.5	203	203	0.0
300	221	800.5	202	203	0.2
350	210	801.5	202	203.5	0.4
400[5]	199	802.5	207	203.5	0.8
450	185	803	201	205	0.9
500	174	804	200	205	1.2
550	164	805.5	198	205.5	1.8
600[5]	153	806.5	206	208.5	0.6
650	142	807	197	208	2.7
700	131	808	196	209	3.2
750	121	808	195	210	3.7
800	110	809	192	211.5	4.8
850	100	809	190	213.5	5.8
900	91	810	188	215	6.7
950	81	810.5	185	216.5	7.8
1000	73	810	180	220	10.0
1050	65	810.5	177	222.5	11.4
1100	57	810.5	173	226	13.3
1150	50	811	171	230	14.7
1200	43	810.5	Buckle	Buckle	Buckle
1250	36	809	Buckle	Buckle	Buckle
1300	30	810.5	Buckle	Buckle	Buckle
1350	24	816.5	Buckle	216	Buckle
1400	20	821.5	180	212	8.2
1450	14	825	184	210	6.6
1500	10	826	188	208.5	5.2
1550	8	827	192	207	3.8
1600	6	828	195	205.5	2.6
1650	4	828	197	204.5	1.9
1700	2	829	199	203.5	1.1
1750	2	829	200	203	0.7
1800	1	829	202	203	0.2
1850	1	829.5	202	202	0.0
1900	0	829.5	202	202	0.0
1950	0	829.5	202	202	0.0

Notes:
1. Measured from Master End of Pipe.
2. Elevation was measured down from the 1300 mm mark to top of pipe.
3. Pipe Diameter in mm measured from 9:00 to 3:00 (front to rear).
4. Pipe Diameter in mm measured from 12:00 to 6:00 (top to bottom).
5. Strain Gauge Location.

Table 5(b) - Post-Test Pipe Location, Elevation, and Ovalization (Slave Side) - Test GSC 01

Location[1] Along Pipe (mm)	Displacement From Pre - Test Position (mm)	Pipe Elevation[2]	D1[3]	D2[4]	% Ovalization
0	317	791	202	203	0.2
50	293	792	202	202	0.0
100	279	792.5	202	202	0.0
150	269	794	202	202	0.0
200	253	795	202	202	0.0
250	241	797.5	202	203	0.2
300	228	799	202	203	0.2
350	215	800.5	202	203.5	0.4
400[5]	202	801	208	203.5	1.1
450	192	802.5	202	203.5	0.4
500	177	803.5	201	204.5	0.9
550	163	804.5	201	205	1.0
600[5]	150	805.5	204	207	0.7
650	140	806.5	199	206	1.7
700	126	807.5	199	207	2.0
750	113	808	197	208	2.7
800	101	809	195	209	3.5
850	89	809.5	194	210	4.0
900	78	810	192	211	4.7
950	68	810	190	213	5.7
1000	59	808	187	217	7.4
1050	51	805	185	222.5	9.2
1100	44	801	Buckle	Buckle	Buckle
1150	36	815	Buckle	Buckle	Buckle
1200	29	814	168	223	14.1
1250	23	814.5	176	222	11.5
1300	17	816.5	183	218	8.7
1350	13	818	187	216	7.2
1400	9	820	191	213	5.4
1450	7	821.5	194	211	4.2
1500	5	822.5	196	208	3.0
1550	3	823.5	199	206.5	1.8
1600	2	824.5	200	206	1.5
1650	1	825	201	204	0.7
1700	0	825.5	202	204	0.5
1750	0	826	202	204	0.5
1800	0	827	202	203	0.2
1850	0	827.5	202	202	0.0

Notes:
1. Measured from Master End of Pipe.
2. Elevation was measured down from the 1300 mm mark to top of pipe.
3. Pipe Diameter in mm measured from 9:00 to 3:00 (front to rear).
4. Pipe Diameter in mm measured from 12:00 to 6:00 (top to bottom).
5. Strain Gauge Location.

List of Figures

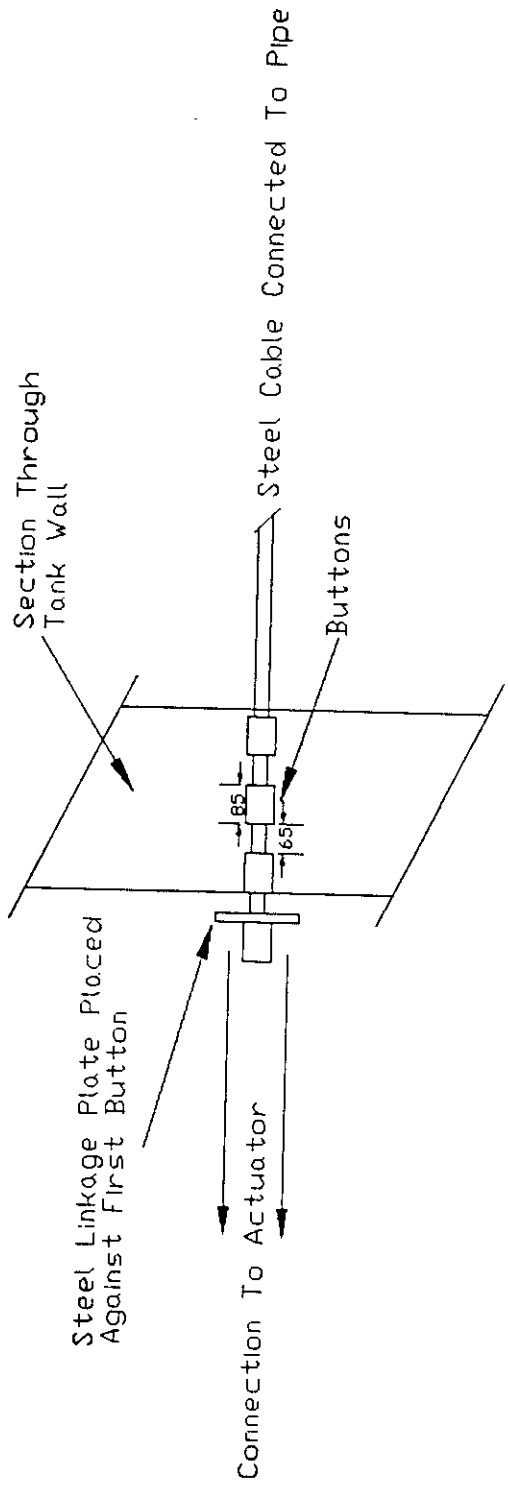

C-CORE

Loading Cable/Steel Button Details

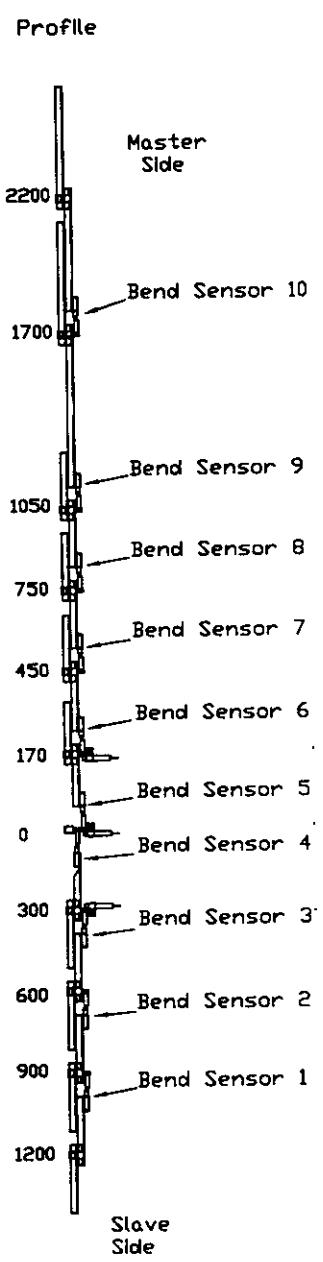
Profile
Master Side
2200
Bend Sensor 10
1700
Bend Sensor 9
1050
Bend Sensor 8
750
Bend Sensor 7
450
Bend Sensor 6
170
Bend Sensor 5
0
Bend Sensor 4
300
Bend Sensor 3
600
Bend Sensor 2
900
Bend Sensor 1
1200
Slave Side

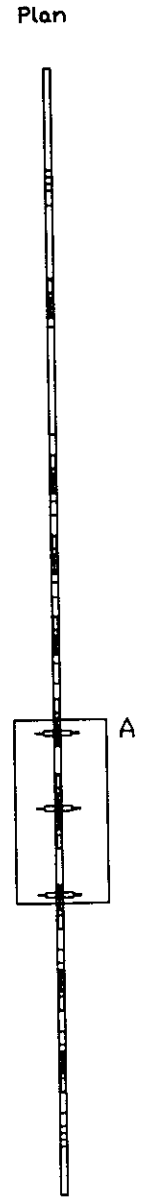
Plan
A

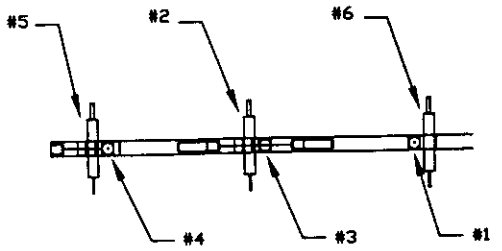
Detail A / Exploded View
LVDT's / Ovalisation Sensors
#5
#2
#6
#4
#3
#1

Pipe:
OD: 203.2mm
Wall: 3.175mm
Length: 5814mm
Material: 1010 Carbon Steel
HREW

Strain Gauges
Excitation, E:5V

Bending Gauge Configuration

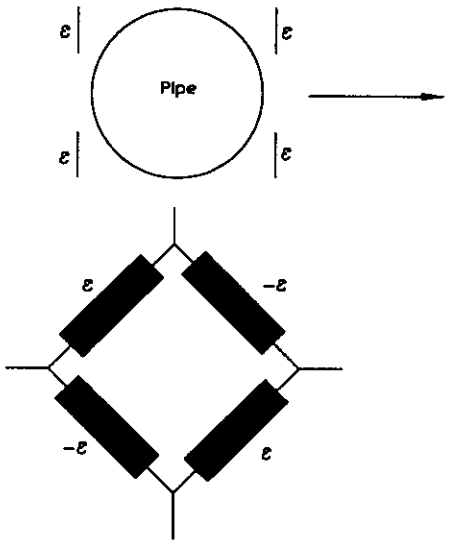

Axial Gauge Configuration

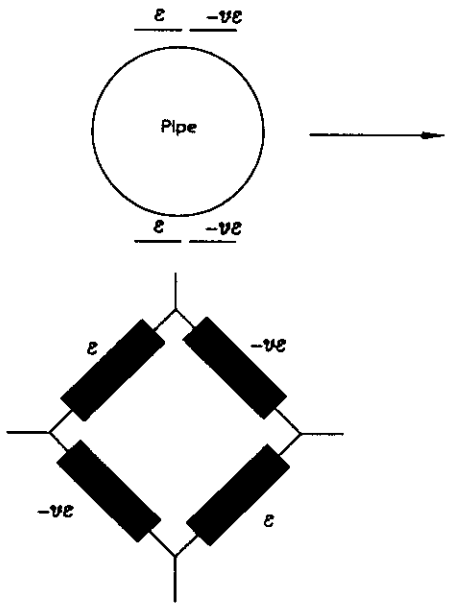

Master

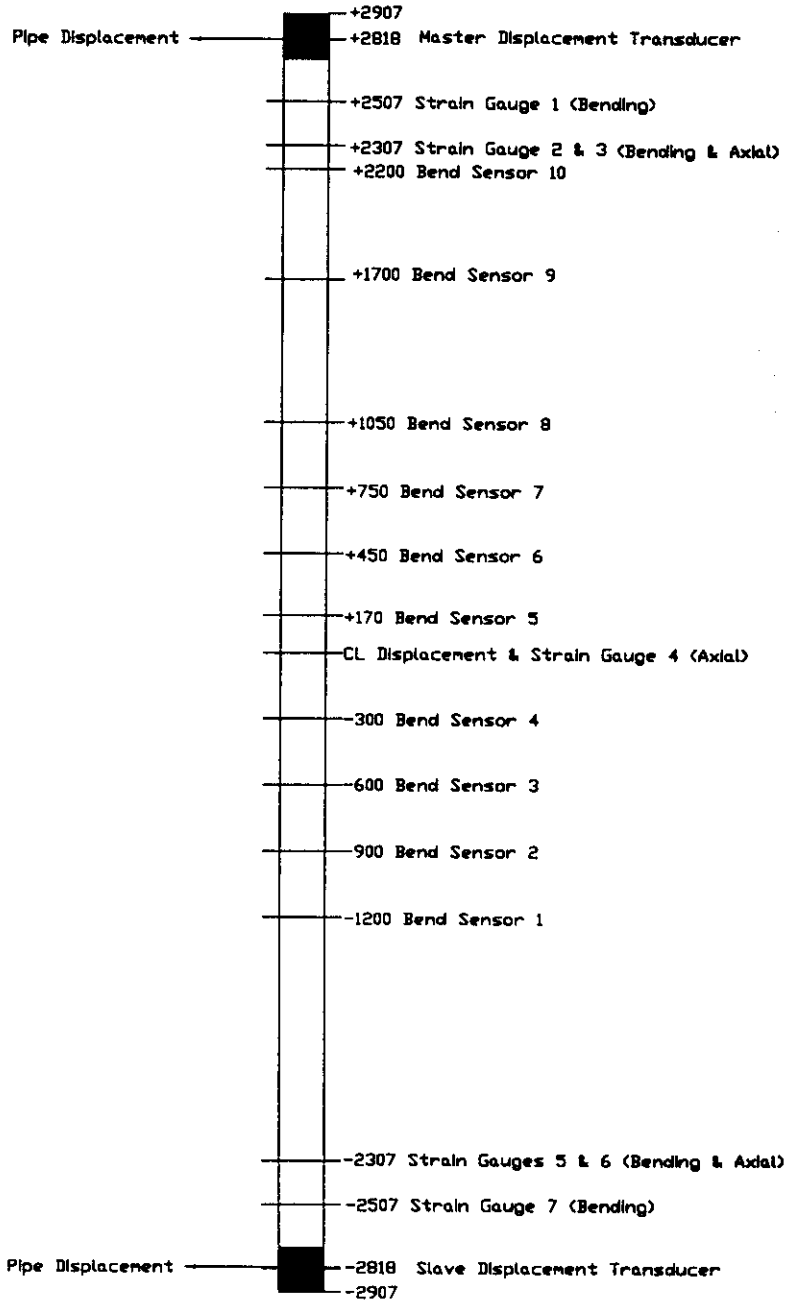

Slave

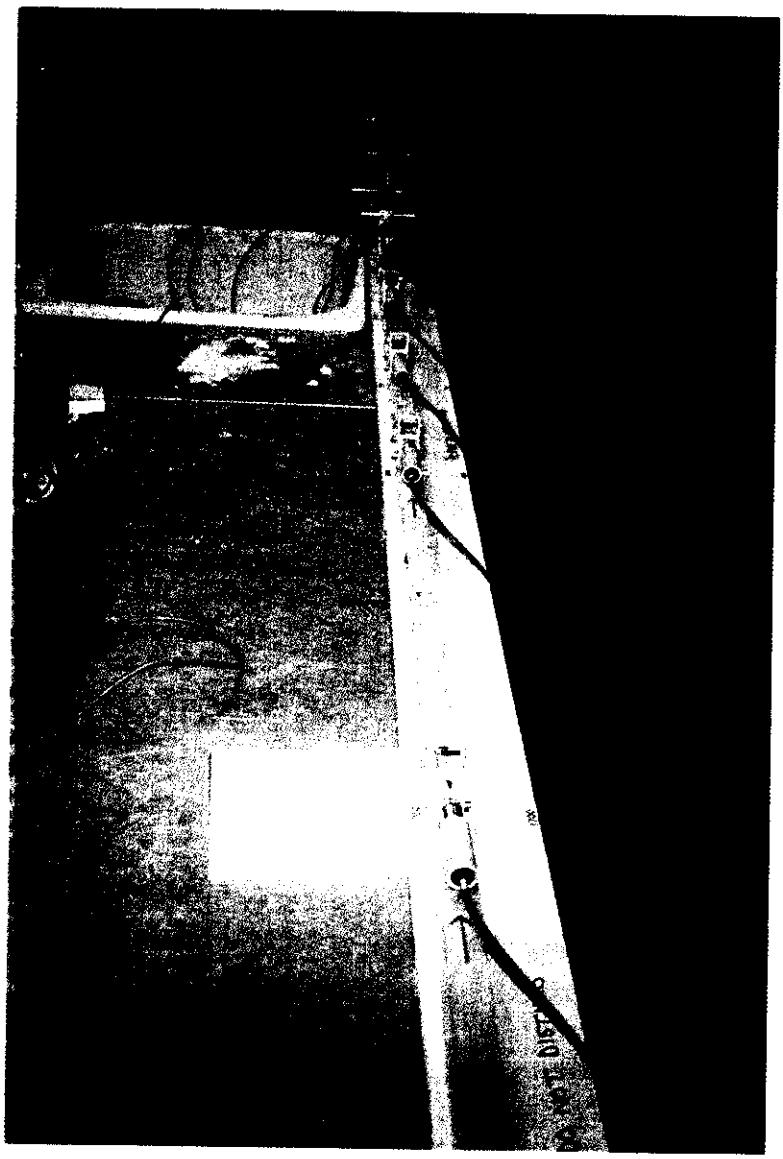

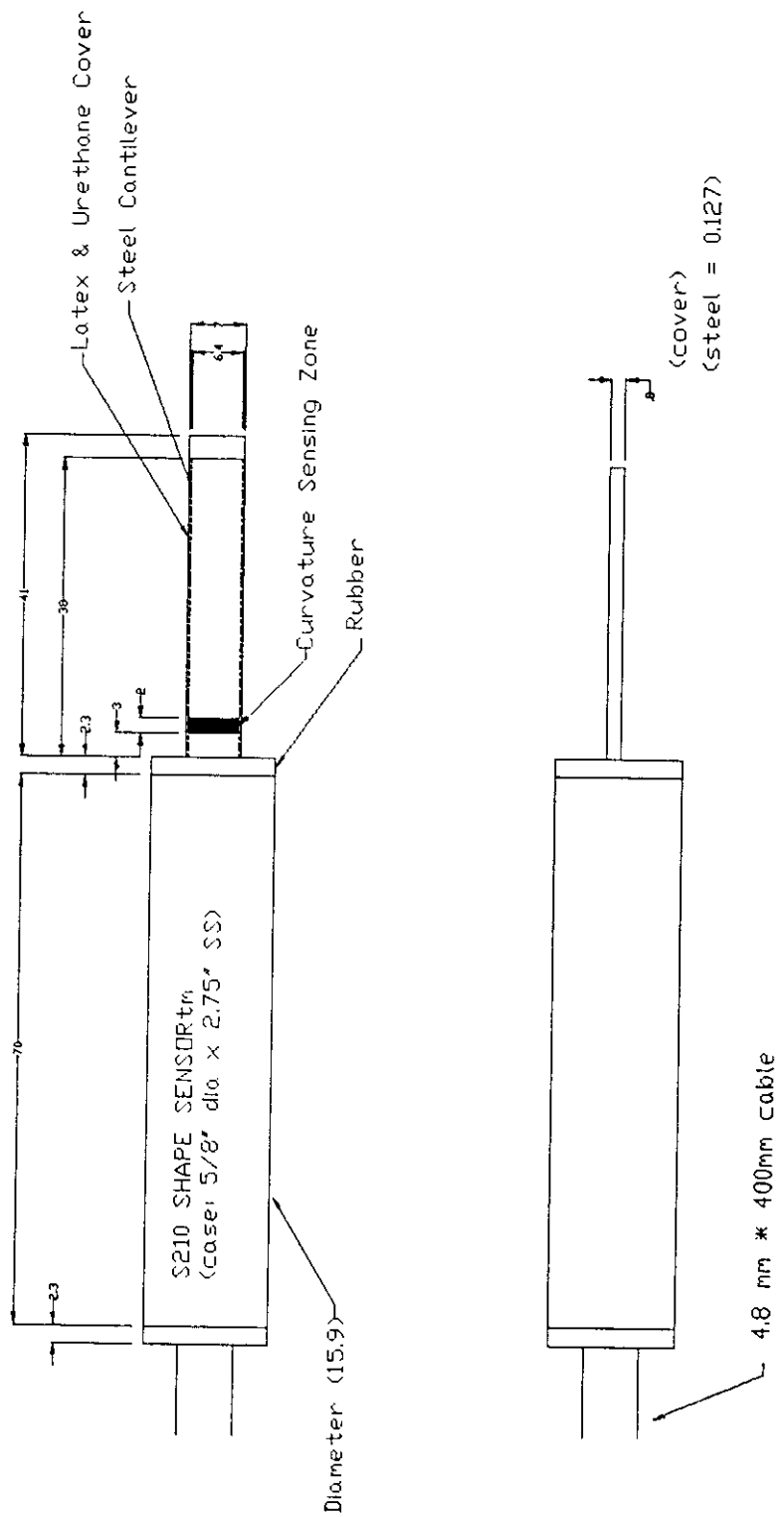
Latex & Urethone Cover
Steel Cantilever
Curvature Sensing Zone
Rubber
S210 SHAPE SENSOR tm
(case: 5/8" dia x 2.75" SS)
Diameter (15.9)
(cover)
(steel = 0.127)
4.8 mm * 400mm cable

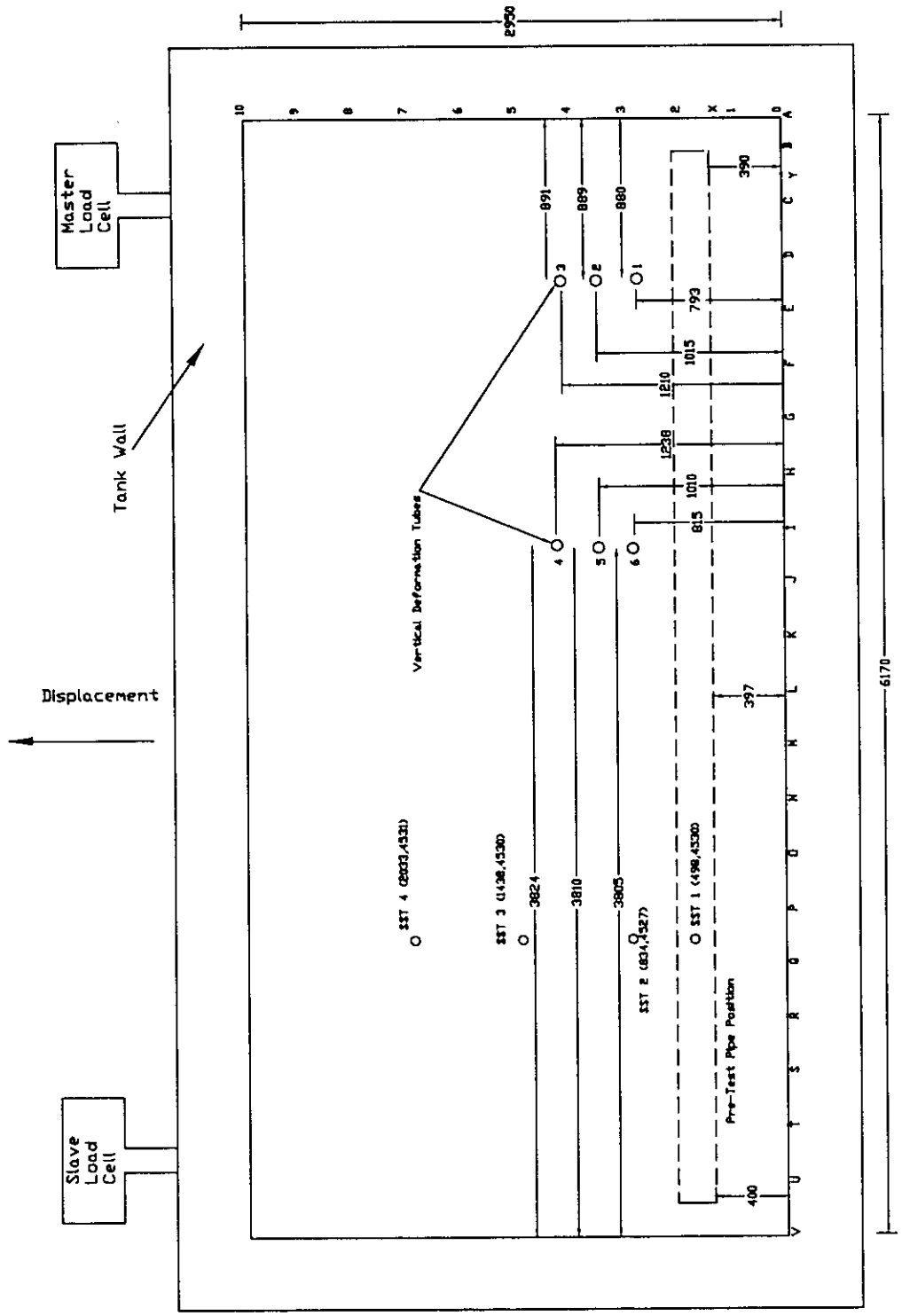

C-CORE

Experimental Setup - Plan View

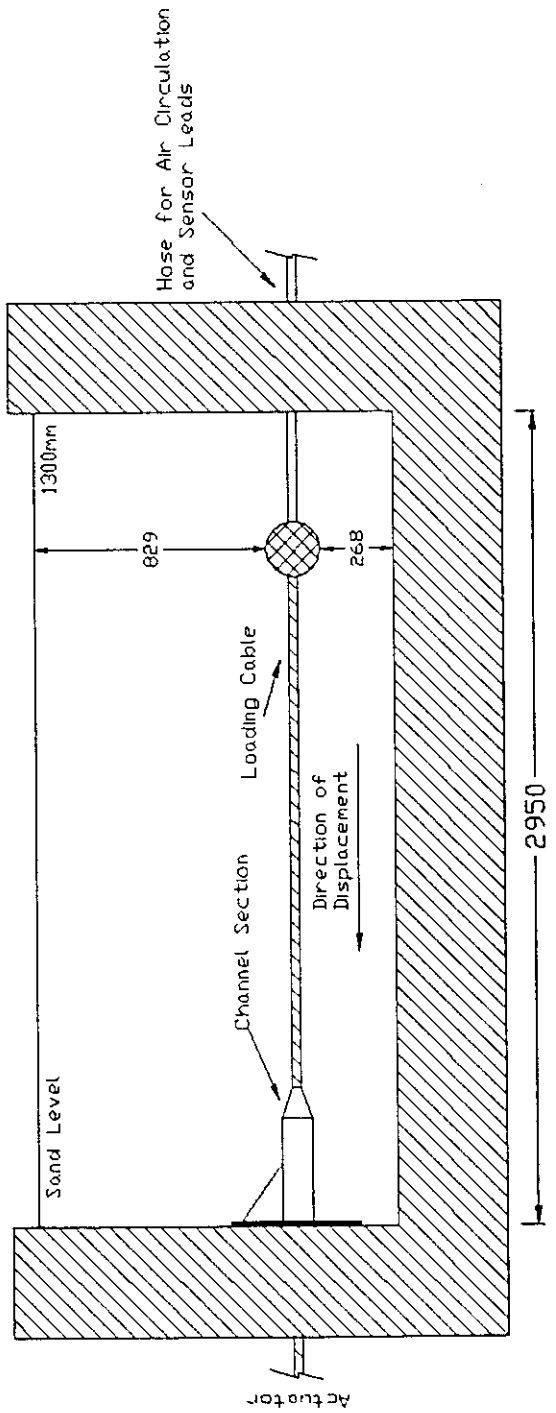
Hose for Air Circulation and Sensor Leads
1300mm
829
268
Loading Cable
Direction of Displacement
2950
Channel Section
Sand Level
Actuator

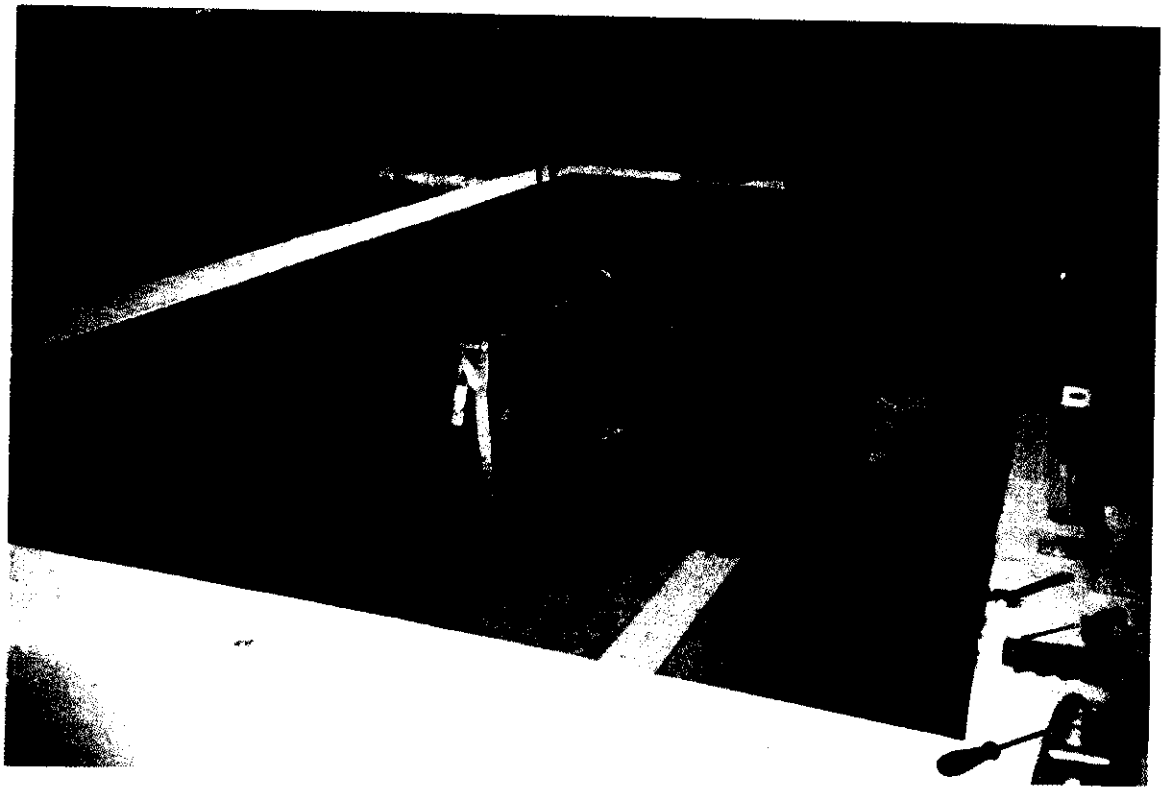

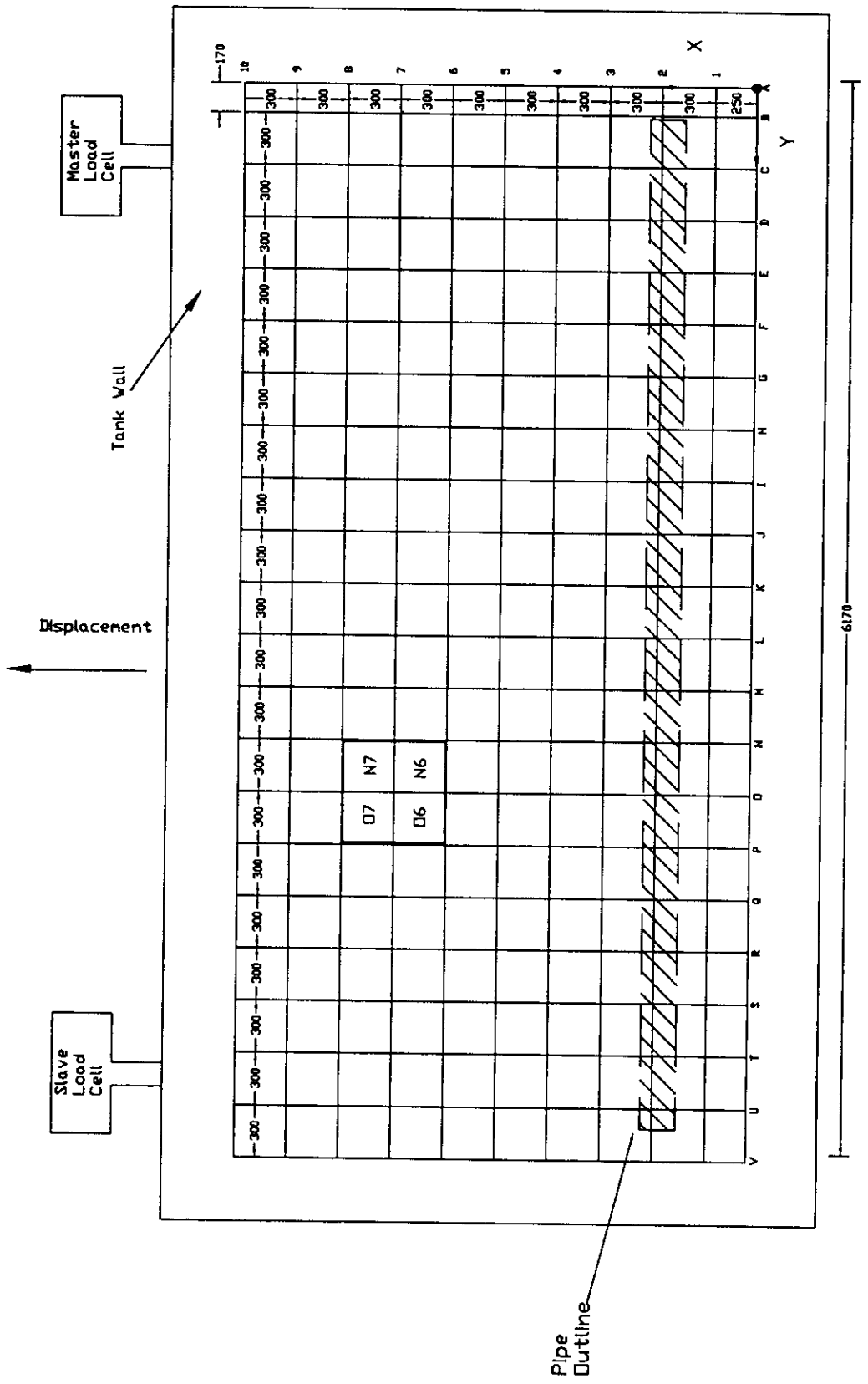

C-CORE

Surface Grid

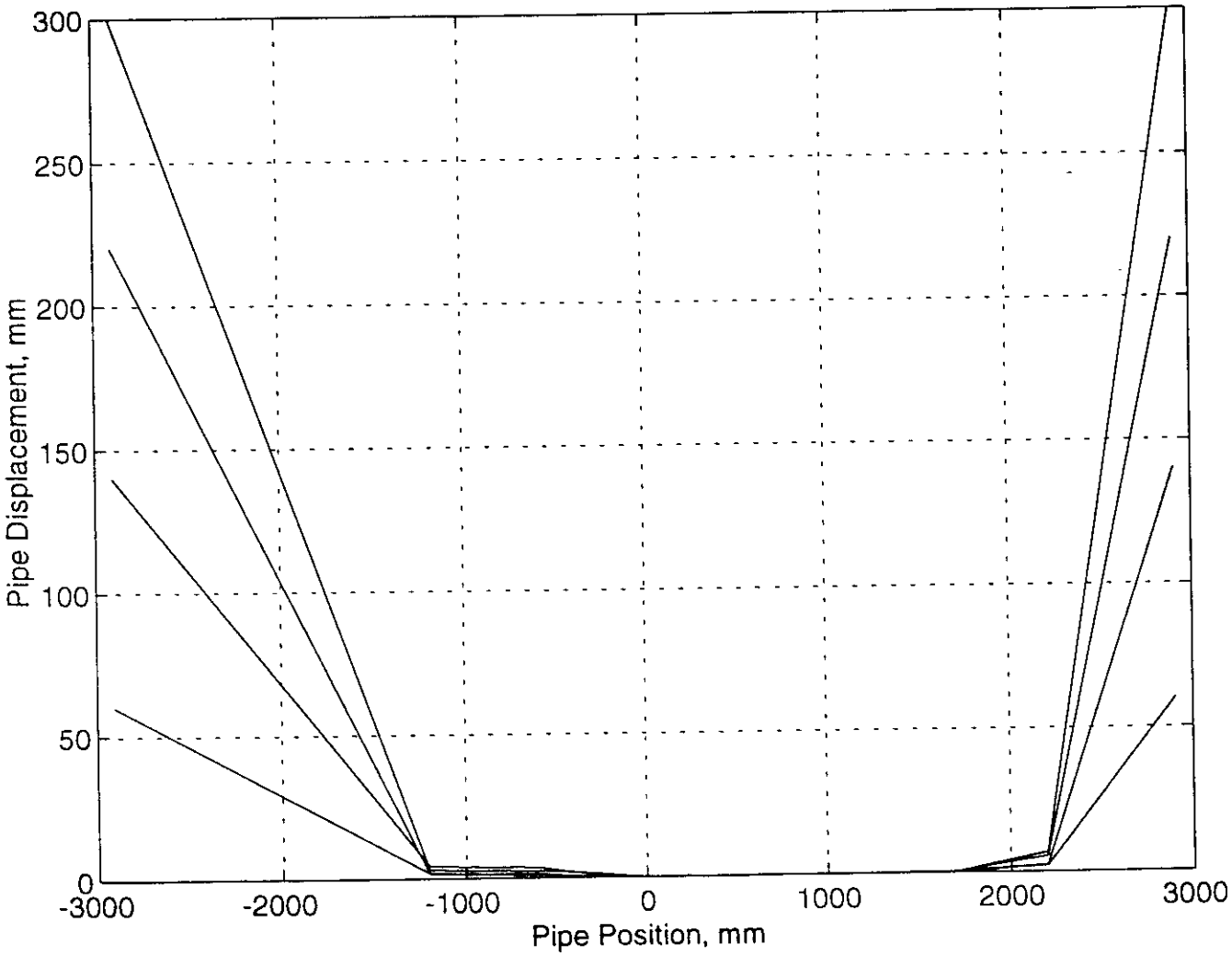

C-CORE

Pipeline Displacement Profiles

29(a)

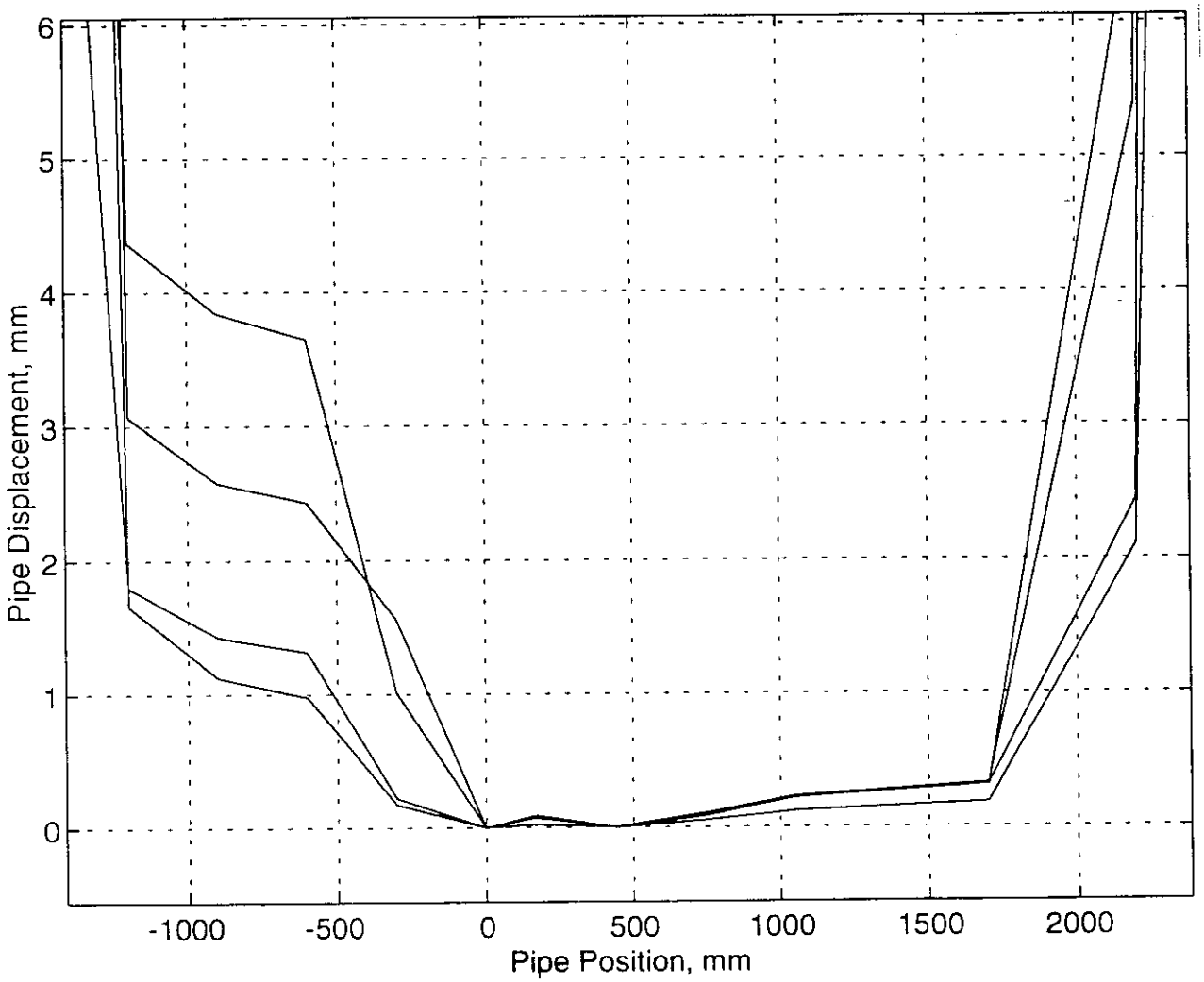

C-CORE

Pipeline Displacement Profiles

29(b)

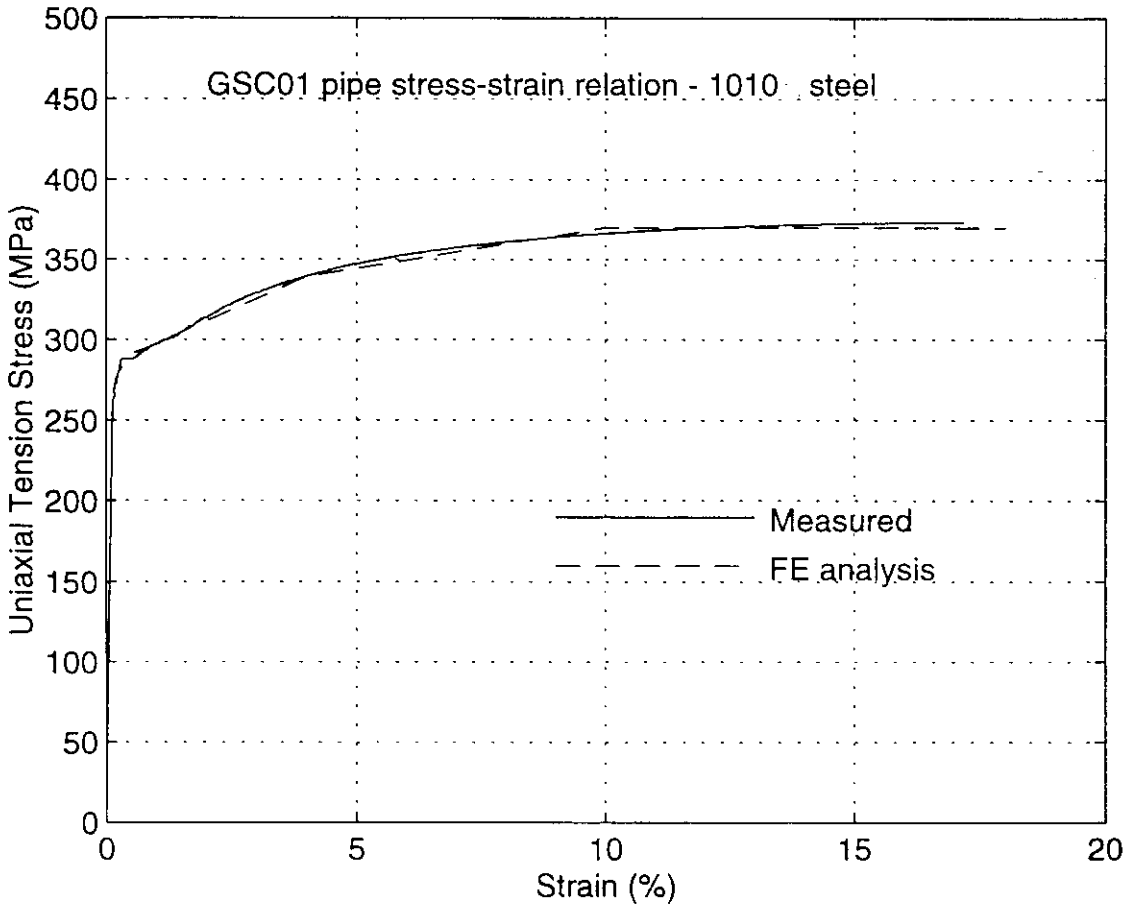
GSC01 pipe stress-strain relation - 1010 steel
Uniaxial Tension Stress (MPa)
Strain (%)
Measured
FE analysis
0
50
100
150
200
250
300
350
400
450
500
0
5
10
15
20

ABAQUS

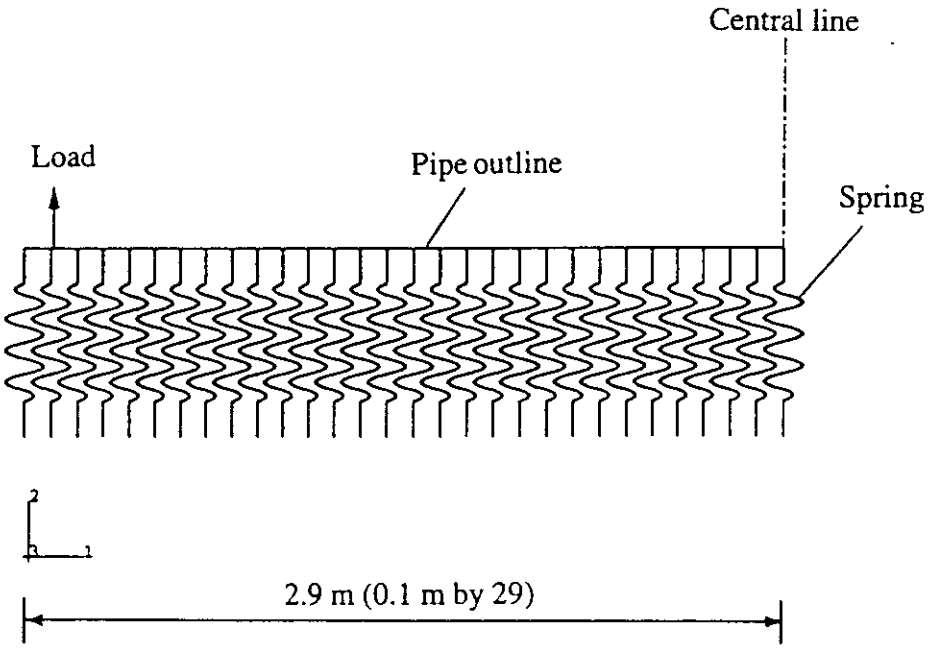

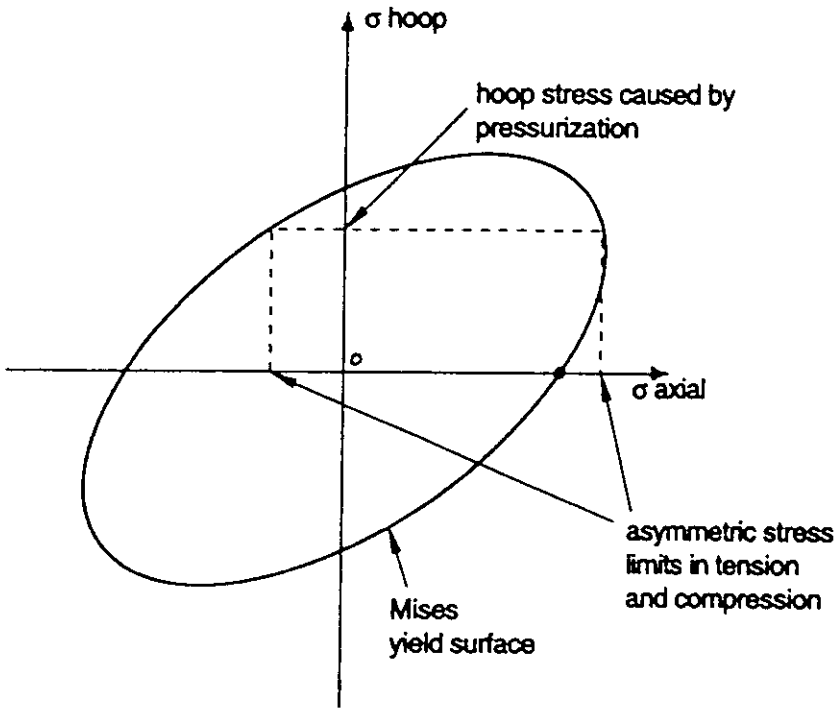

Mises Yield Surface (from Hibbet et al., 1997)

ABAQUS

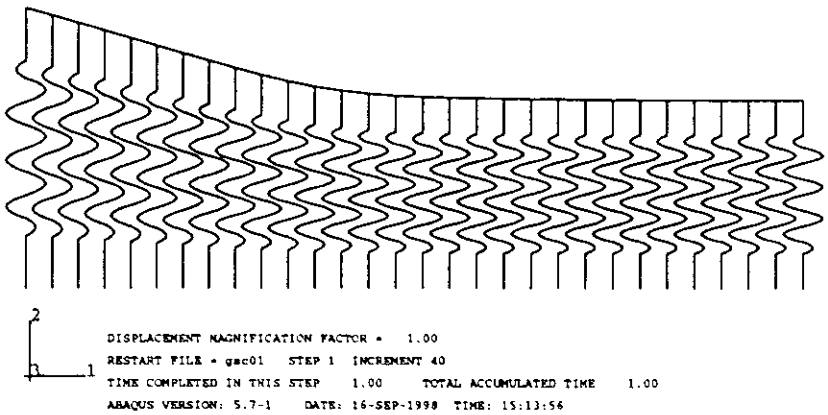
2
3
1
DISPLACEMENT MAGNIFICATION FACTOR = 1.00
RESTART FILE = gac01 STEP 1 INCREMENT 40
TIME COMPLETED IN THIS STEP 1.00 TOTAL ACCUMULATED TIME 1.00
ABAQUS VERSION: 5.7-1 DATE: 16-SEP-1998 TIME: 15:13:56

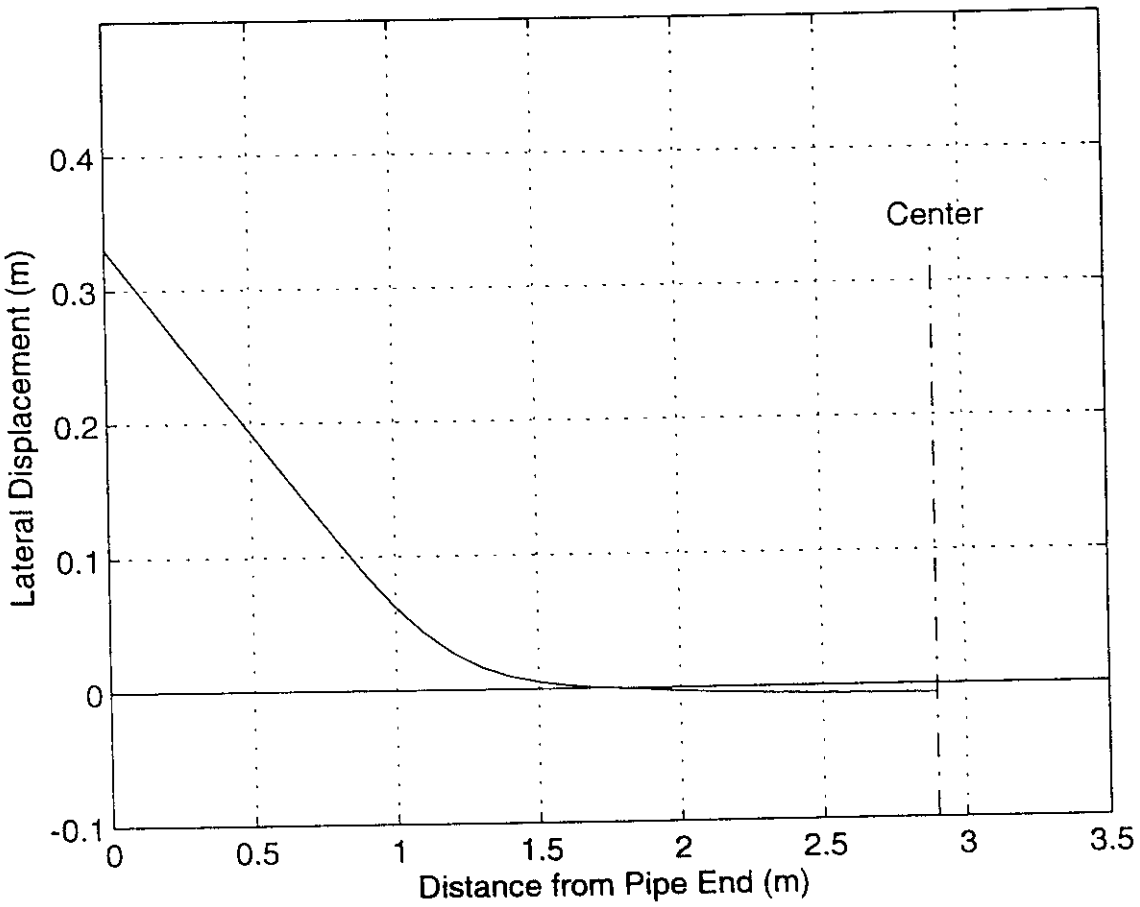
Center
Lateral Displacement (m)
Distance from Pipe End (m)
0.4
0.3
0.2
0.1
0
-0.1
0
0.5
1
1.5
2
2.5
3
3.5

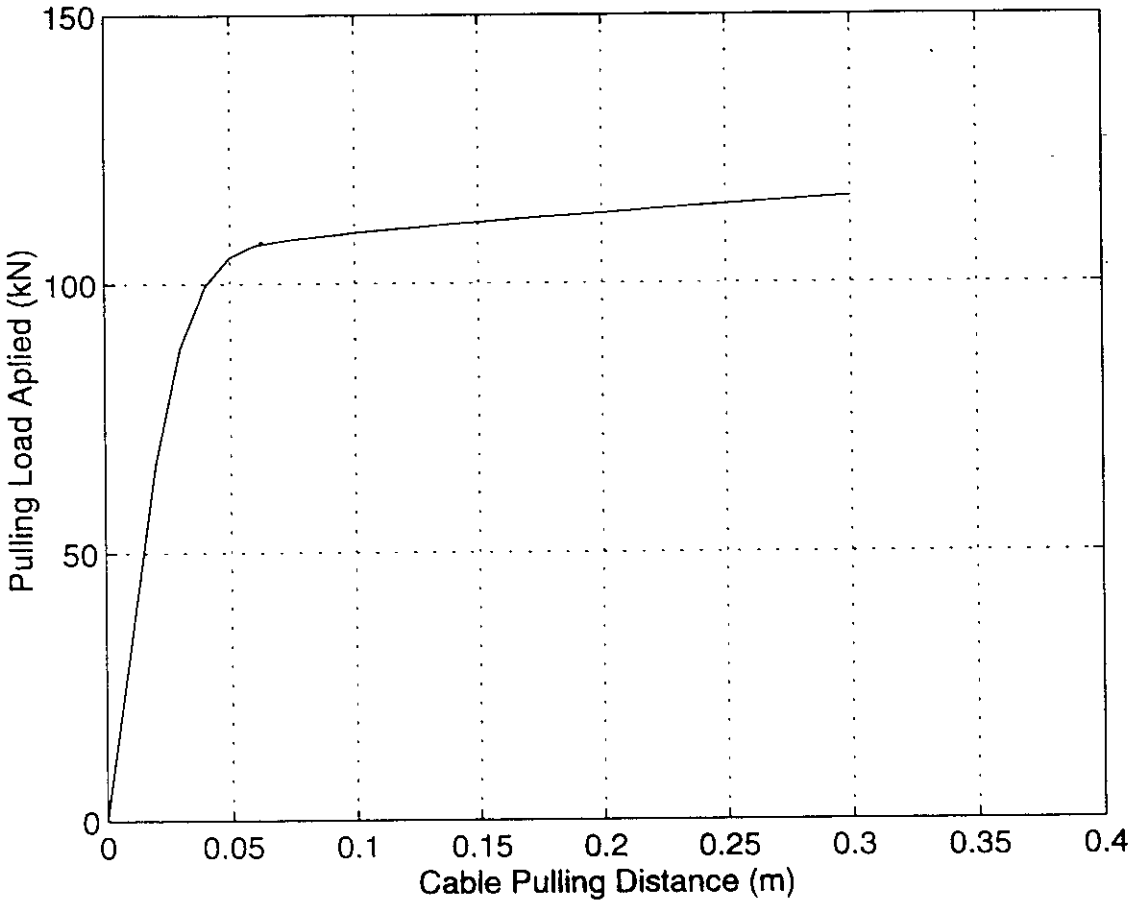
150
100
50
0
Pulling Load Aplied (kN)
0
0.05
0.1
0.15
0.2
0.25
0.3
0.35
0.4
Cable Pulling Distance (m)

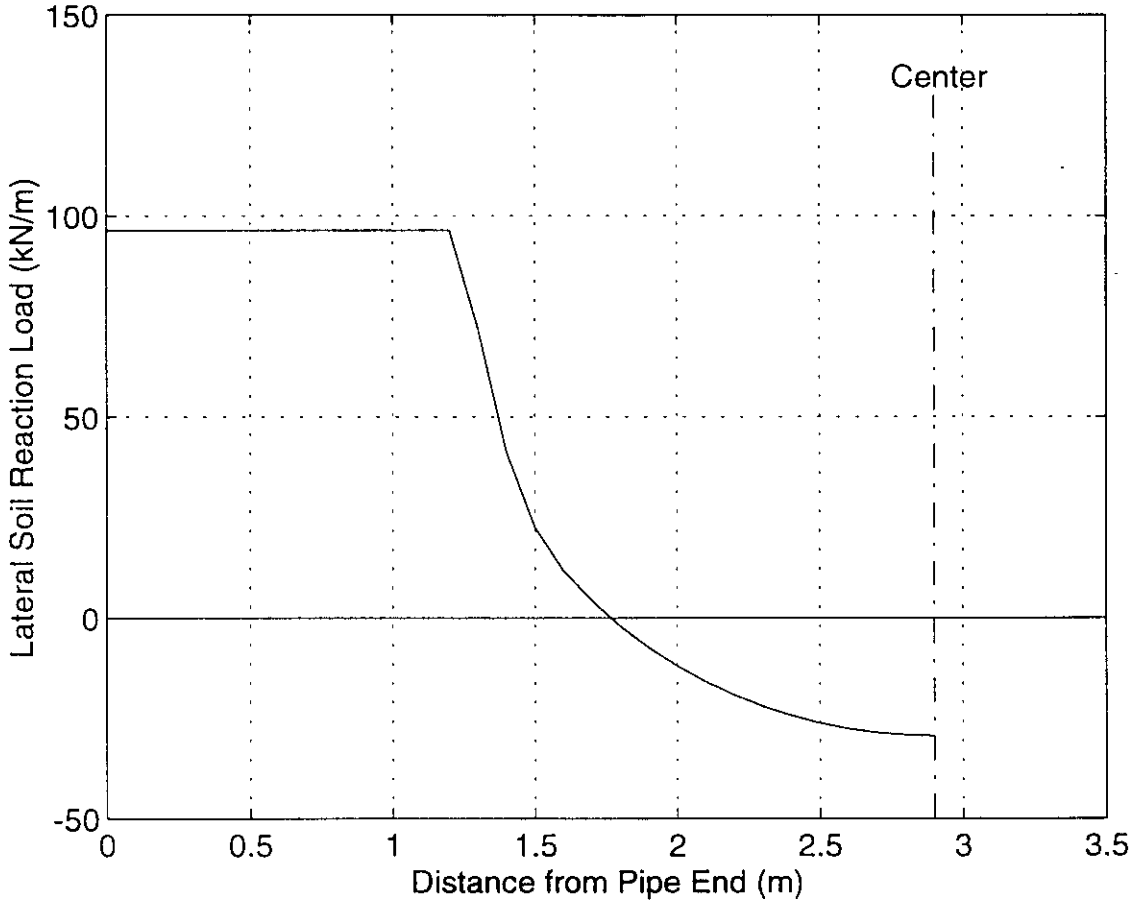
150
100
50
0
-50
0
0.5
1
1.5
2
2.5
3
3.5
Center
Lateral Soil Reaction Load (kN/m)
Distance from Pipe End (m)

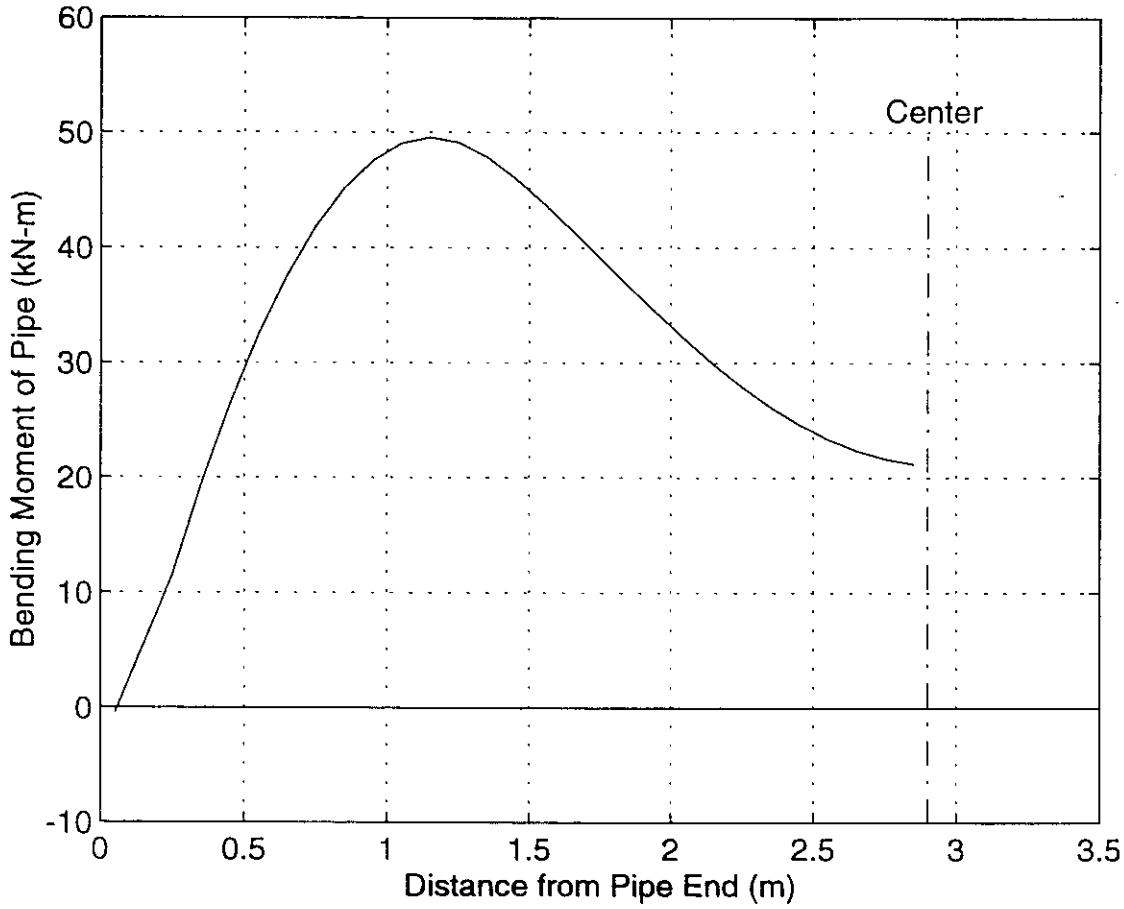
Center
Bending Moment of Pipe (kN-m)
Distance from Pipe End (m)
60
50
40
30
20
10
0
-10
0
0.5
1
1.5
2
2.5
3
3.5

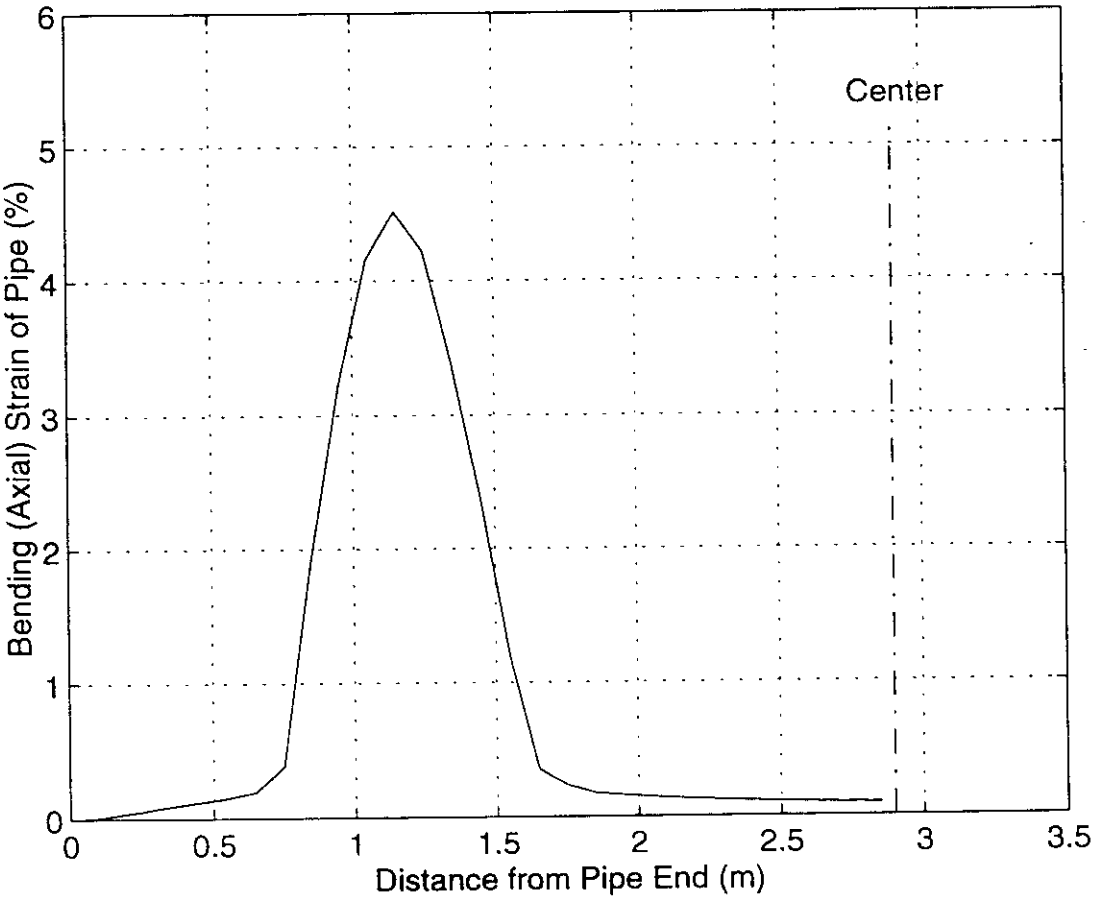
Center
Bending (Axial) Strain of Pipe (%)
Distance from Pipe End (m)
0
1
2
3
4
5
6
0
0.5
1
1.5
2
2.5
3
3.5

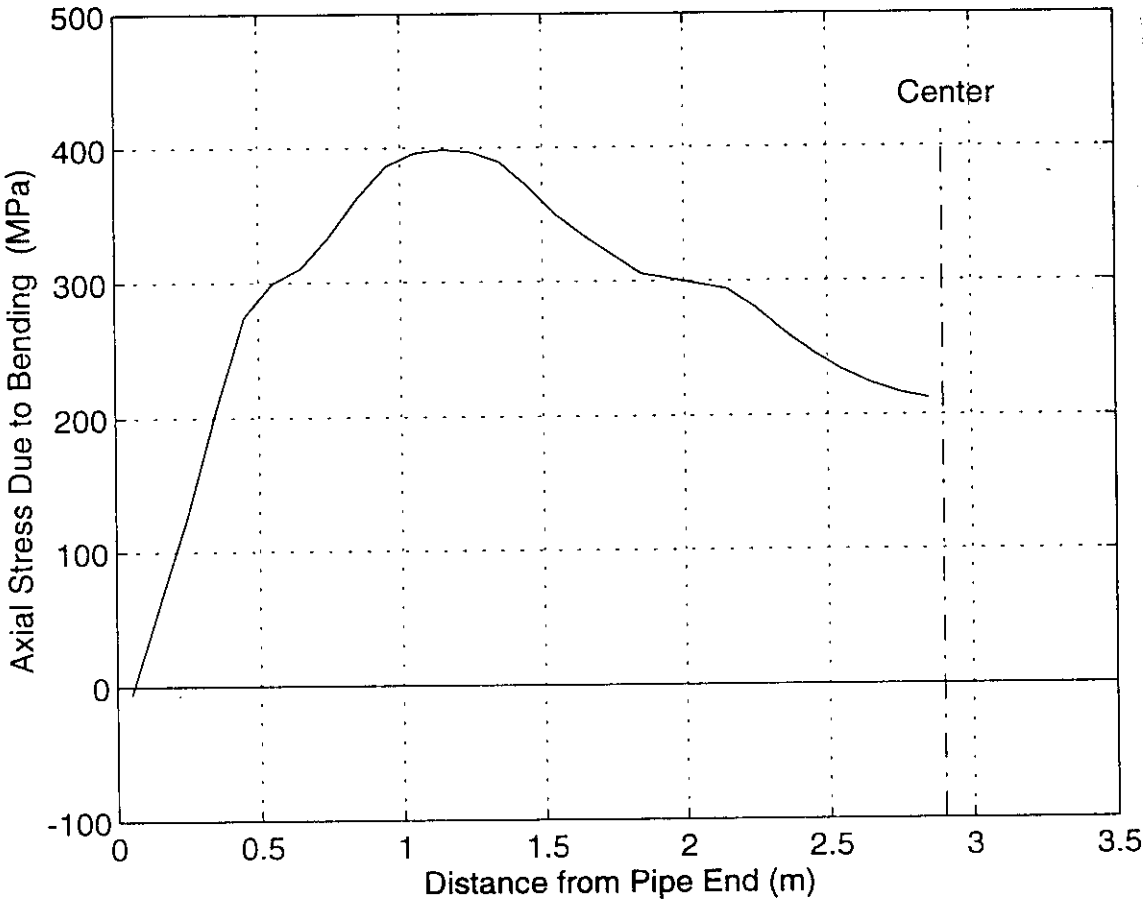
Center
Axial Stress Due to Bending (MPa)
Distance from Pipe End (m)
500
400
300
200
100
0
-100
0
0.5
1
1.5
2
2.5
3
3.5

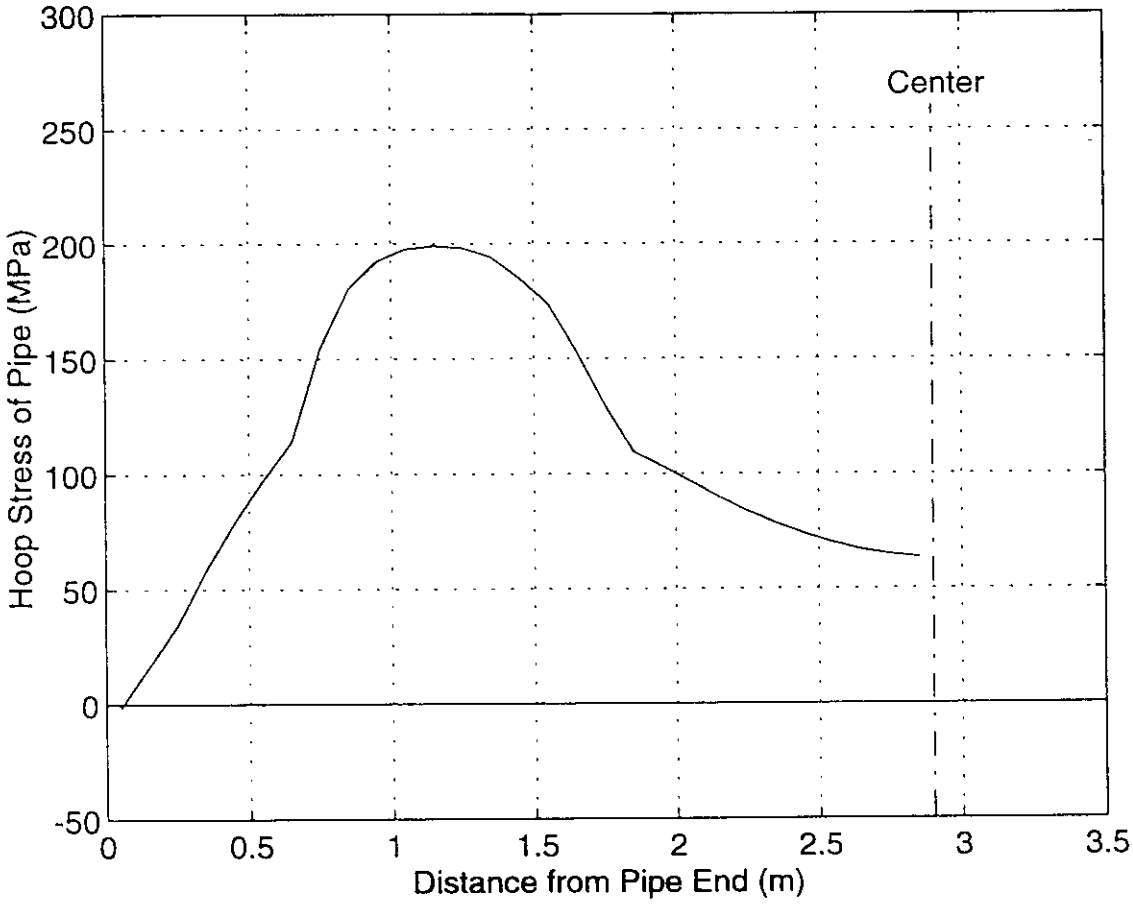
Center
Hoop Stress of Pipe (MPa)
Distance from Pipe End (m)
300
250
200
150
100
50
0
-50
0
0.5
1
1.5
2
2.5
3
3.5

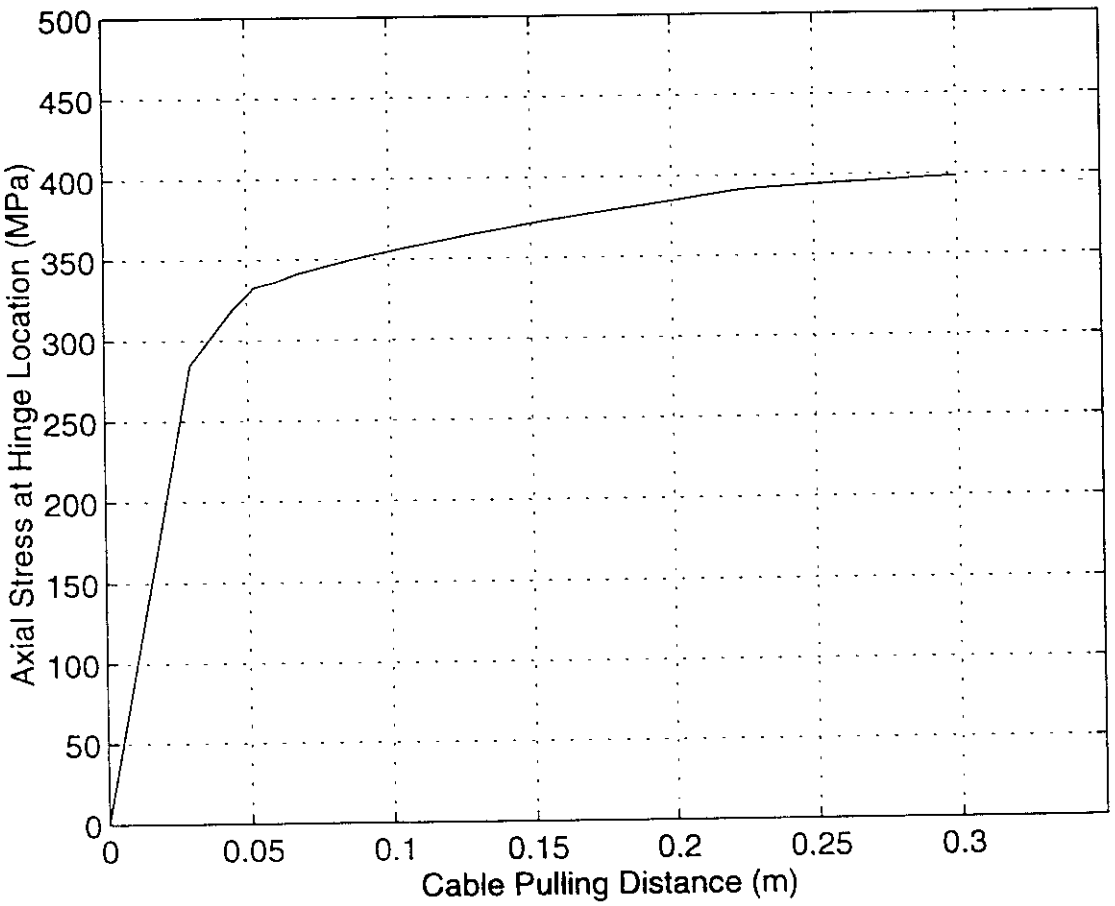
Axial Stress at Hinge Location (MPa)
500
450
400
350
300
250
200
150
100
50
0
0
0.05
0.1
0.15
0.2
0.25
0.3
Cable Pulling Distance (m)

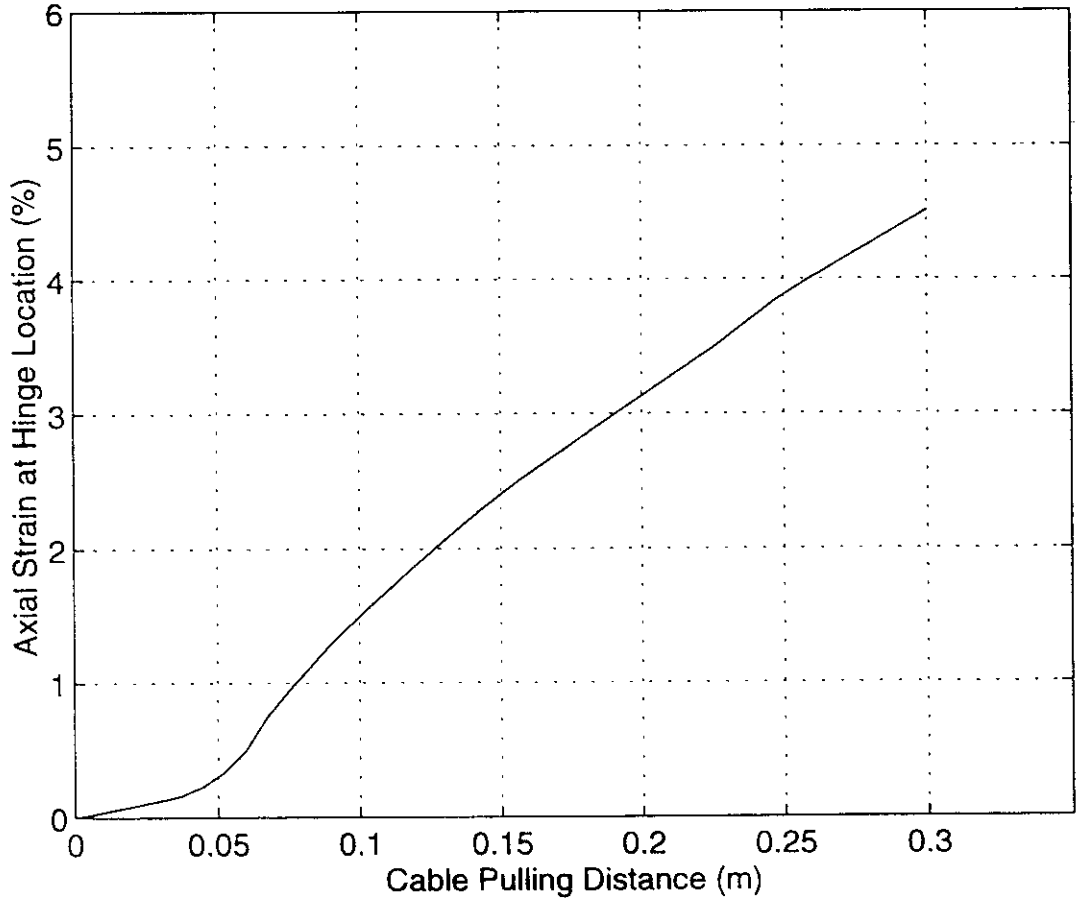
Axial Strain at Hinge Location (%)
Cable Pulling Distance (m)
0
1
2
3
4
5
6
0
0.05
0.1
0.15
0.2
0.25
0.3

Appendix B

Acoustic Surface Profiles

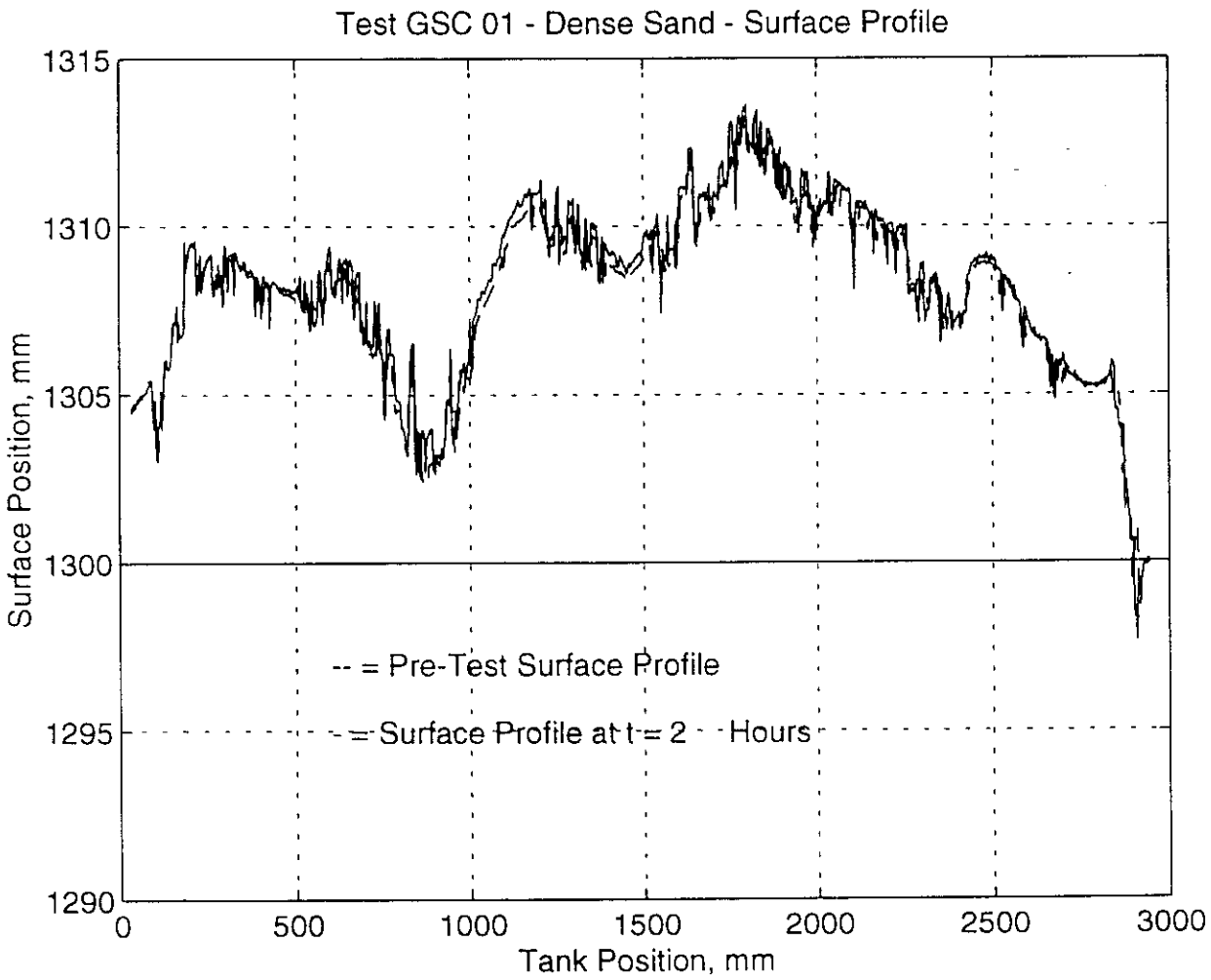
Test GSC 01 - Dense Sand - Surface Profile
Surface Position, mm
1315
1310
1305
1300
1295
1290
0
500
1000
1500
2000
2500
3000
Tank Position, mm
-- = Pre-Test Surface Profile
- = Surface Profile at t = 2 Hours

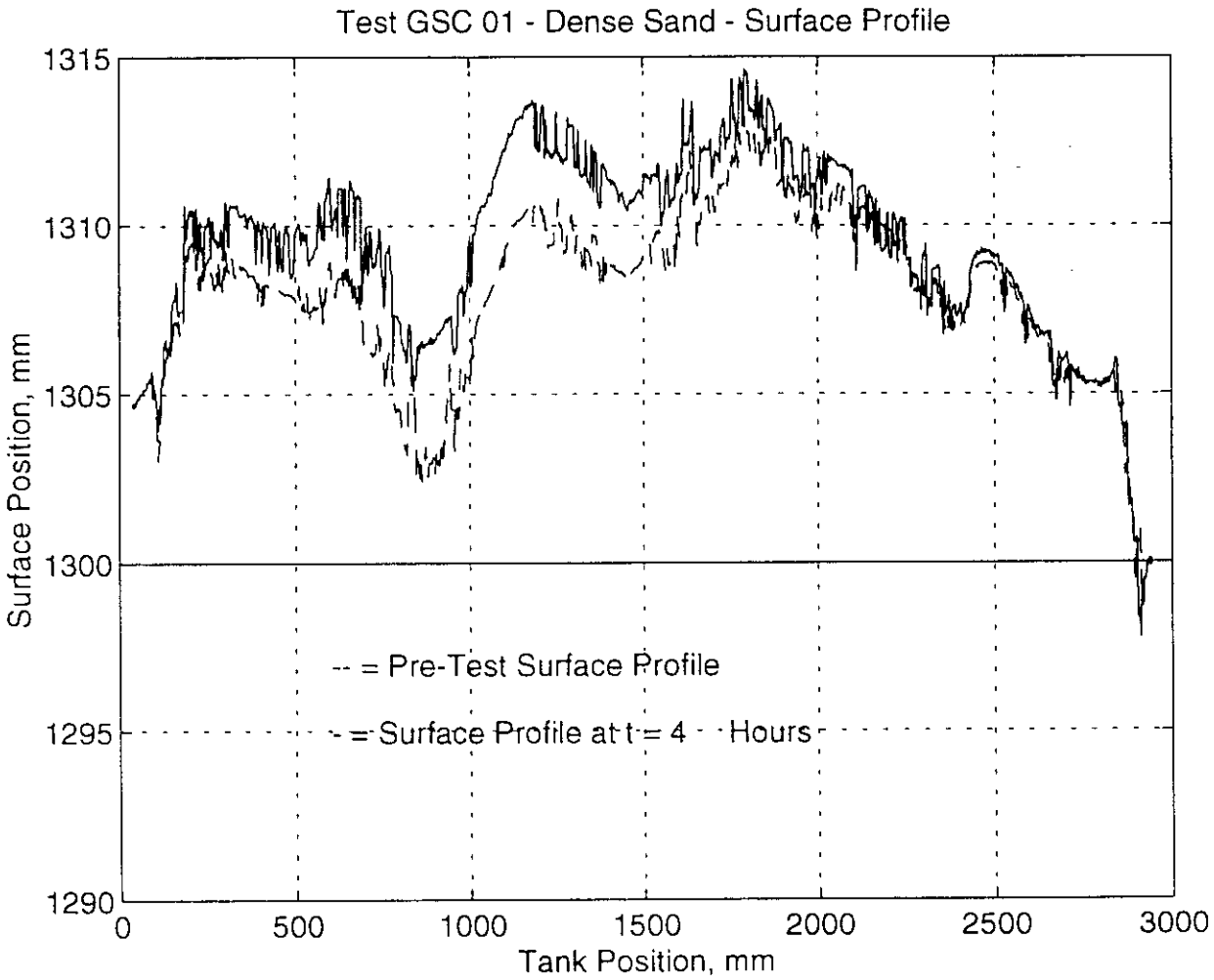
Test GSC 01 - Dense Sand - Surface Profile
Surface Position, mm
1315
1310
1305
1300
1295
1290
0
500
1000
1500
2000
2500
3000
Tank Position, mm
-- = Pre-Test Surface Profile
- = Surface Profile at t = 4 Hours

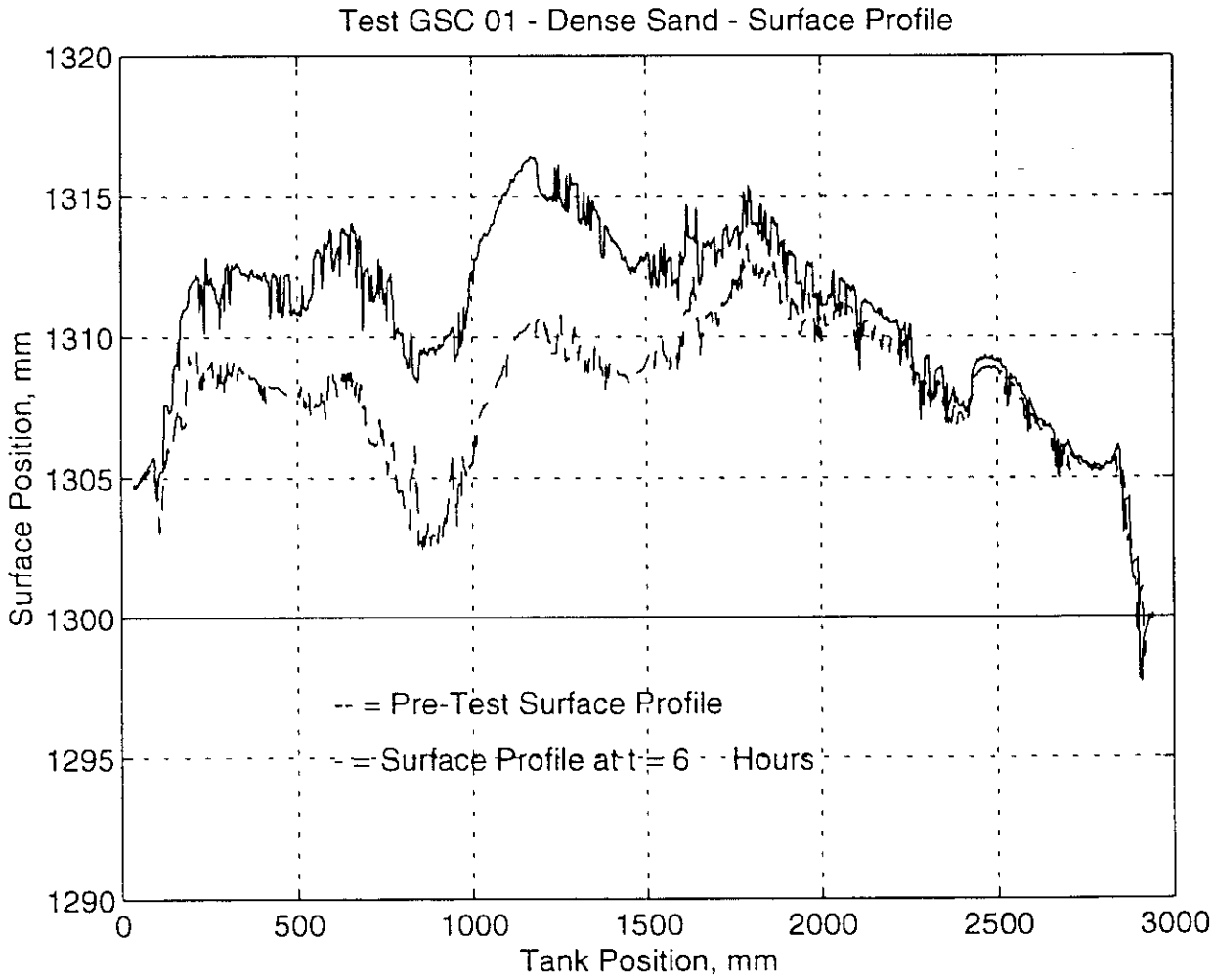
Test GSC 01 - Dense Sand - Surface Profile
Surface Position, mm
1320
1315
1310
1305
1300
1295
1290
0
500
1000
1500
2000
2500
3000
Tank Position, mm
-- = Pre-Test Surface Profile
- = Surface Profile at t = 6 Hours

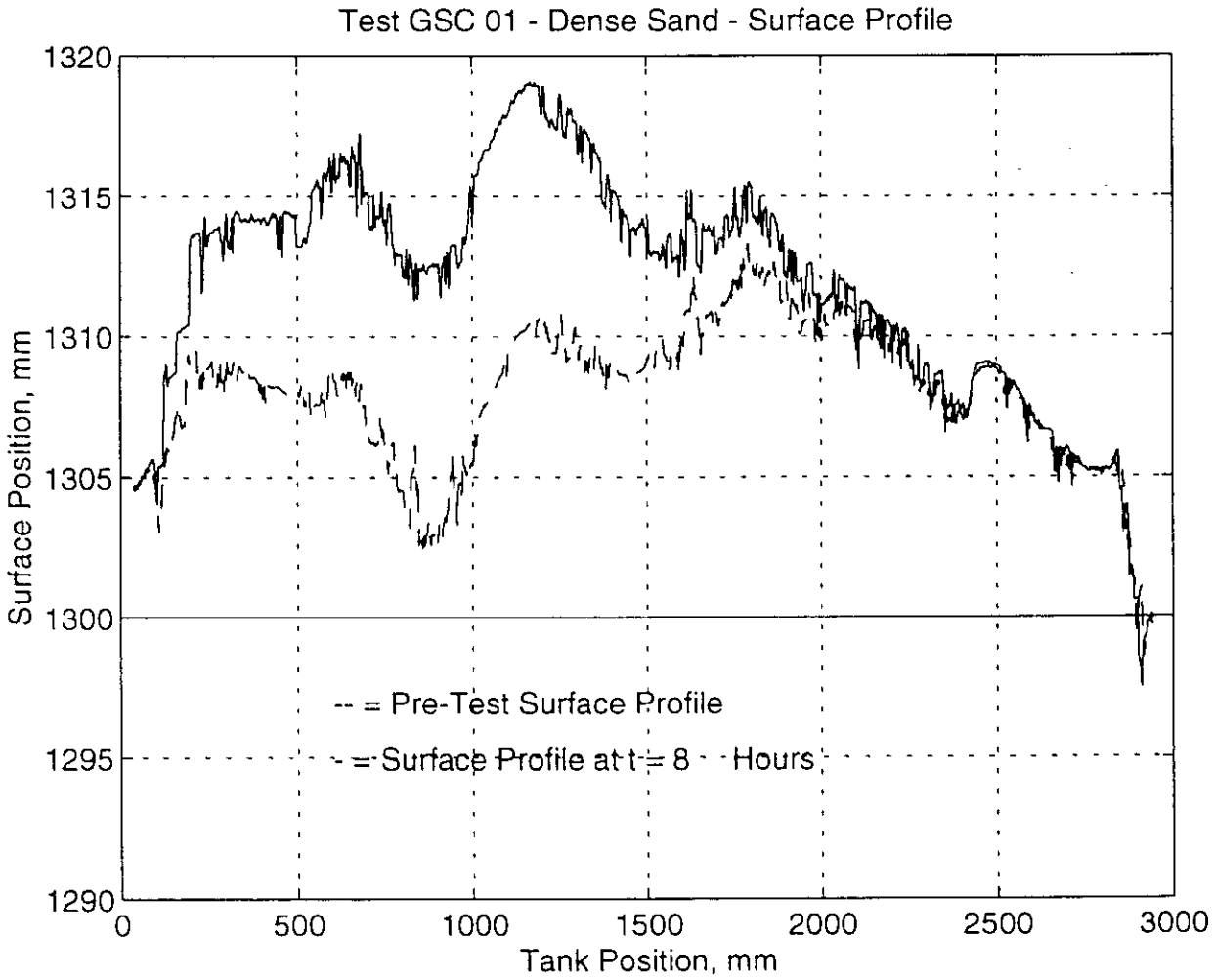
Test GSC 01 - Dense Sand - Surface Profile
Surface Position, mm
1320
1315
1310
1305
1300
1295
1290
0
500
1000
1500
2000
2500
3000
Tank Position, mm
-- = Pre-Test Surface Profile
- = Surface Profile at t = 8 Hours

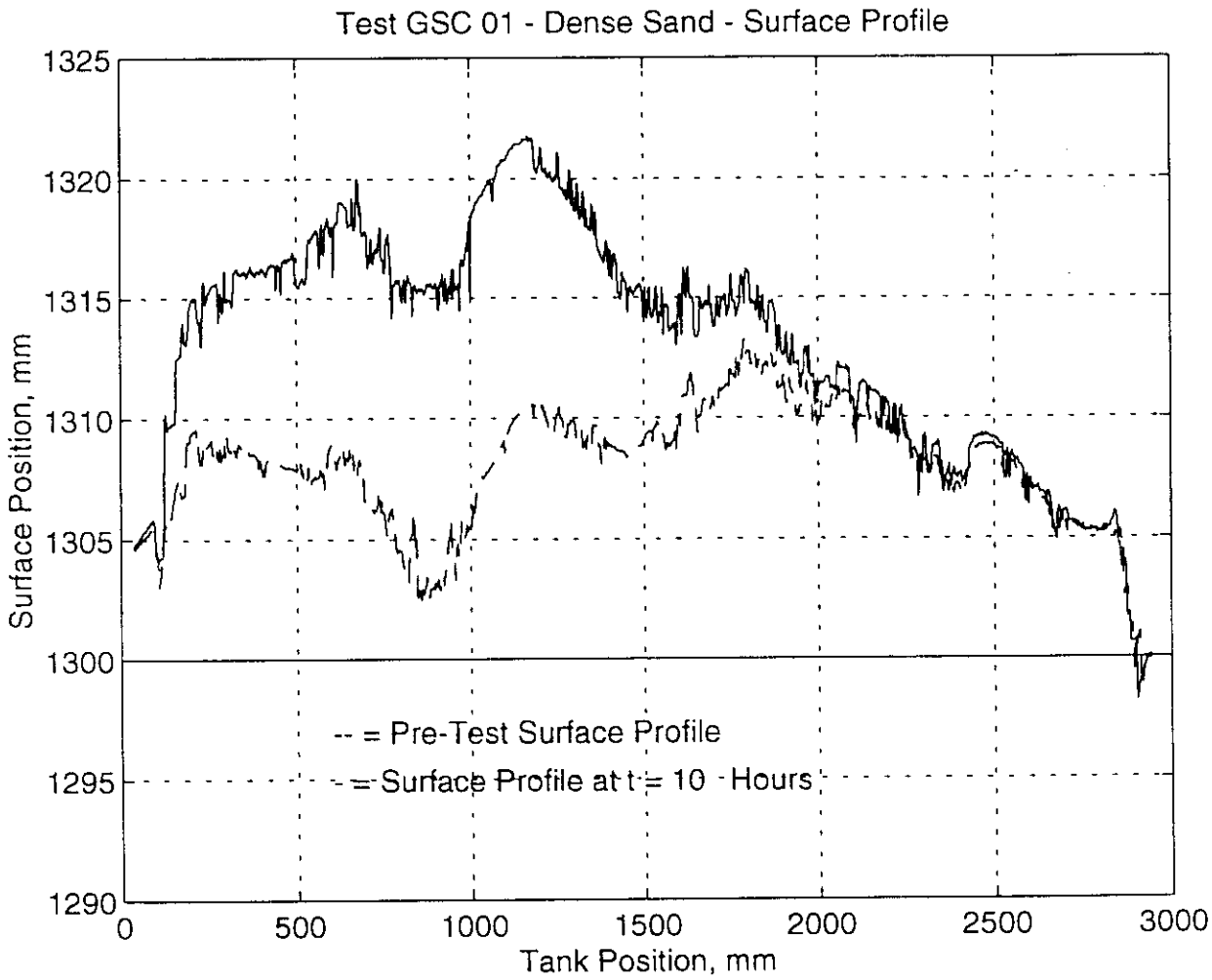
Test GSC 01 - Dense Sand - Surface Profile
Surface Position, mm
Tank Position, mm
1325
1320
1315
1310
1305
1300
1295
1290
0
500
1000
1500
2000
2500
3000
-- = Pre-Test Surface Profile
- = Surface Profile at t = 10 Hours

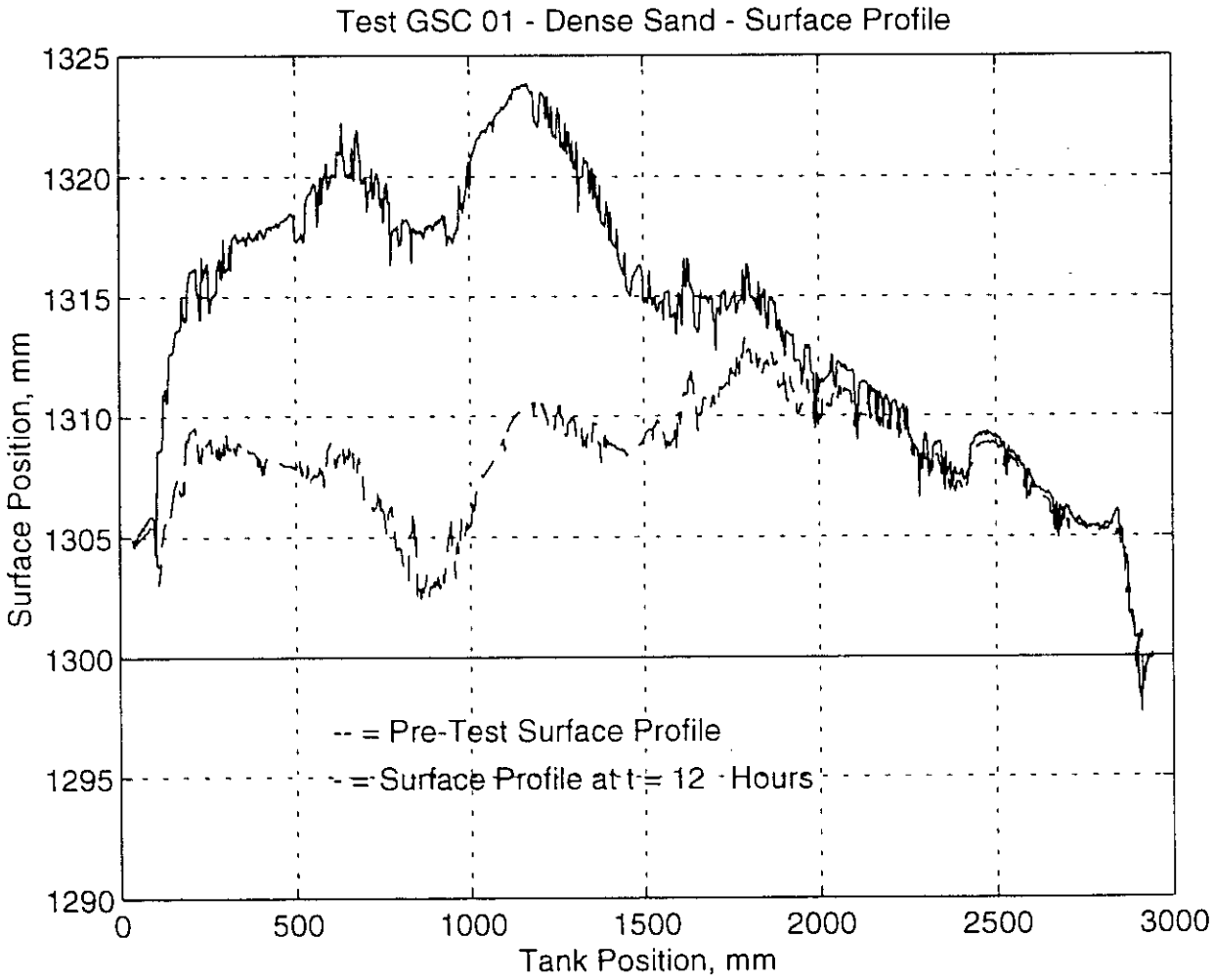
Test GSC 01 - Dense Sand - Surface Profile
Surface Position, mm
1325
1320
1315
1310
1305
1300
1295
1290
0
500
1000
1500
2000
2500
3000
Tank Position, mm
-- = Pre-Test Surface Profile
- = Surface Profile at t = 12 Hours

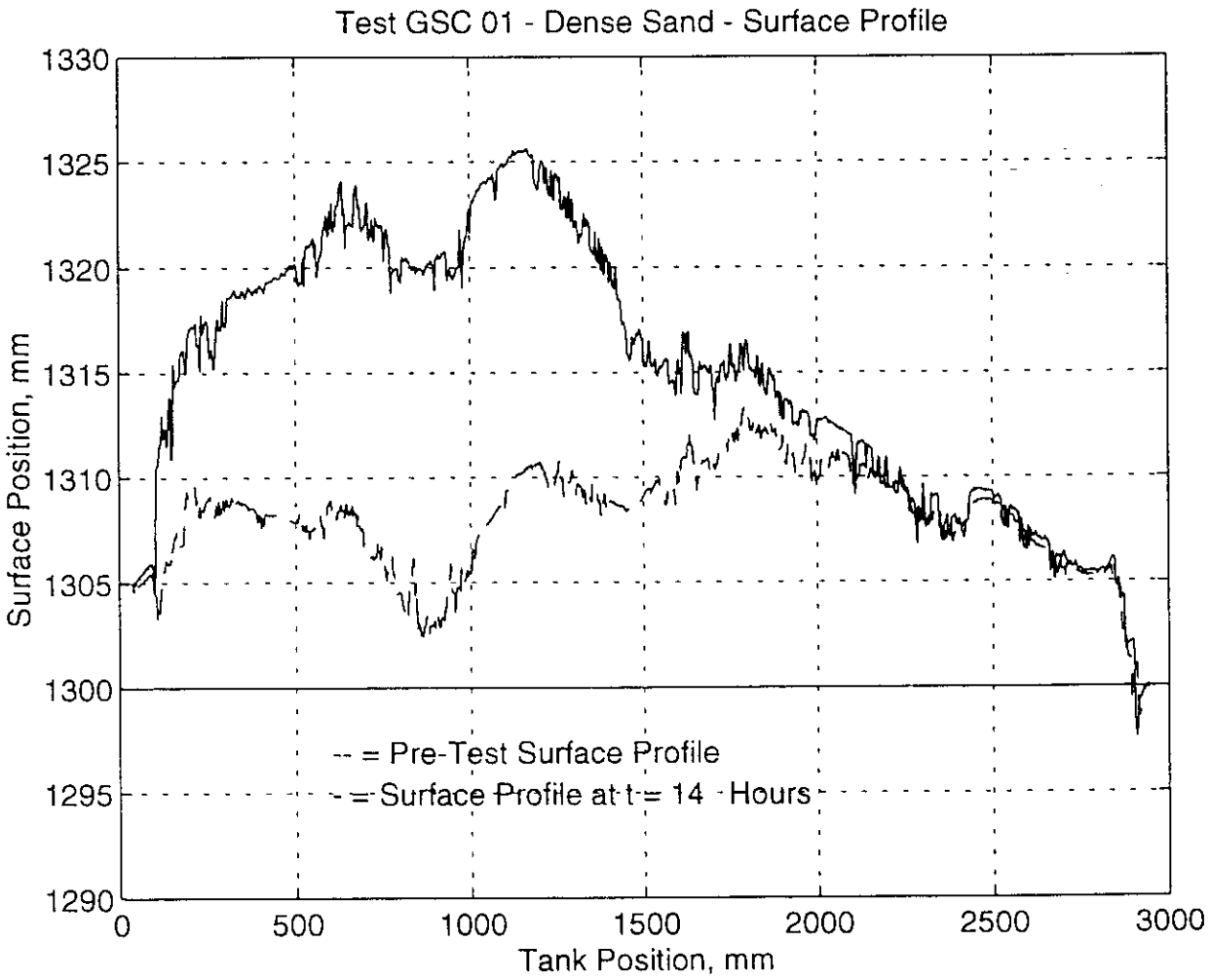
Test GSC 01 - Dense Sand - Surface Profile
Surface Position, mm
Tank Position, mm
1330
1325
1320
1315
1310
1305
1300
1295
1290
0
500
1000
1500
2000
2500
3000
-- = Pre-Test Surface Profile
- = Surface Profile at t = 14 Hours

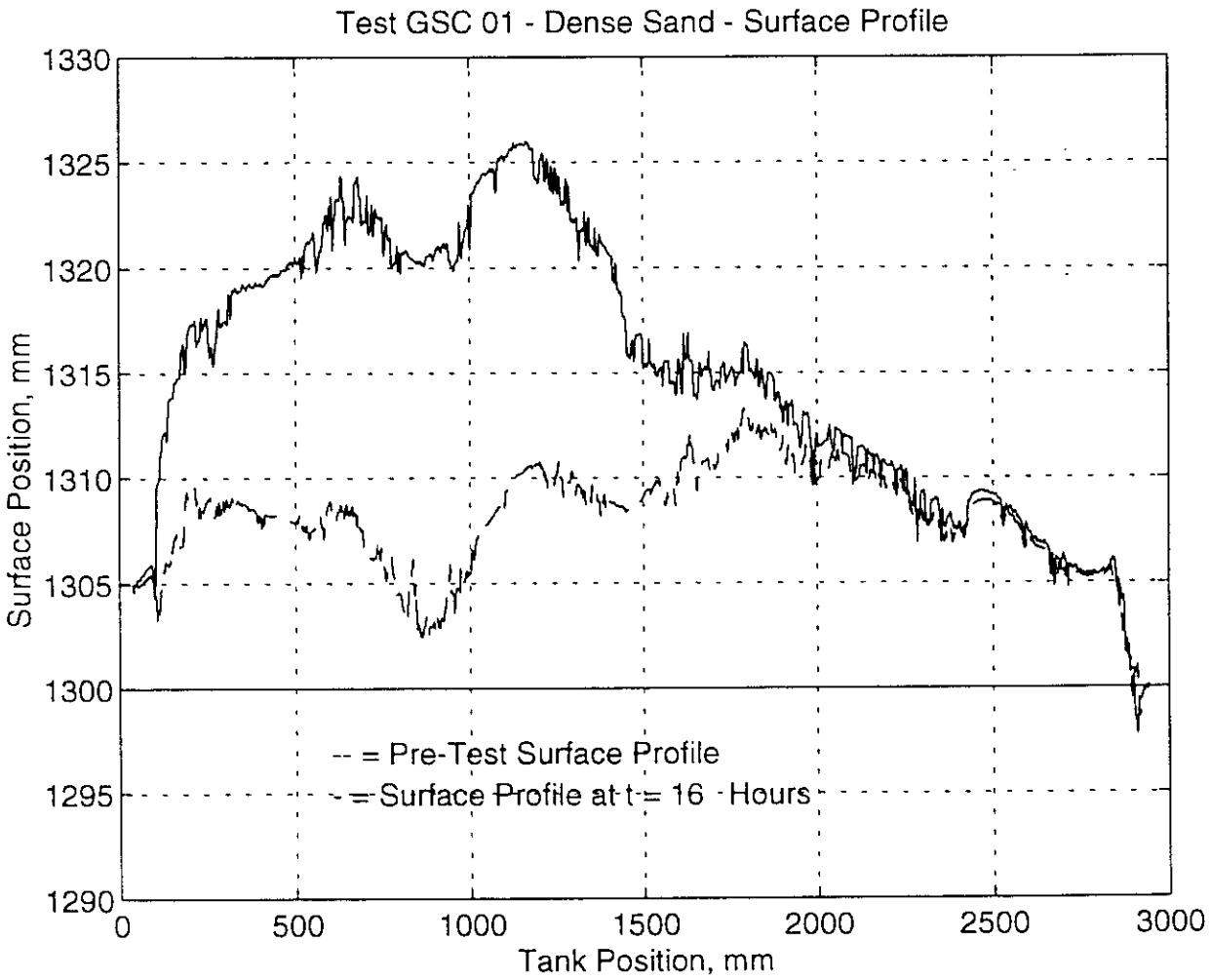
Test GSC 01 - Dense Sand - Surface Profile
Surface Position, mm
Tank Position, mm
1330
1325
1320
1315
1310
1305
1300
1295
1290
0
500
1000
1500
2000
2500
3000
-- = Pre-Test Surface Profile
- = Surface Profile at t = 16 Hours

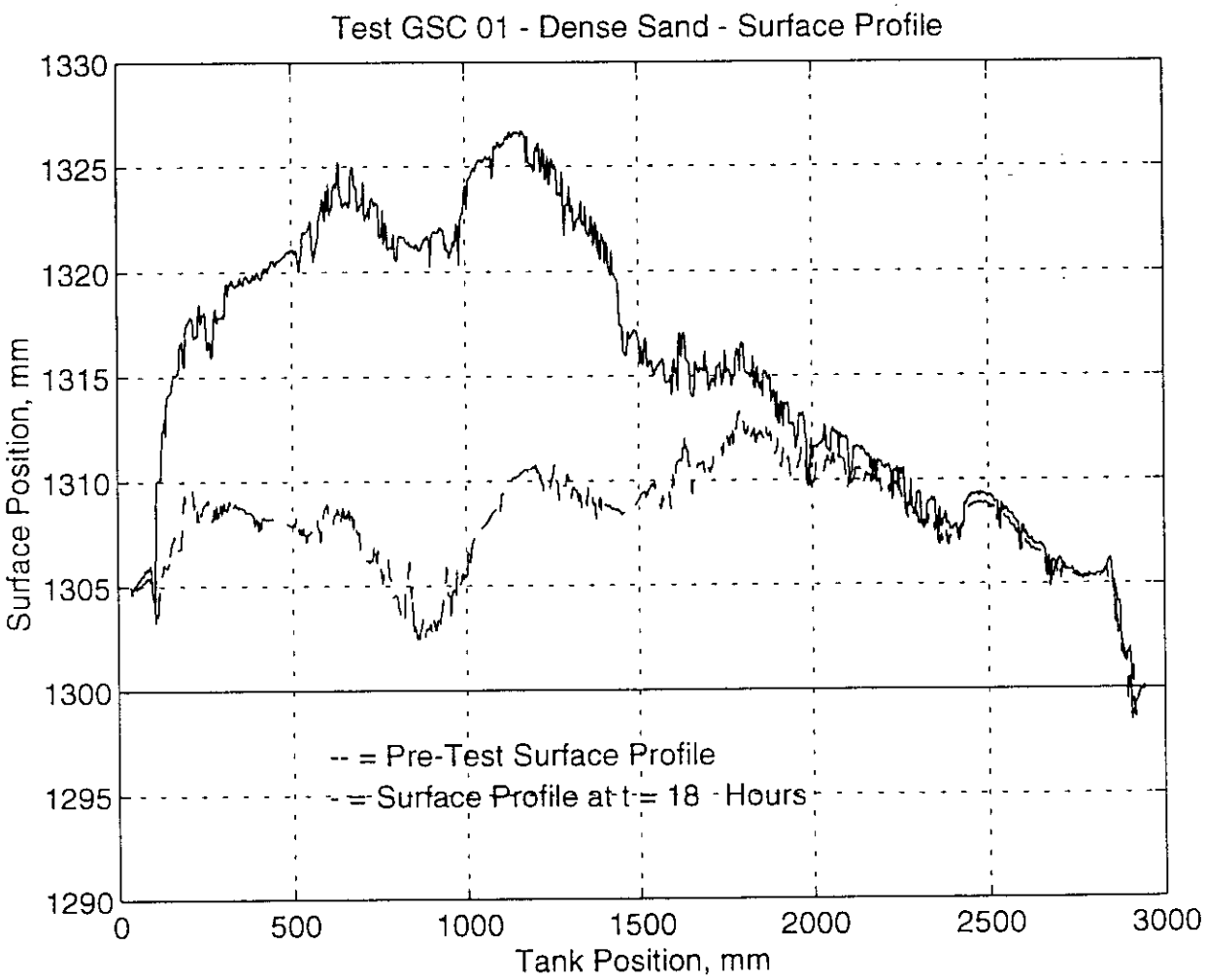
Test GSC 01 - Dense Sand - Surface Profile
Surface Position, mm
Tank Position, mm
1330
1325
1320
1315
1310
1305
1300
1295
1290
0
500
1000
1500
2000
2500
3000
-- = Pre-Test Surface Profile
- = Surface Profile at t = 18 Hours

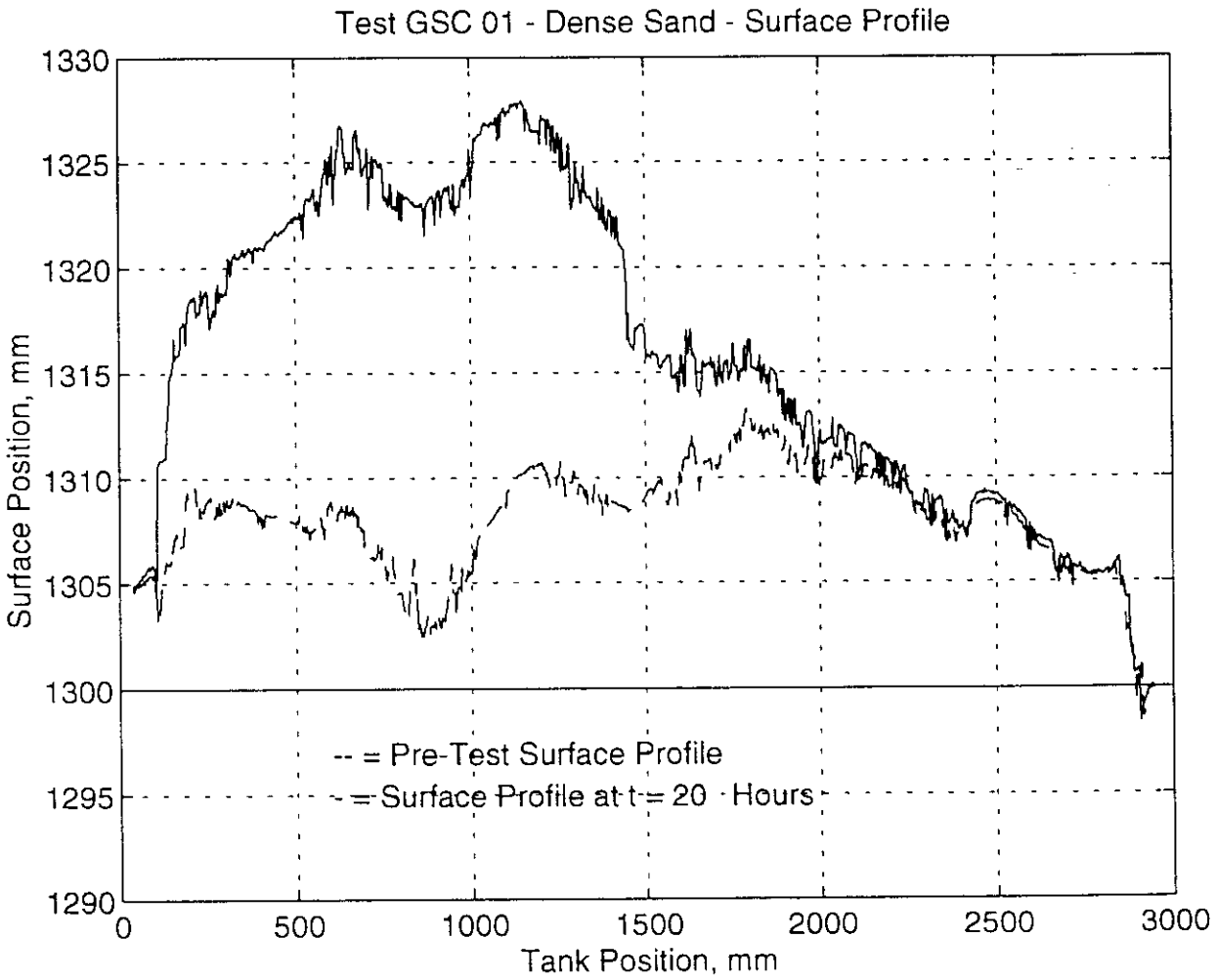
Test GSC 01 - Dense Sand - Surface Profile
Surface Position, mm
Tank Position, mm
1330
1325
1320
1315
1310
1305
1300
1295
1290
0
500
1000
1500
2000
2500
3000
-- = Pre-Test Surface Profile
- = Surface Profile at t = 20 Hours

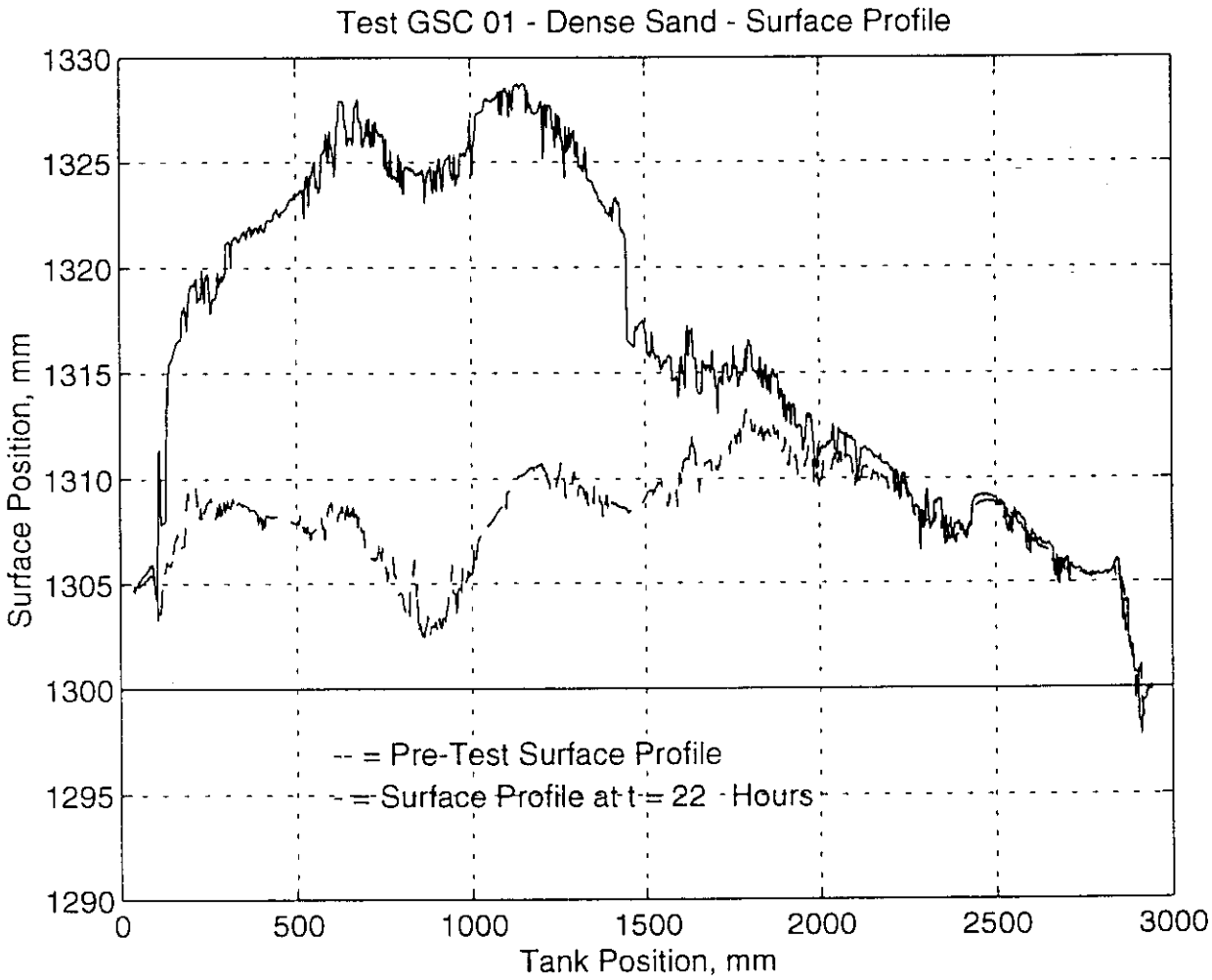
Test GSC 01 - Dense Sand - Surface Profile
Surface Position, mm
Tank Position, mm
1330
1325
1320
1315
1310
1305
1300
1295
1290
0
500
1000
1500
2000
2500
3000
-- = Pre-Test Surface Profile
- = Surface Profile at t = 22 Hours

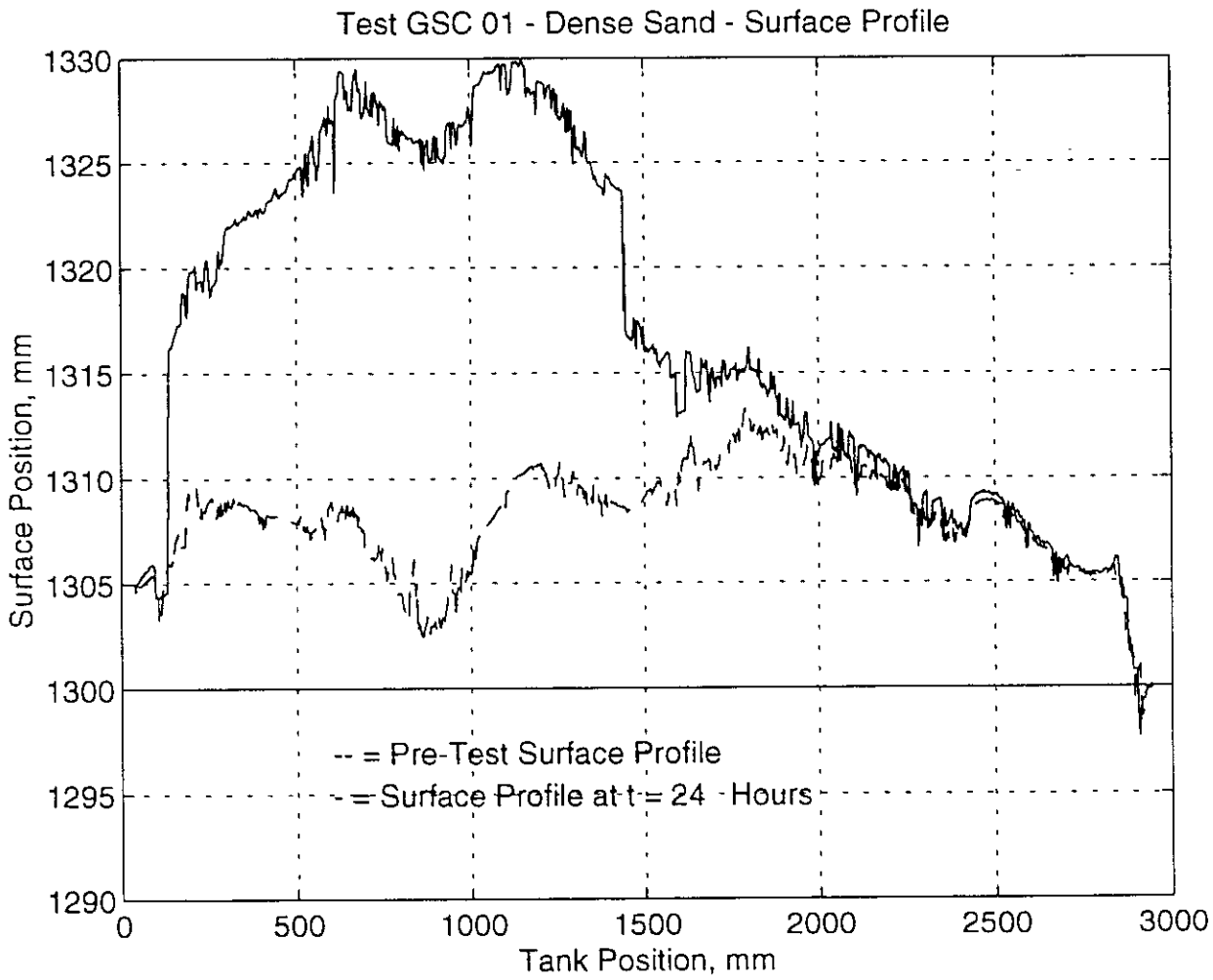
Test GSC 01 - Dense Sand - Surface Profile
Surface Position, mm
Tank Position, mm
1330
1325
1320
1315
1310
1305
1300
1295
1290
0
500
1000
1500
2000
2500
3000
-- = Pre-Test Surface Profile
- = Surface Profile at t = 24 Hours

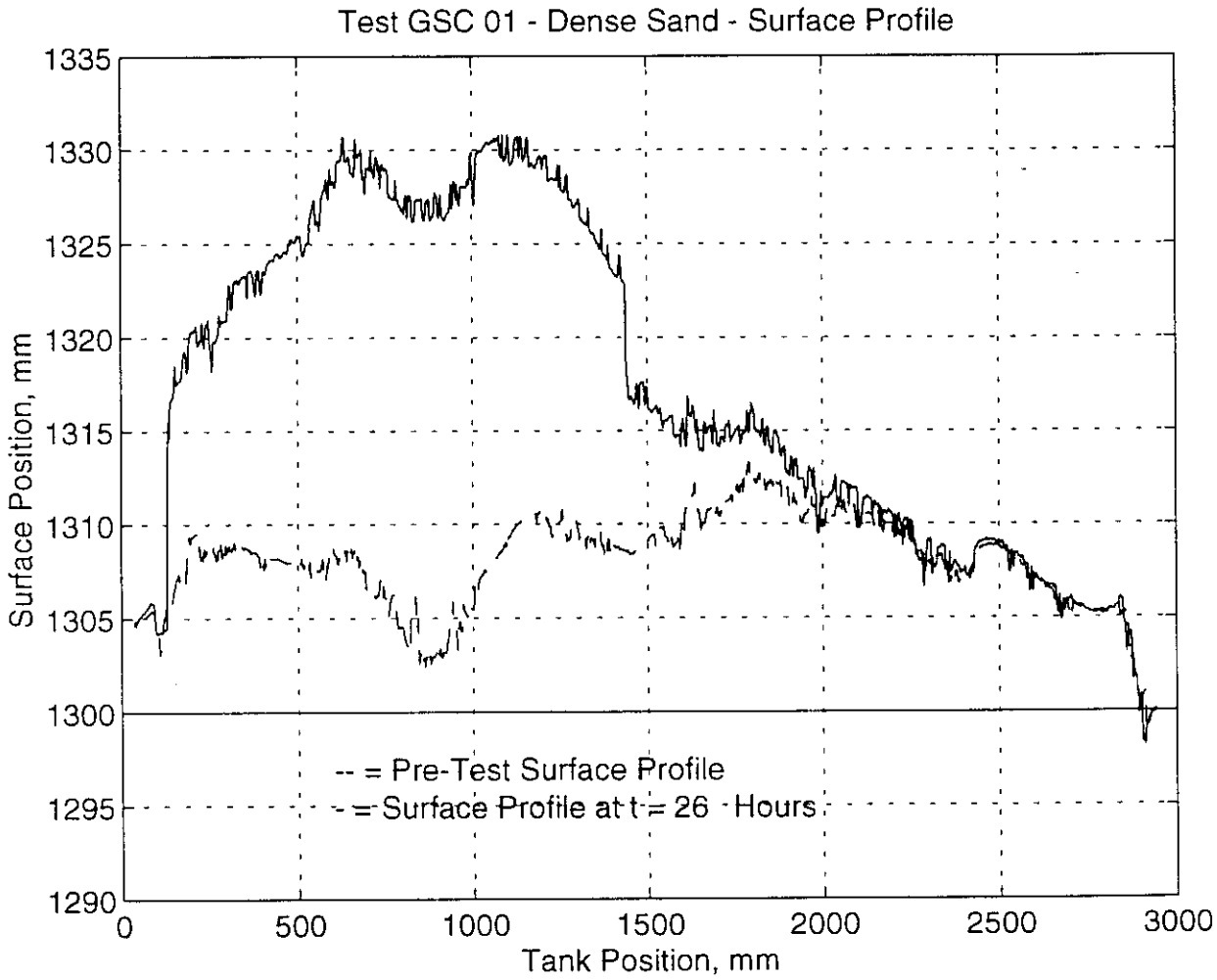
Test GSC 01 - Dense Sand - Surface Profile
Surface Position, mm
Tank Position, mm
1335
1330
1325
1320
1315
1310
1305
1300
1295
1290
0
500
1000
1500
2000
2500
3000
-- = Pre-Test Surface Profile
- = Surface Profile at t = 26 Hours

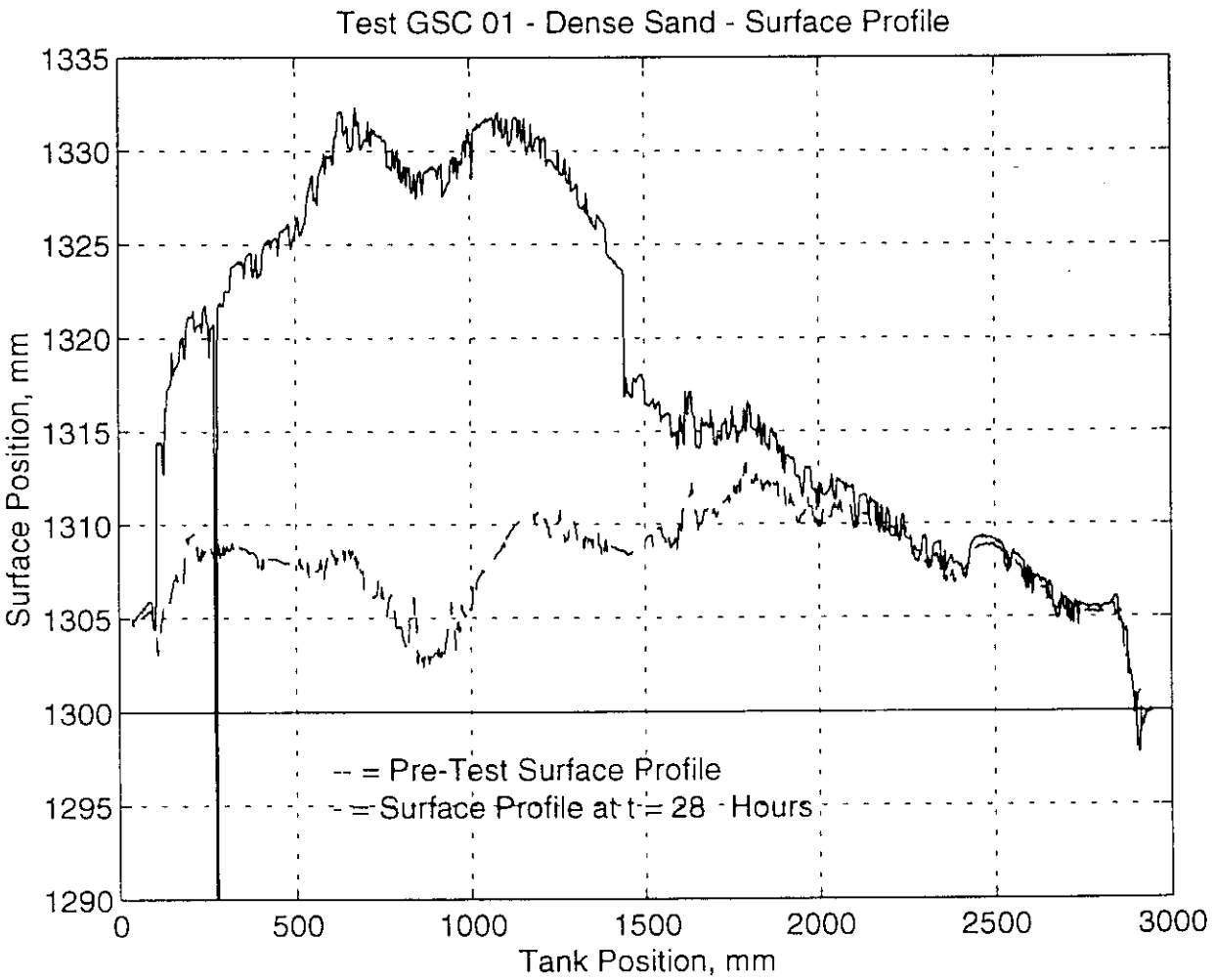
Test GSC 01 - Dense Sand - Surface Profile
Surface Position, mm
Tank Position, mm
1335
1330
1325
1320
1315
1310
1305
1300
1295
1290
0
500
1000
1500
2000
2500
3000
-- = Pre-Test Surface Profile
- = Surface Profile at t = 28 Hours

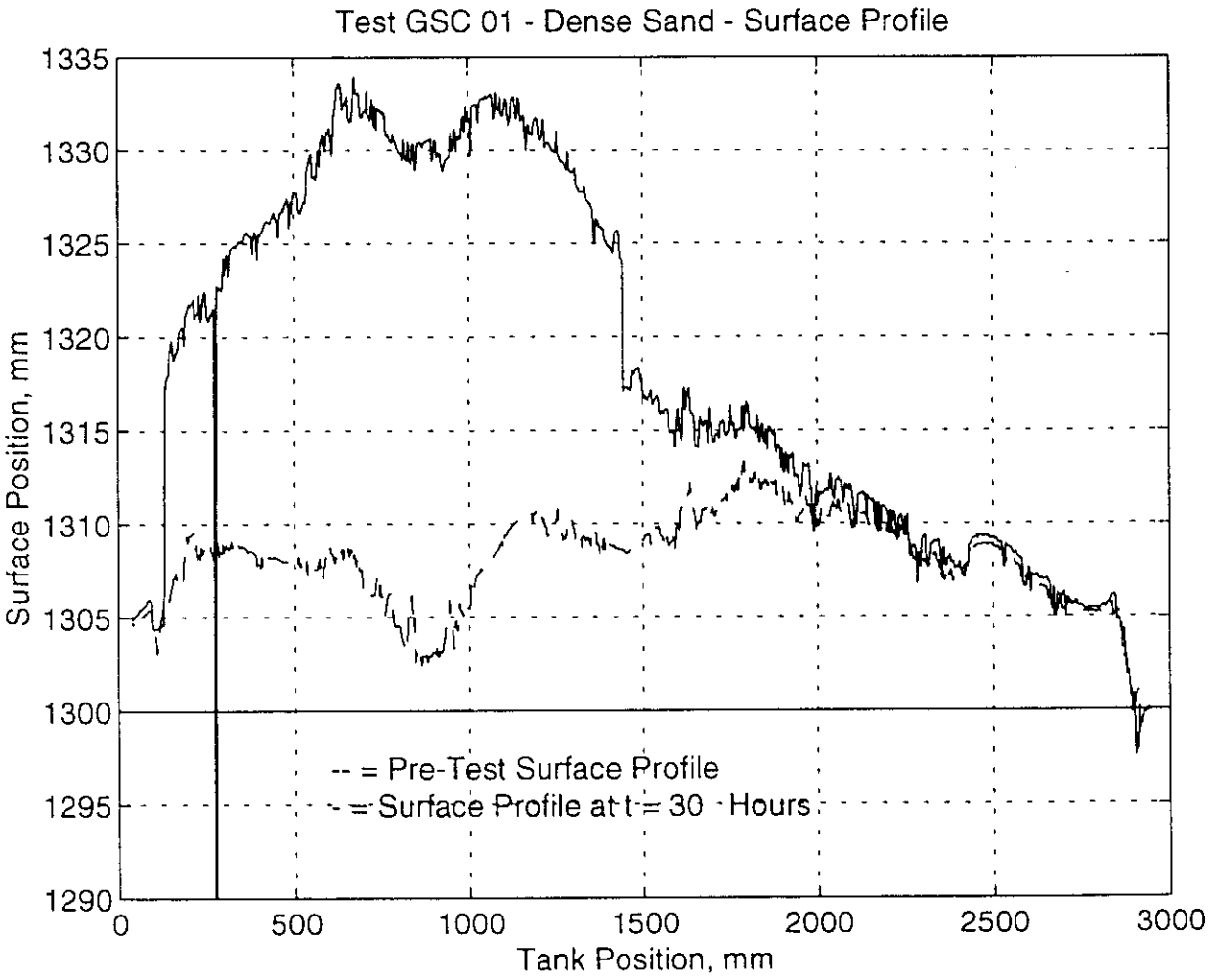
Test GSC 01 - Dense Sand - Surface Profile
Surface Position, mm
Tank Position, mm
1335
1330
1325
1320
1315
1310
1305
1300
1295
1290
0
500
1000
1500
2000
2500
3000
-- = Pre-Test Surface Profile
- = Surface Profile at t = 30 Hours

Appendix C

Tecnotest Probe Data

Tecnotest Probe Data - Test GSC01 - Post Test - June 16, 1998.

Cone Diameter: 35.7 mm Soil Density: 1792 kg/m^3

Tank Position: X = 1300 mm Y = 3425 mm **Test #1**

Activity	Initial Soil to Ref. (mm)	Final Soil to Ref. (mm)	Penetration (mm)	Cumulative Penetration (mm)	SPT Blow Count	Blows per 100 mm	Comments
Insert Probe	1223	1048	175	175	N/A	N/A	Probe penetration under self weight
SPT #1	1048	942	106	281	5	4.72	
SPT #2	942	841	101	382	14	13.86	
SPT #3	841	740	101	483	24	23.76	
SPT #4	740	641	99	582	34	34.34	
SPT #5	641	538	103	685	39	37.86	
SPT #6	538	439	99	784	43	43.43	
SPT #7	439	344	95	879	46	48.42	

Tank Position: X = 2365 mm Y = 3427 mm **Test #2**

Activity	Initial Soil to Ref. (mm)	Final Soil to Ref. (mm)	Penetration (mm)	Cumulative Penetration (mm)	SPT Blow Count	Blows per 100 mm	Comments
Insert Probe	1222	1057	165	165	N/A	N/A	Probe Penetration under self weight
SPT #1	1057	941	116	281	6	5.17	
SPT #2	941	835	106	387	16	15.09	
SPT #3	835	736	99	486	26	26.26	
SPT #4	736	638	98	584	34	34.69	
SPT #5	638	539	99	683	41	41.41	
SPT #6	539	437	102	785	50	49.02	
SPT #7	437	336	101	886	55	54.46	

Tecnotest Probe Data - Test GSC01 - Post Test - June 16, 1998.

Cone Diameter: 35.7 mm Soil Density: 1792 kg/m^3

Tank Position: X = 1898 Y = 4625 mm **Test #3**

Activity	Initial Soil to Ref. (mm)	Final Soil to Ref. (mm)	Penetration (mm)	Cumulative Penetration (mm)	SPT Blow Count	Blows per 100 mm	Comments
Insert Probe	1224	1051	173	173	N/A	N/A	Probe penetration under self weight
SPT #1	1051	936	115	288	7	6.09	
SPT #2	936	835	101	389	15	14.85	
SPT #3	835	735	100	489	25	25.00	
SPT #4	735	637	98	587	34	34.69	
SPT #5	637	535	102	689	44	43.14	
SPT #6	535	436	99	788	50	50.51	
SPT #7	436	338	98	886	57	58.16	

Tank Position: X = 2335 Y = 1732 mm **Test #4**

Activity	Initial Soil to Ref. (mm)	Final Soil to Ref. (mm)	Penetration (mm)	Cumulative Penetration (mm)	SPT Blow Count	Blows per 100 mm	Comments
Insert Probe	1220	1048	172	172	N/A	N/A	Probe penetration under self weight
SPT #1	1048	937	111	283	6	5.41	
SPT #2	937	833	104	387	16	15.38	
SPT #3	833	735	98	485	25	25.51	
SPT #4	735	636	99	584	33	33.33	
SPT #5	636	535	101	685	43	42.57	
SPT #6	535	435	100	785	47	47.00	
SPT #7	435	335	100	885	50	50.00	

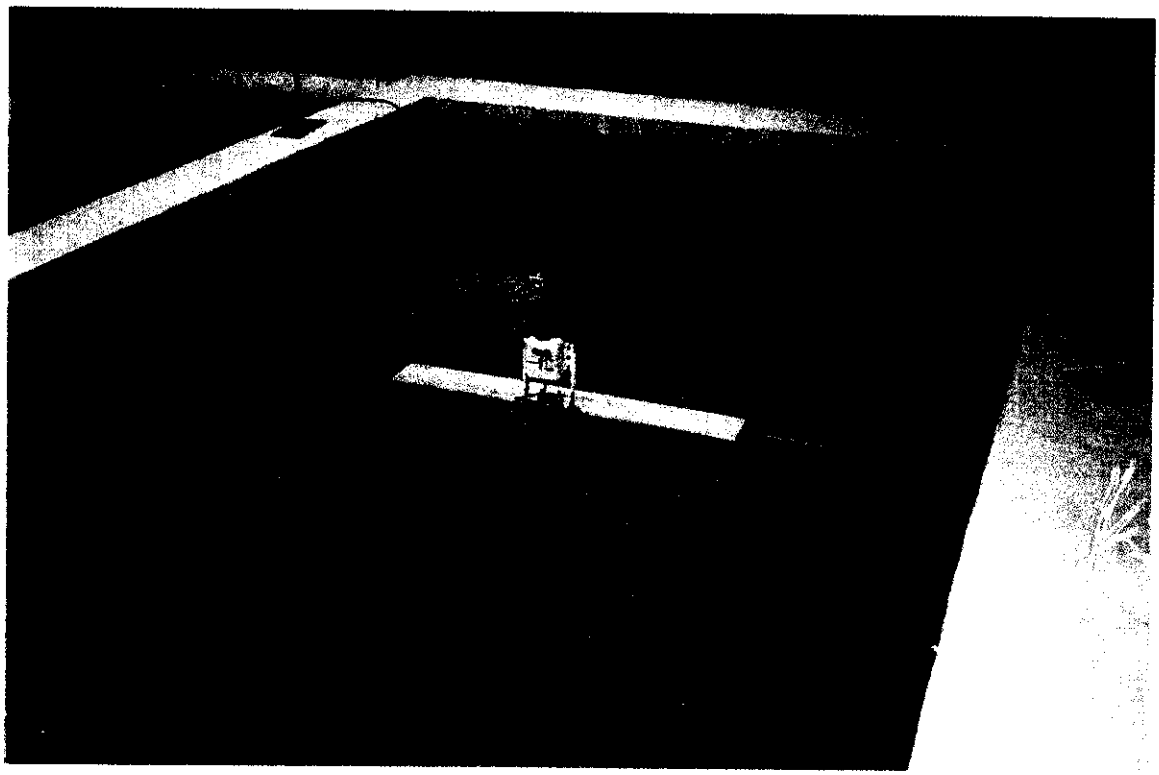

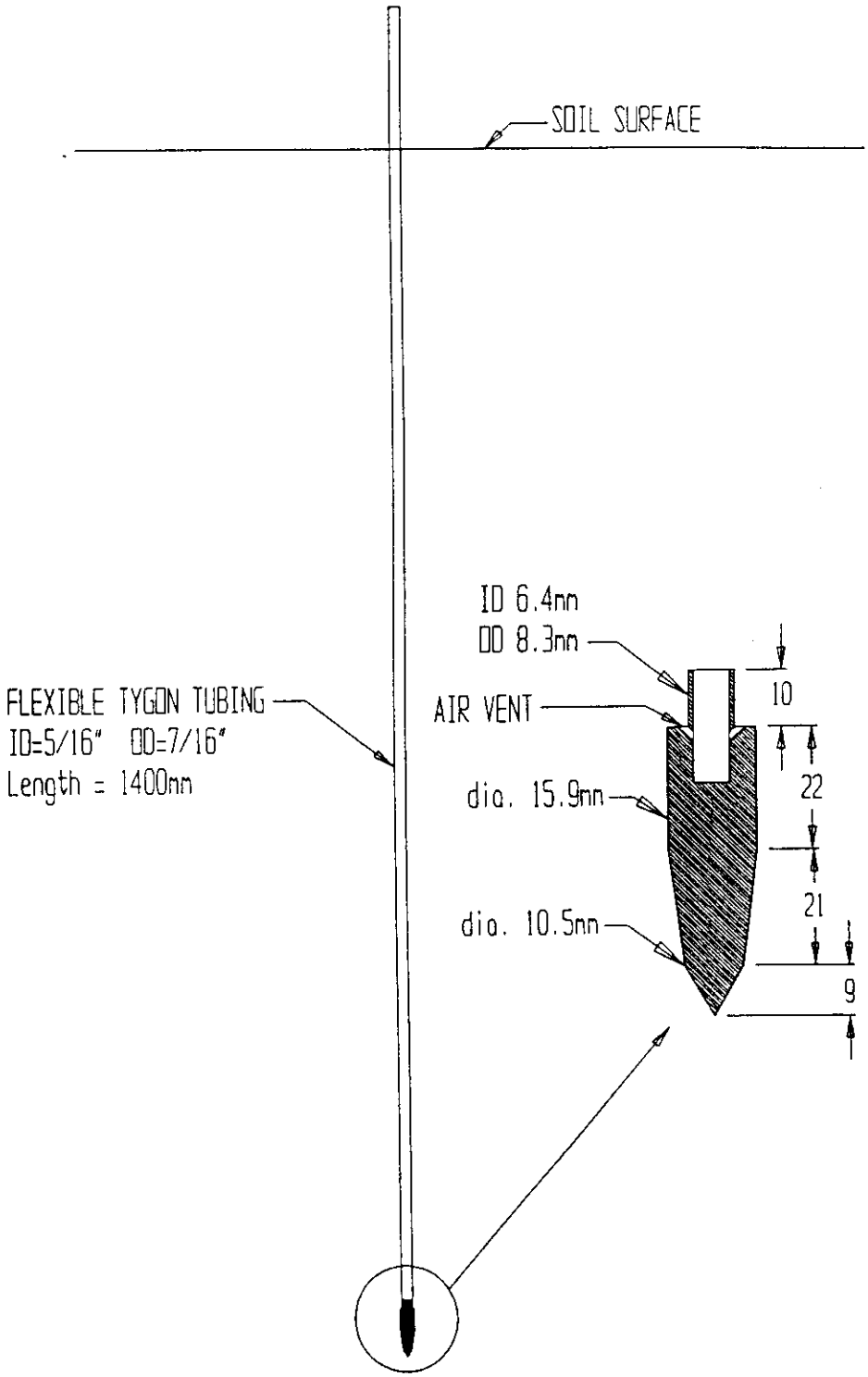
SOIL SURFACE
ID 6.4mm
OD 8.3mm
AIR VENT
FLEXIBLE TYGON TUBING
ID=5/16" OD=7/16"
Length = 1400mm
dia. 15.9mm
dia. 10.5mm
10
22
21
9

C-CORE

Vertical Deformation Tube Placement
Profile View

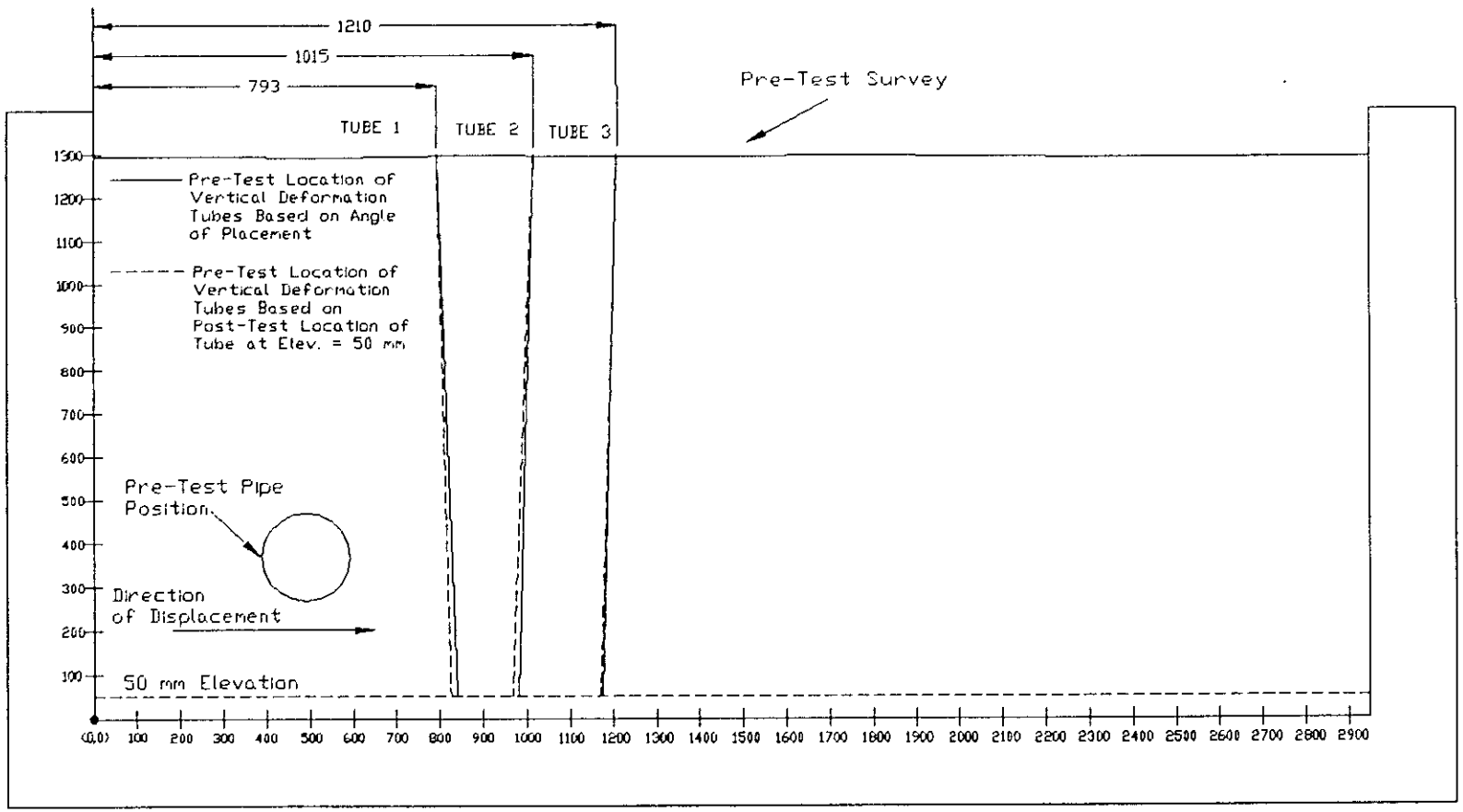

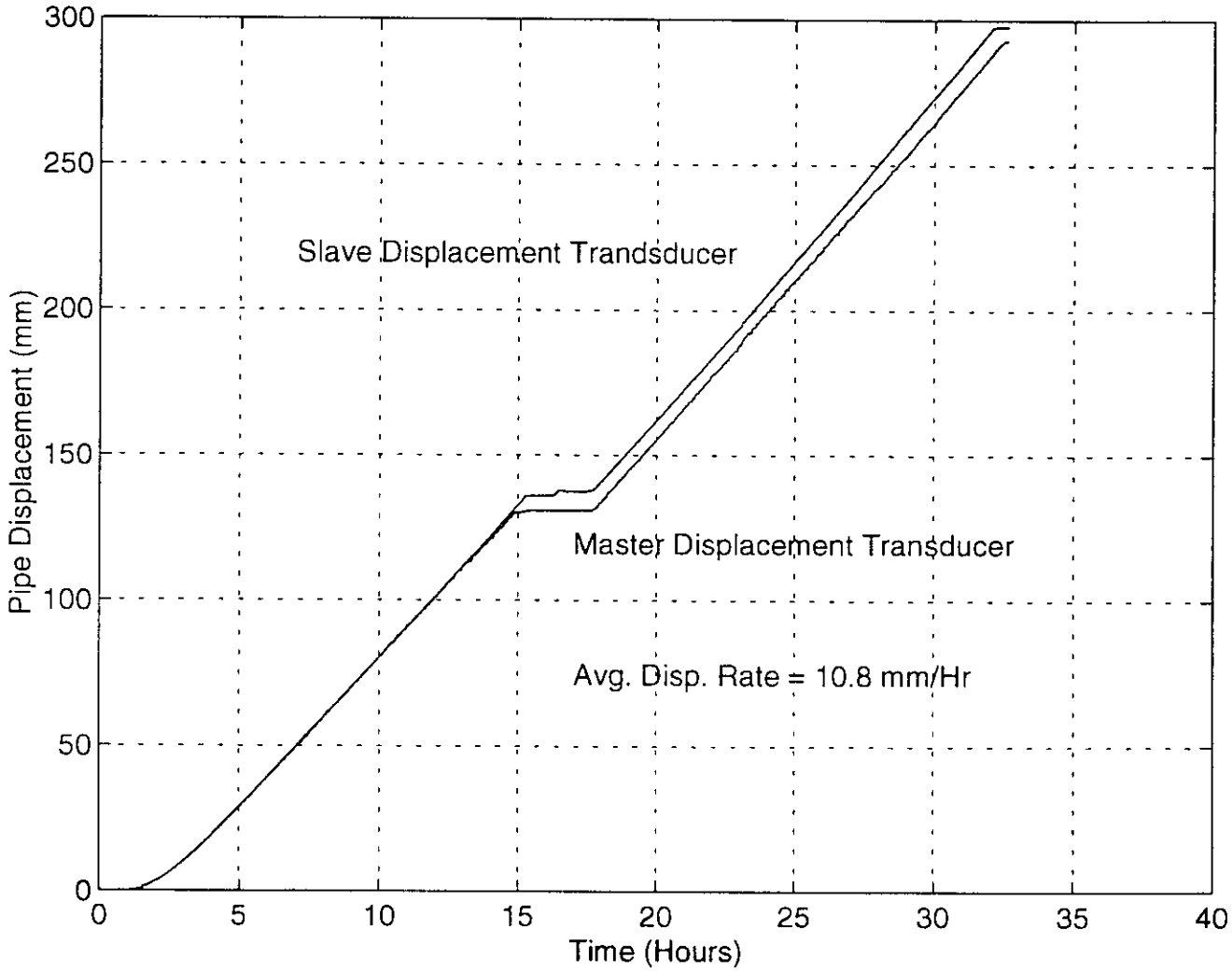
300
250
200
150
100
50
0
Pipe Displacement (mm)
0
5
10
15
20
25
30
35
40
Time (Hours)
Slave Displacement Trandsducer
Master Displacement Transducer
Avg. Disp. Rate = 10.8 mm/Hr

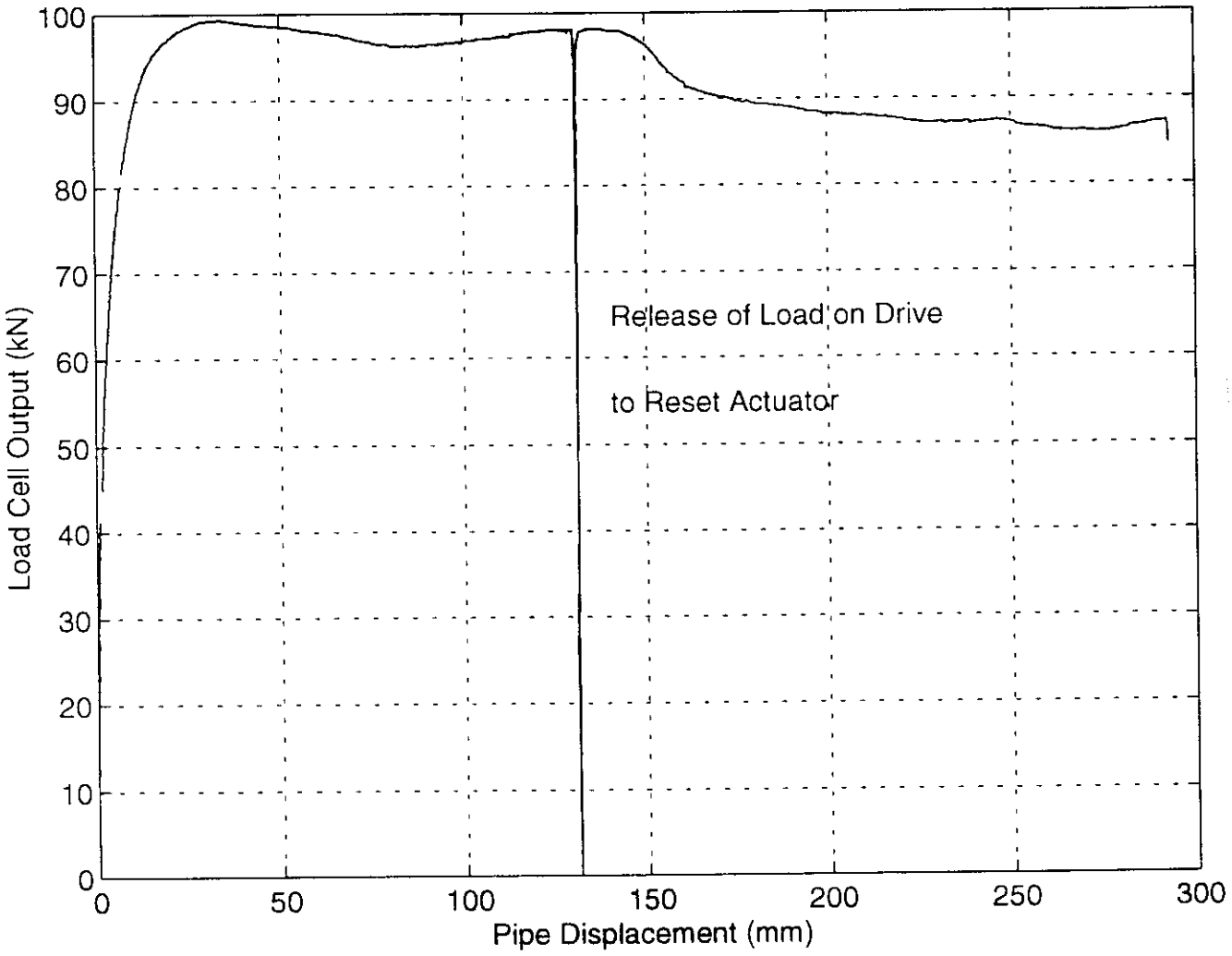

C-CORE

Load vs. Displacement - Master Load Cell

13(a)

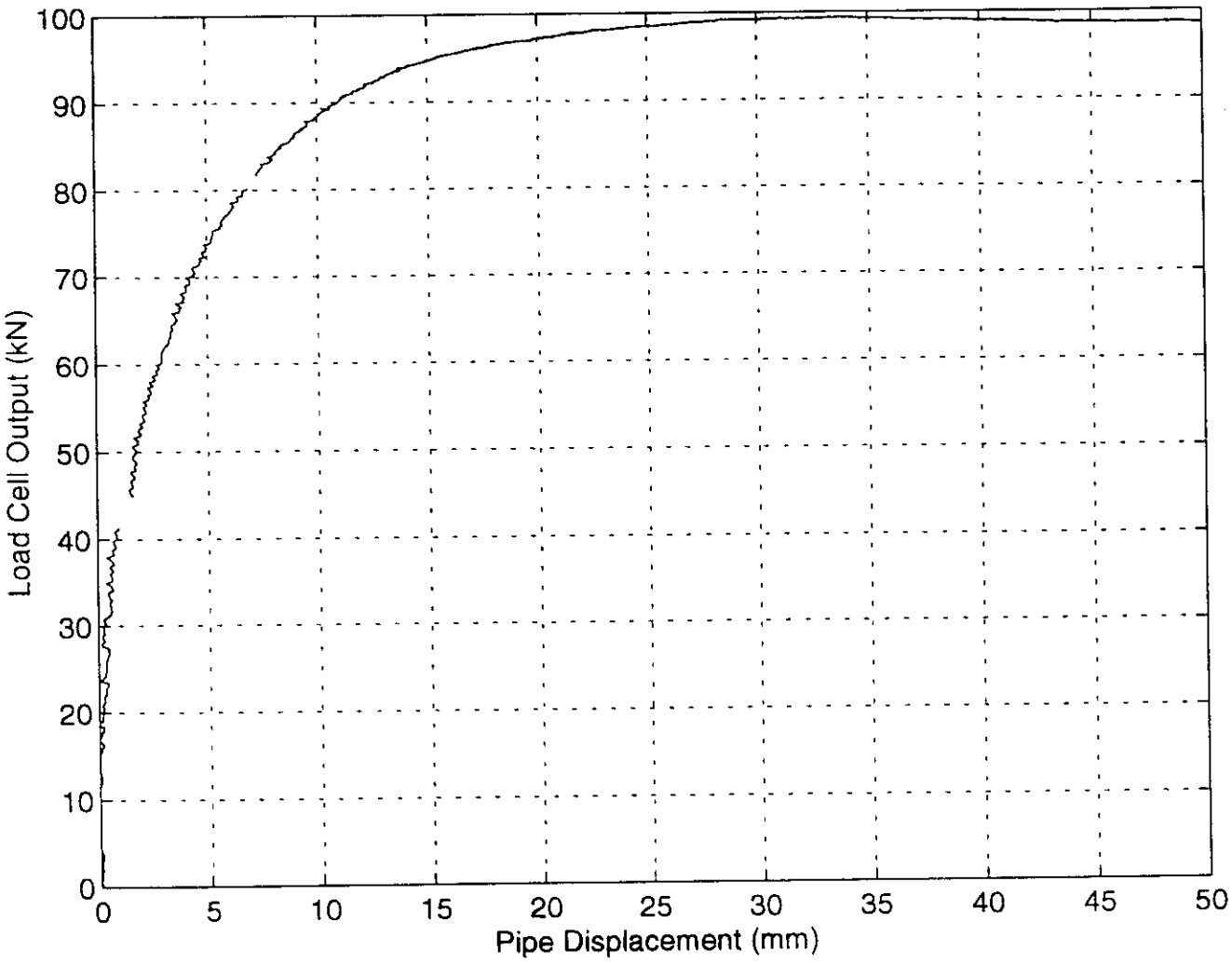

C-CORE

Load vs. Displacement - Master Load Cell

13(b)

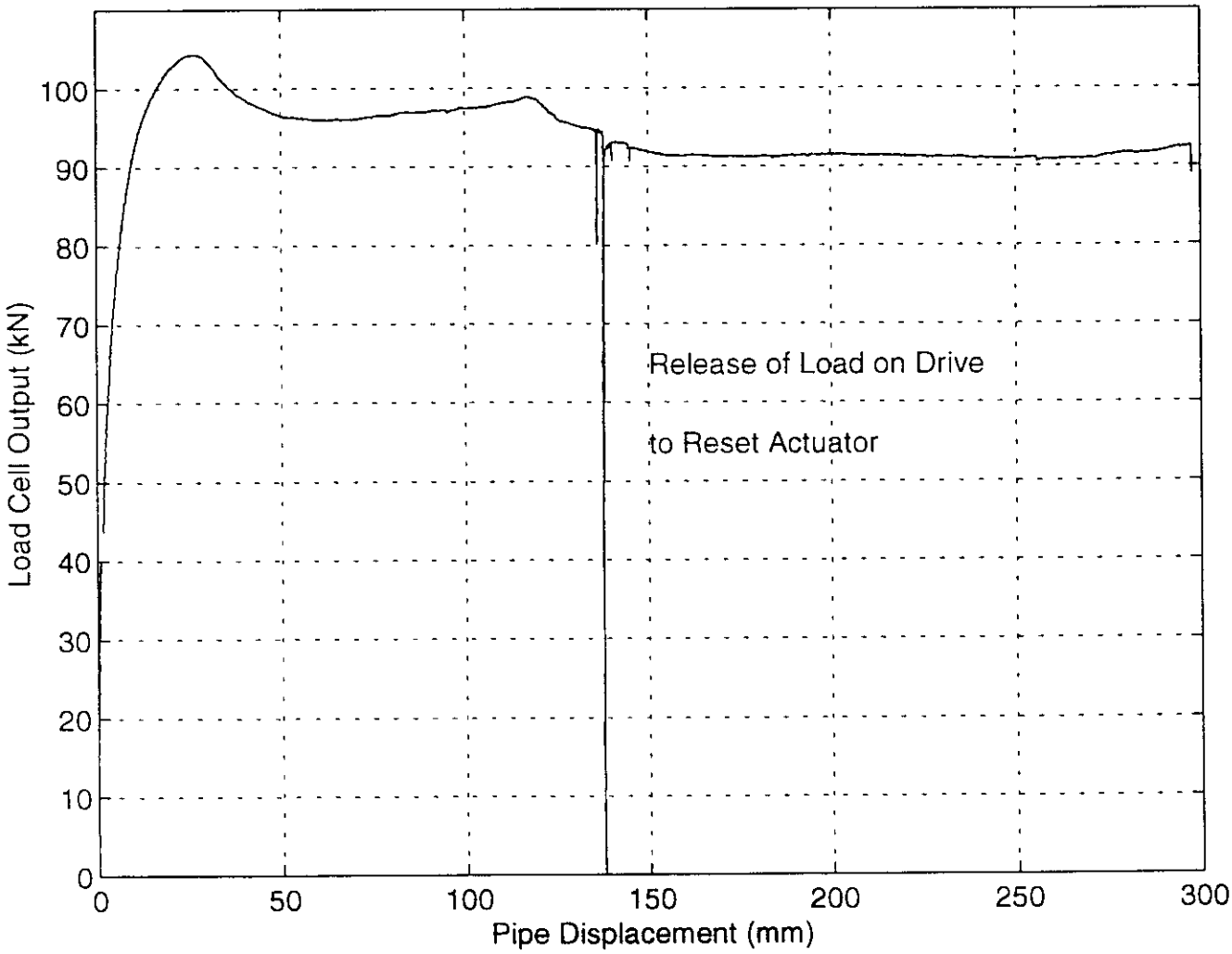

C-CORE

Load vs. Displacement - Slave Load Cell

14(a)

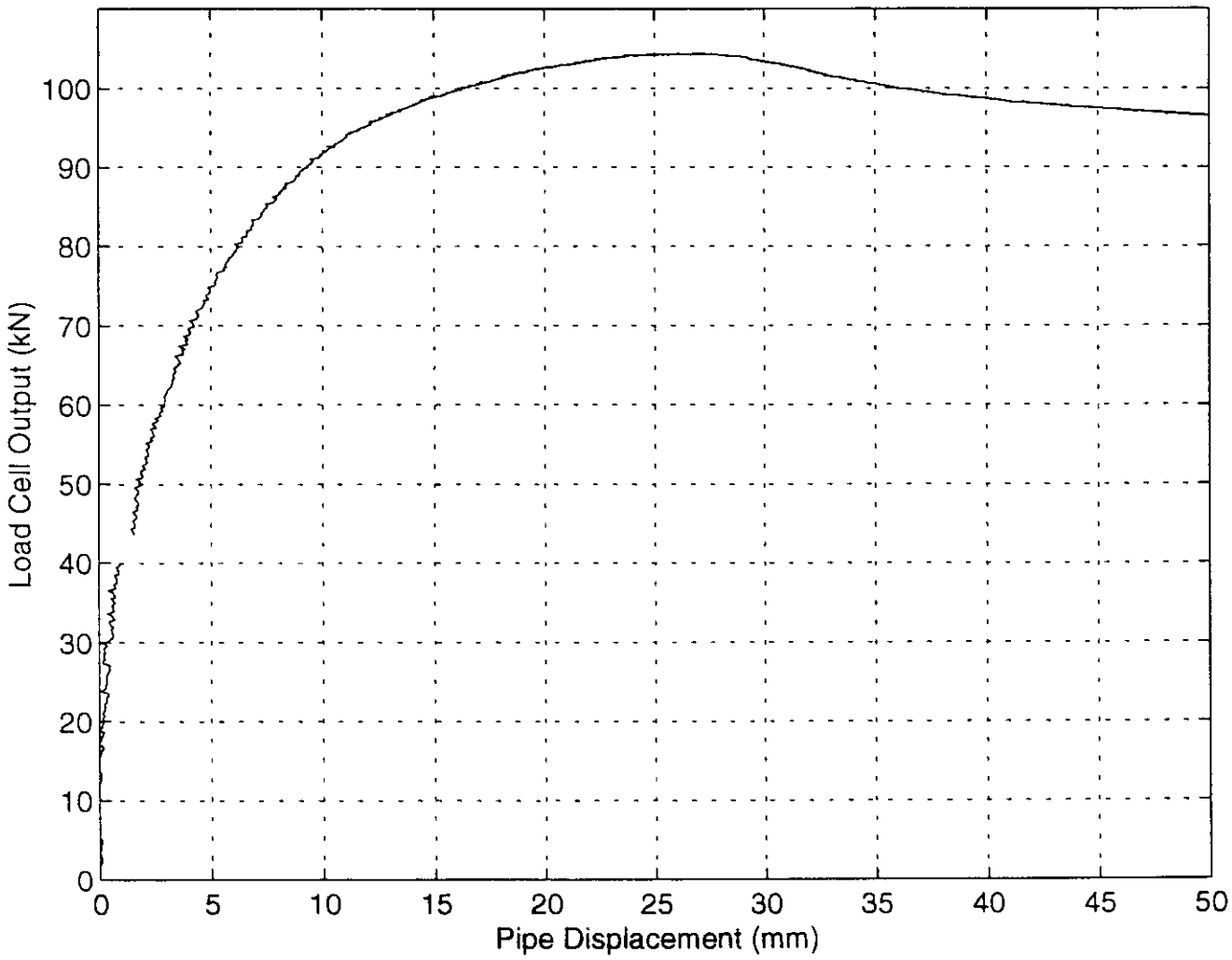

C-CORE

Load vs. Displacement - Slave Load Cell

14(b)

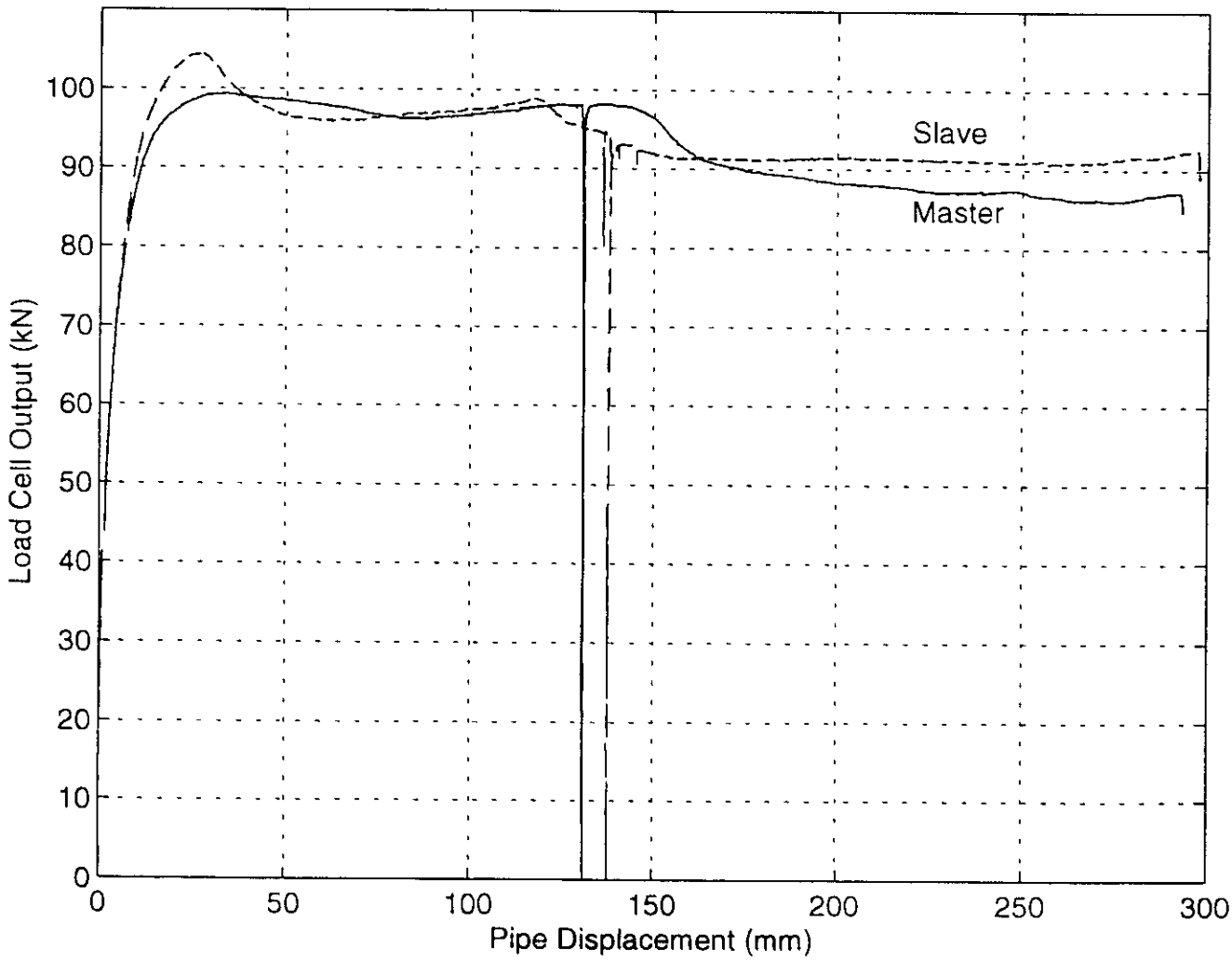

C-CORE

Comparison of Load Displacement Curves

15(a)

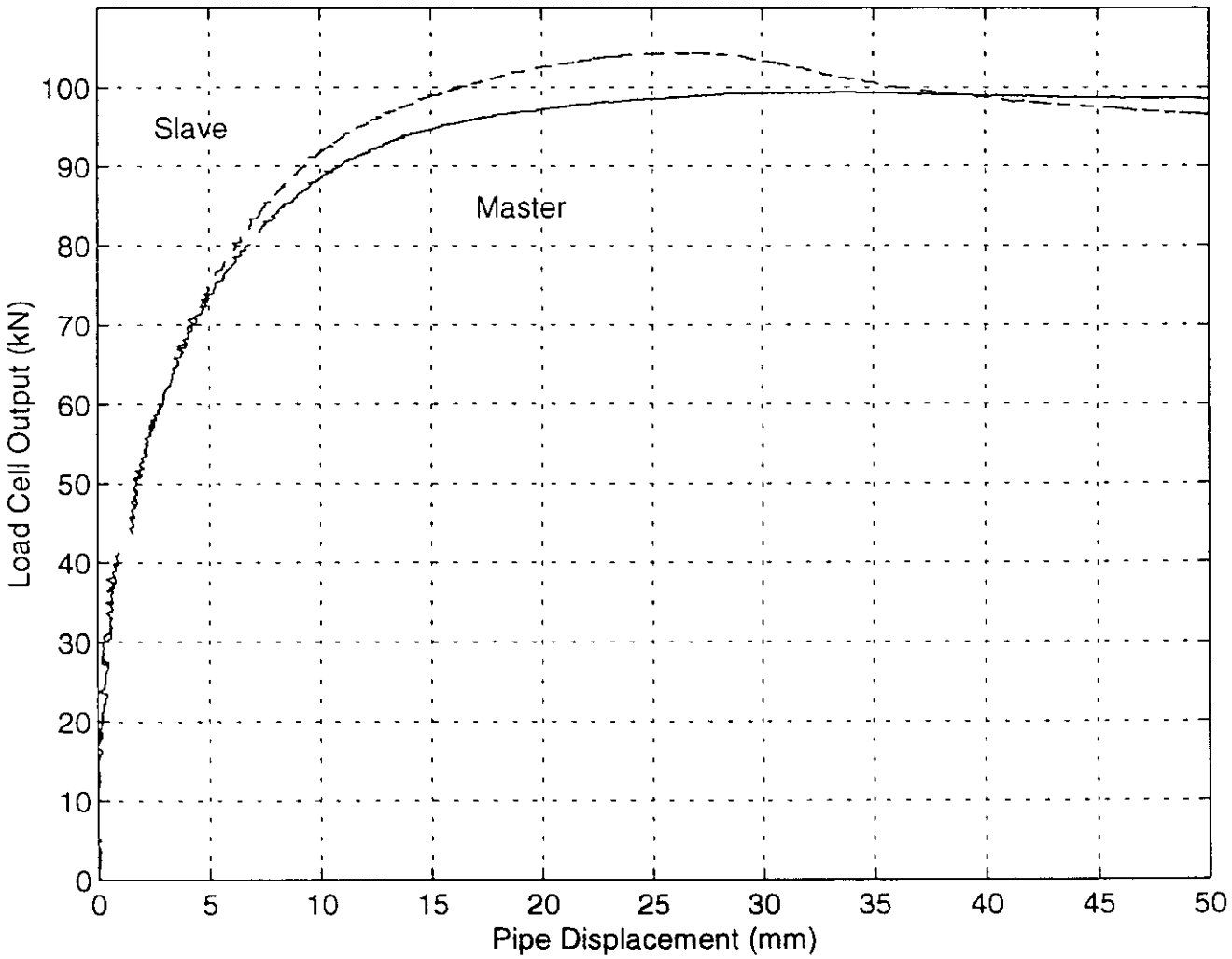

C-CORE

Comparison of Load Displacement Curves

15(b)

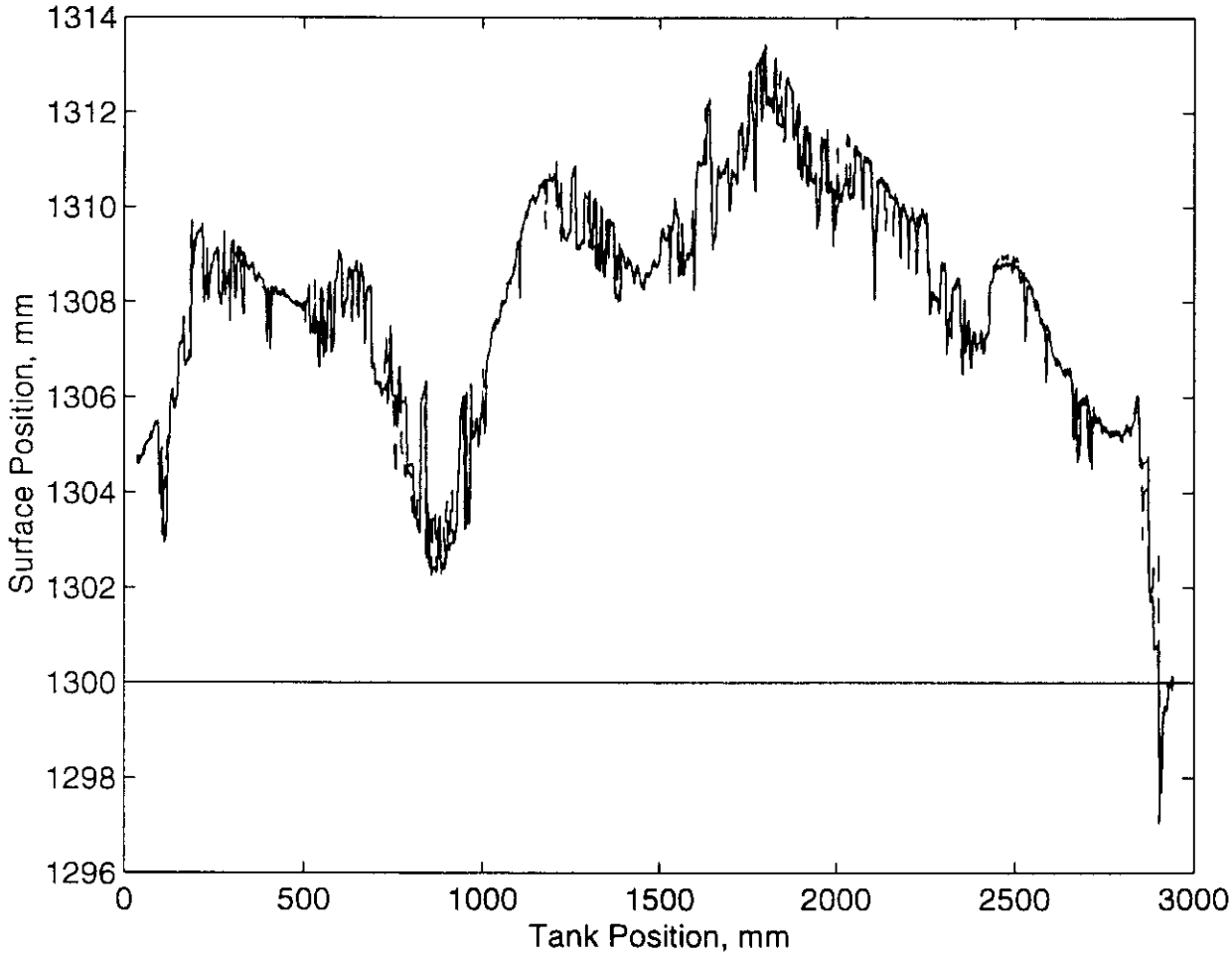
1314
1312
1310
1308
1306
1304
1302
1300
1298
1296
Surface Position, mm
0
500
1000
1500
2000
2500
3000
Tank Position, mm

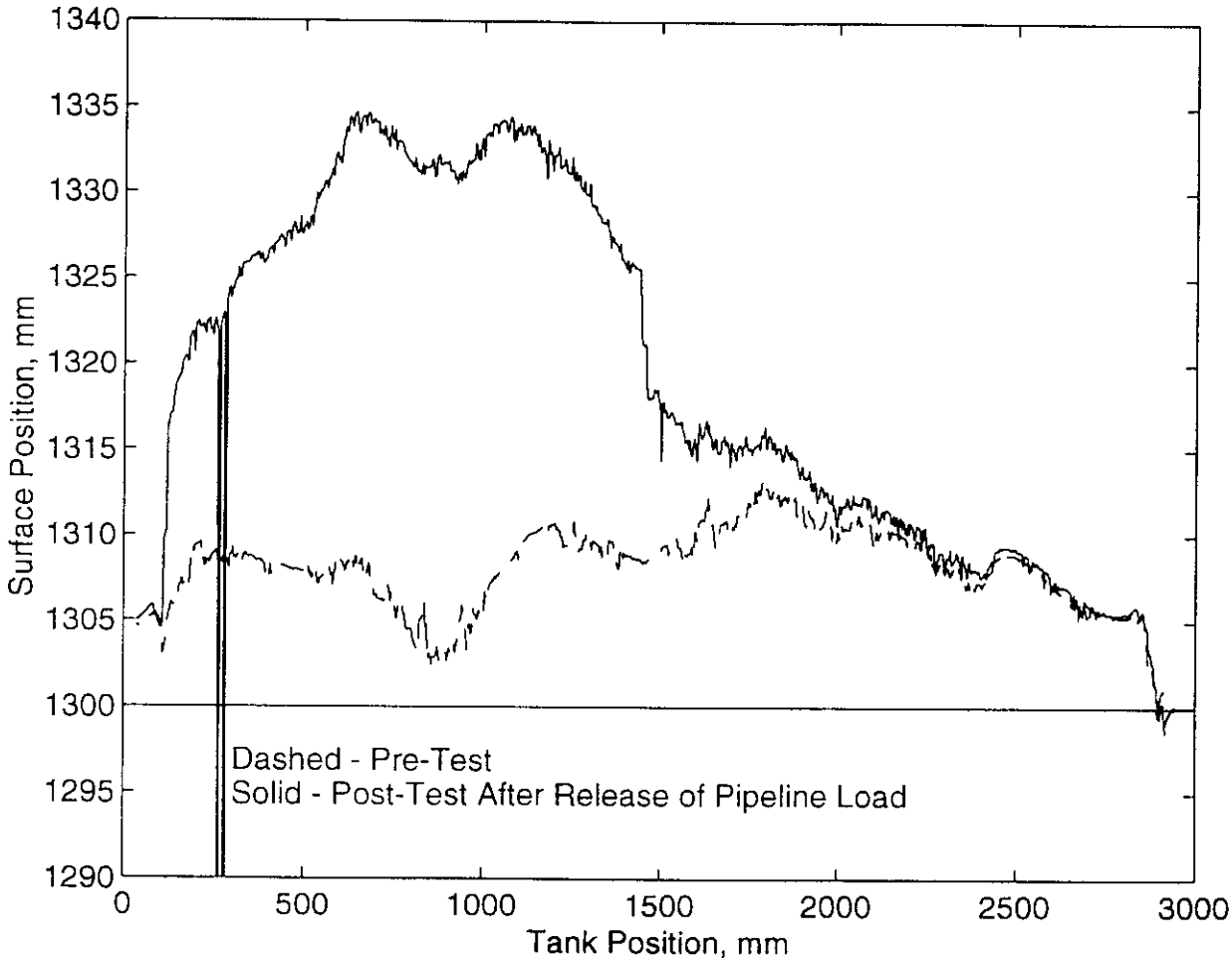
1340
1335
1330
1325
1320
1315
1310
1305
1300
1295
1290
Surface Position, mm
0
500
1000
1500
2000
2500
3000
Tank Position, mm
Dashed - Pre-Test
Solid - Post-Test After Release of Pipeline Load

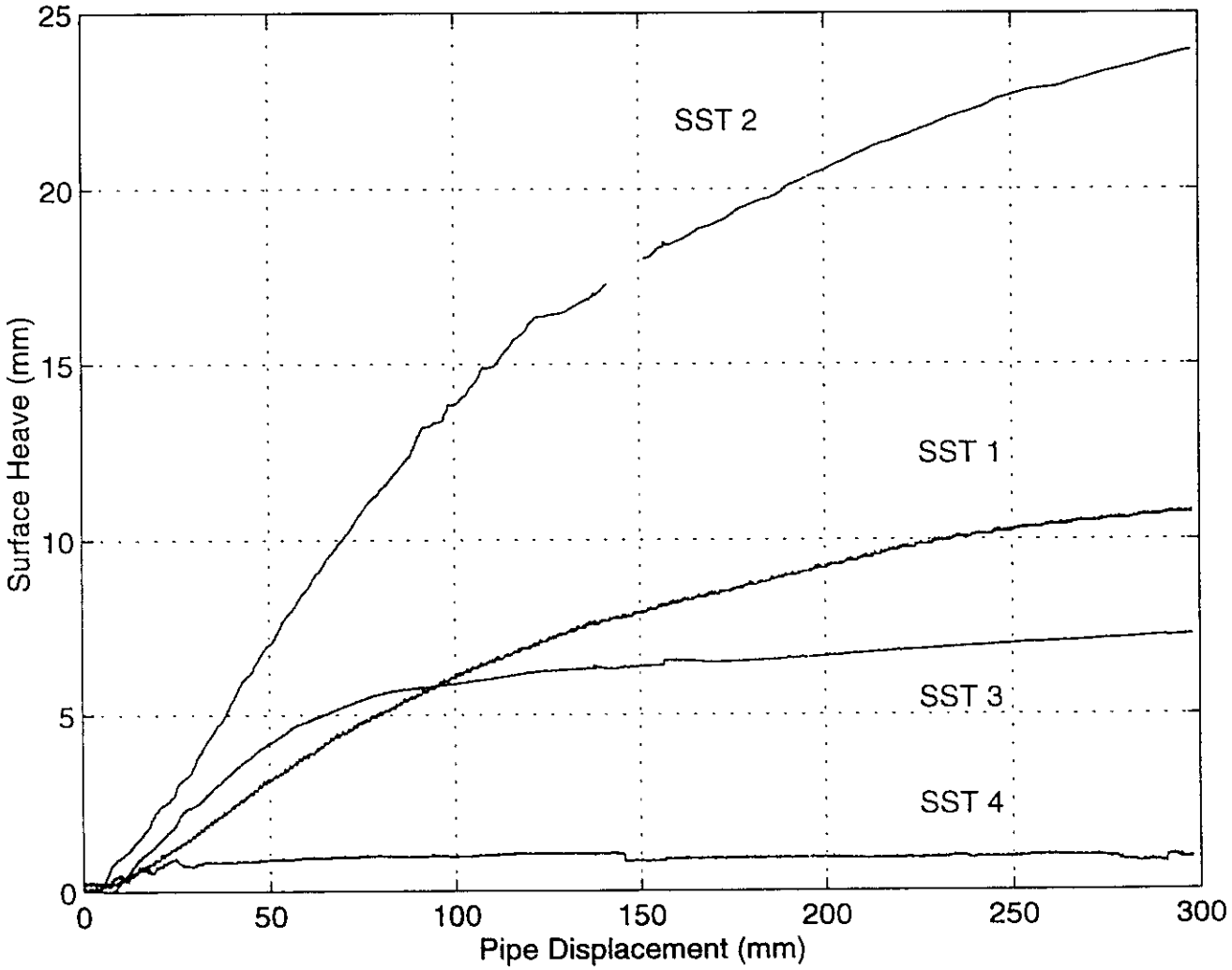
25
20
15
10
5
0
Surface Heave (mm)
0
50
100
150
200
250
300
Pipe Displacement (mm)
SST 2
SST 1
SST 3
SST 4

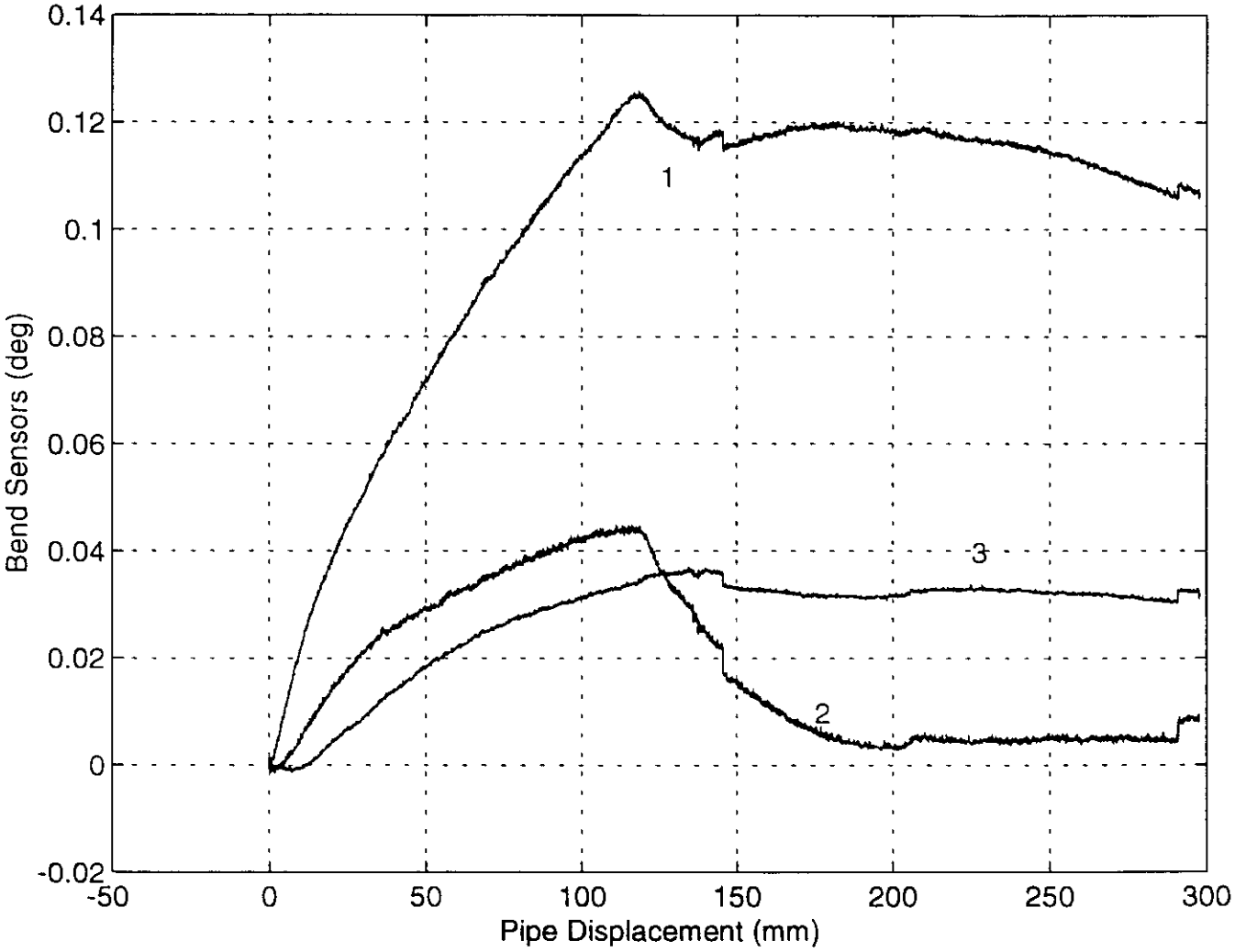

C-CORE

Bend Sensor Output vs. Pipeline Displacement

19(a)

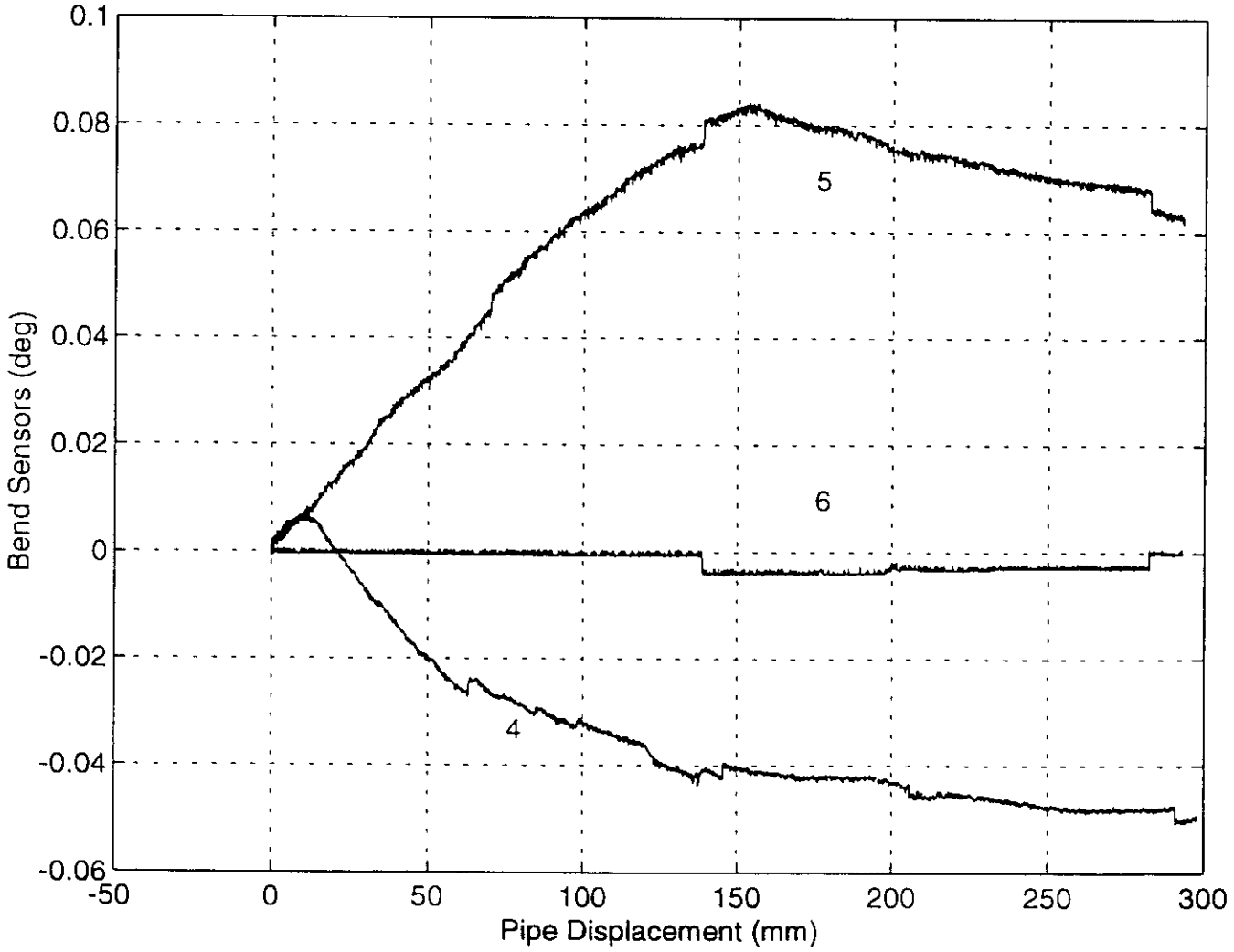

C-CORE

Bend Sensor Output vs. Pipeline Displacement

19(b)

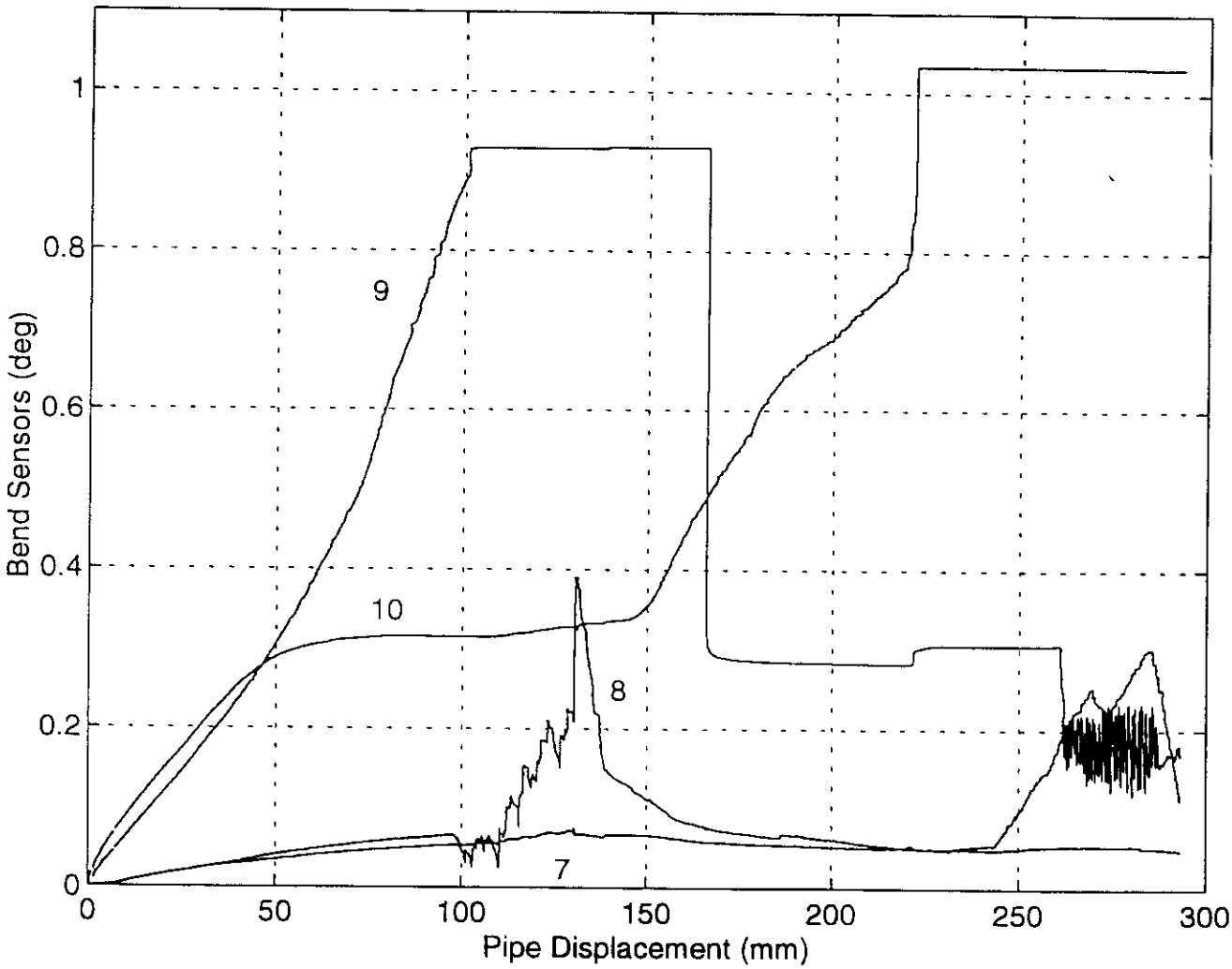

C-CORE

Bend Sensor Output vs. Pipeline Displacement

19(c)

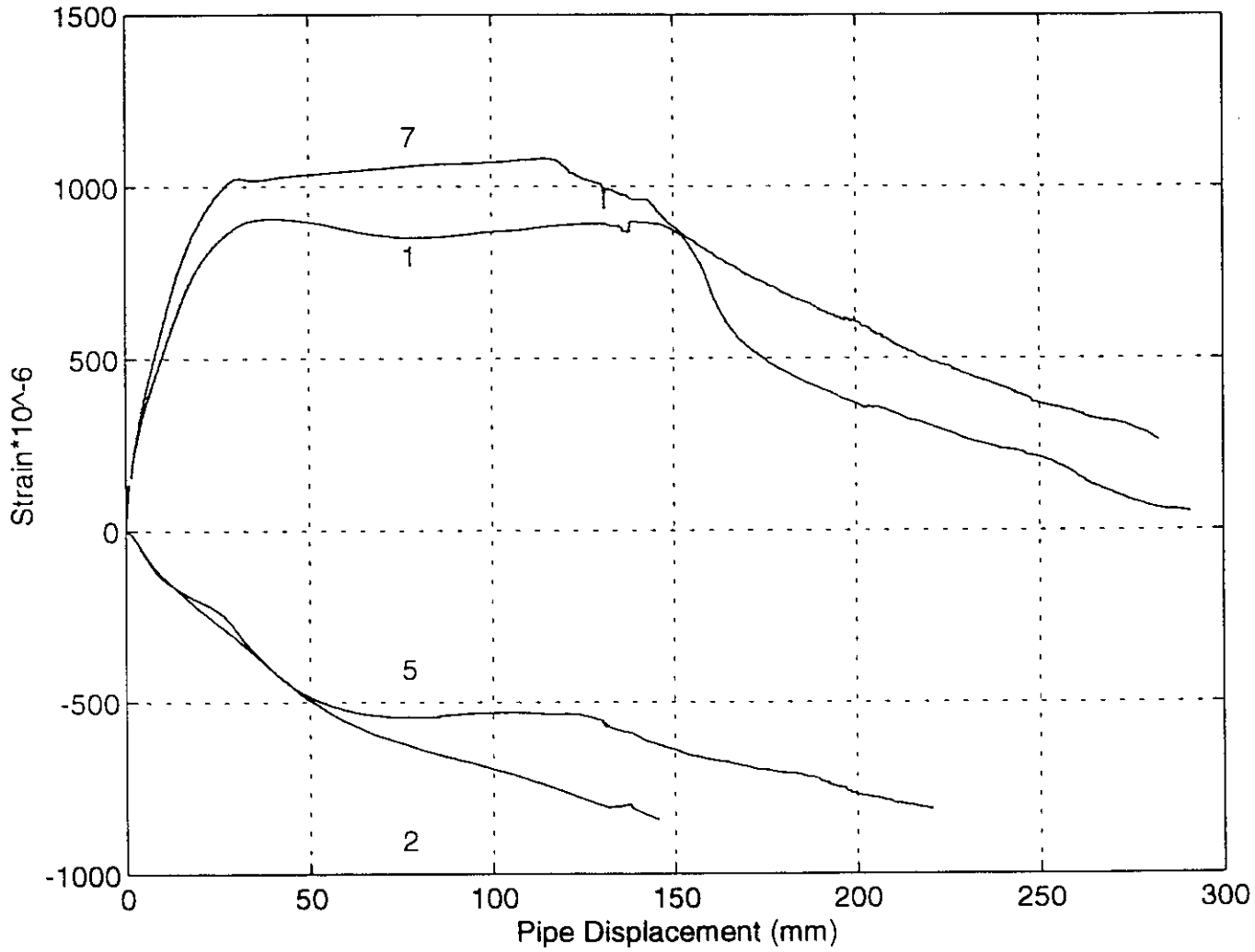

C-CORE

Bending Strain Gauge Output vs. Pipeline Displacement

20(a)

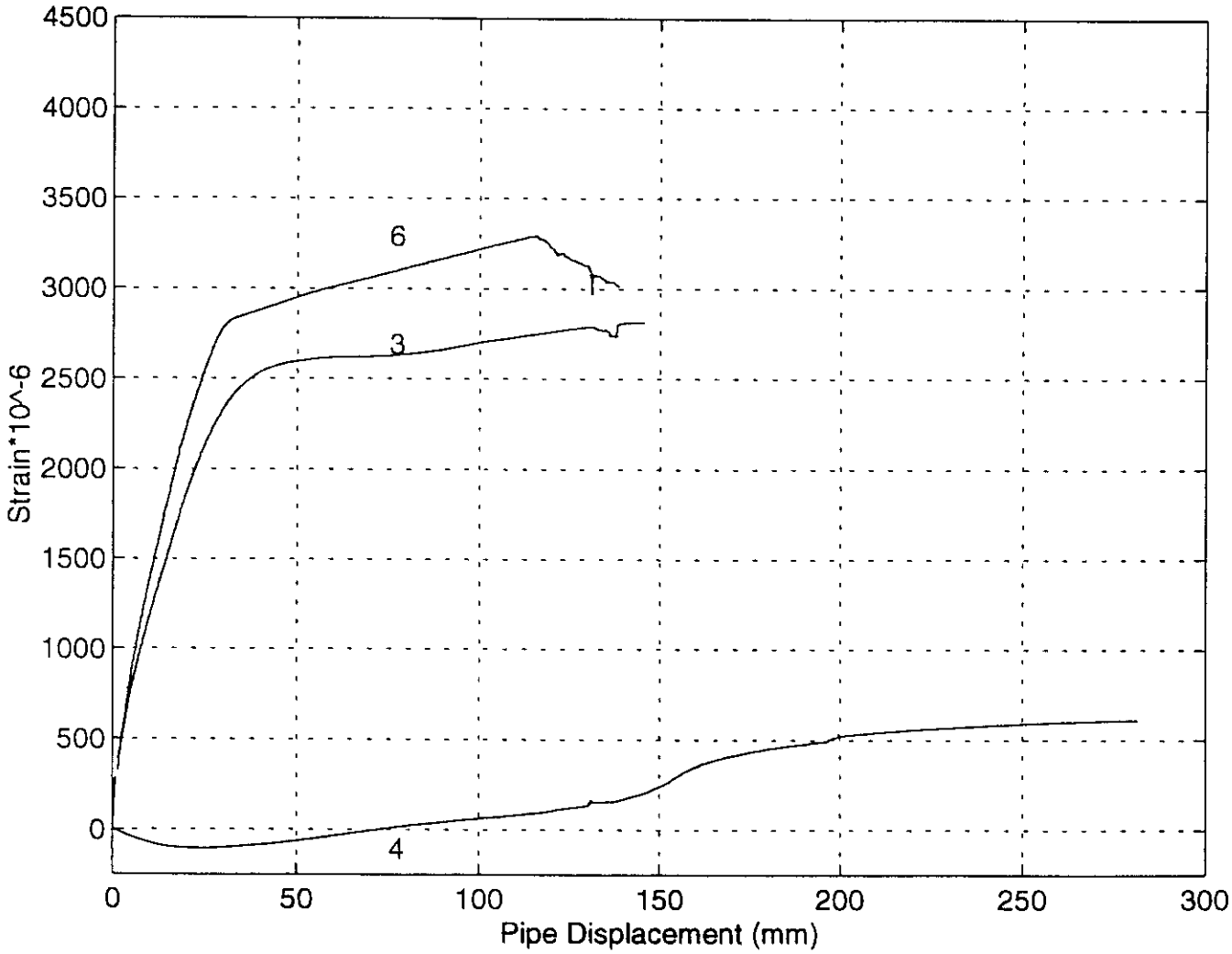

C-CORE	Axial Strain Gauge Output vs. Pipeline Displacement	20(b)

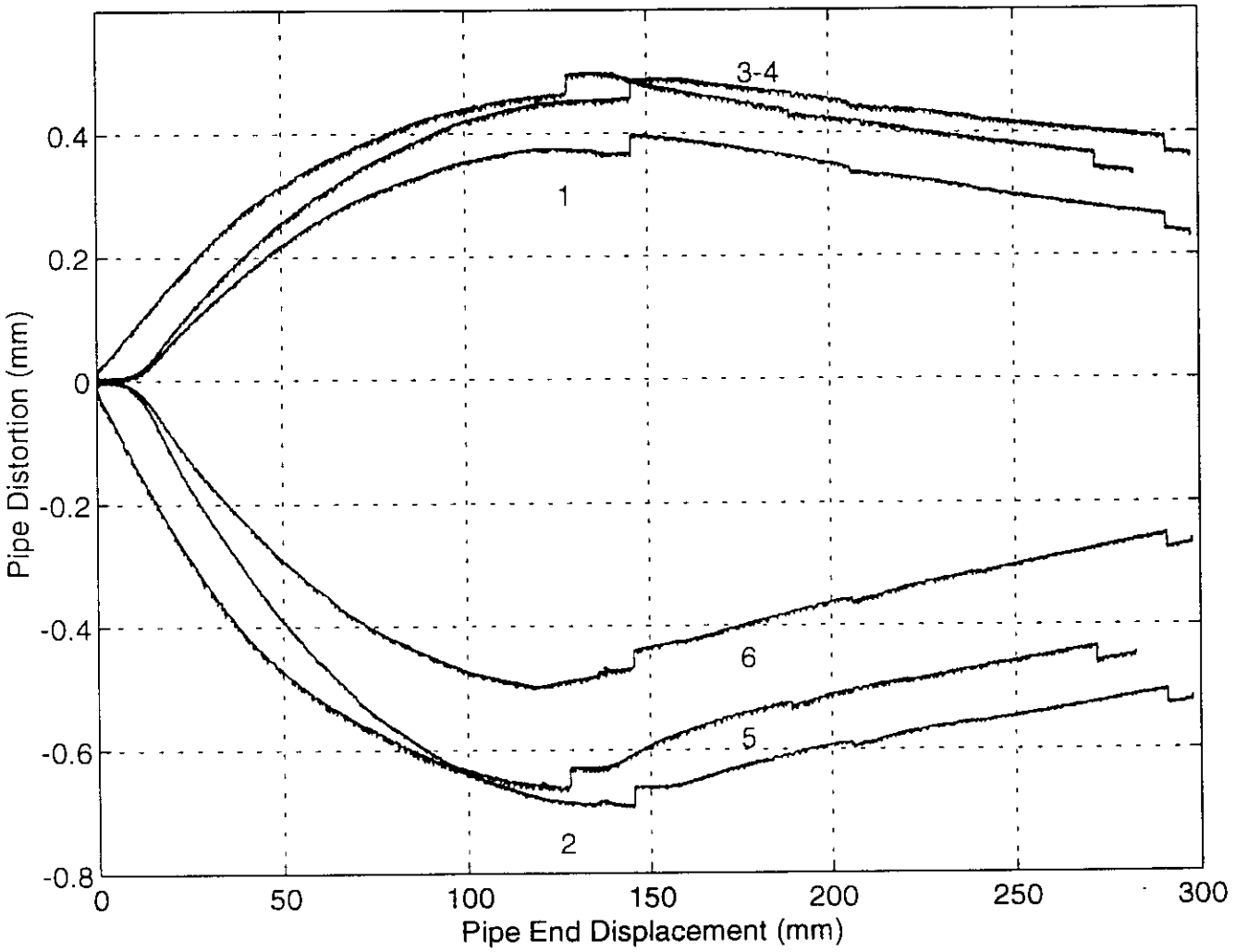

C-CORE

Displacement (Ovalisation) Measurements
vs. Pipeline Displacement

21(a)

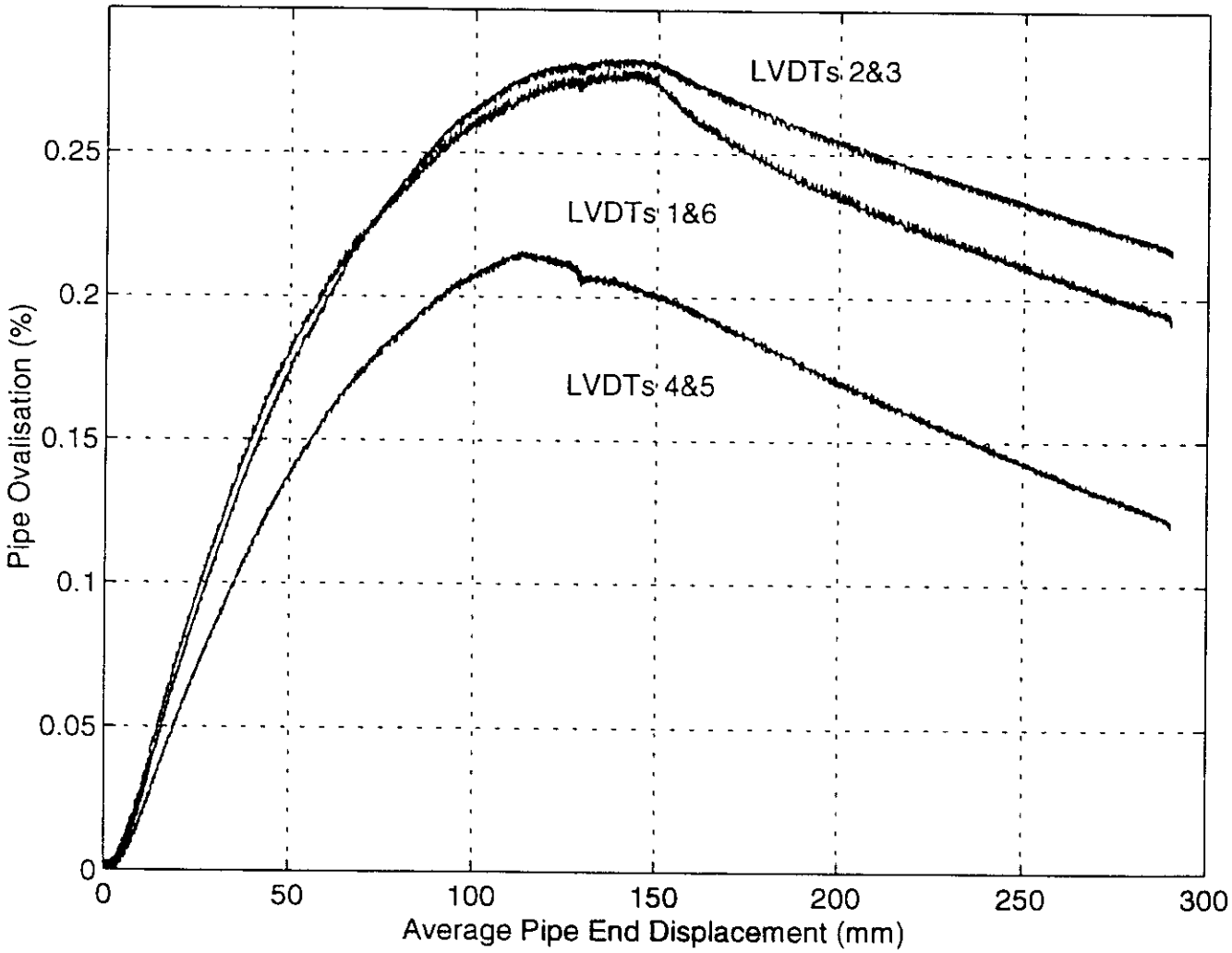

C-CORE

Displacement (Ovalisation) Measurements
vs. Pipeline Displacement

21(b)

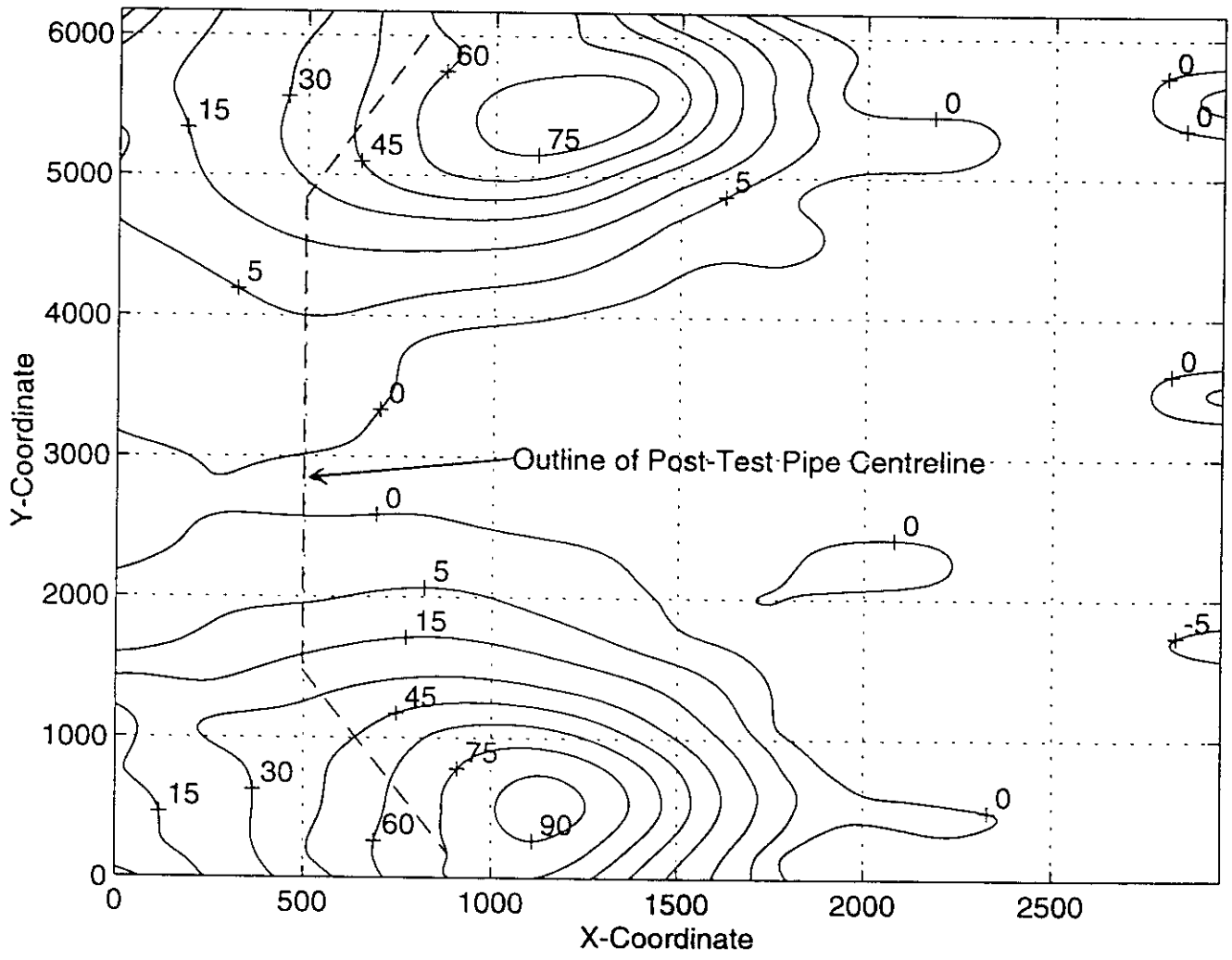
Y-Coordinate
X-Coordinate
Outline of Post-Test Pipe Centreline
6000
5000
4000
3000
2000
1000
0
0
500
1000
1500
2000
2500
60
30
15
45
75
5
0
-5
90

C-CORE

Post-Test Vertical Deformation Tubes

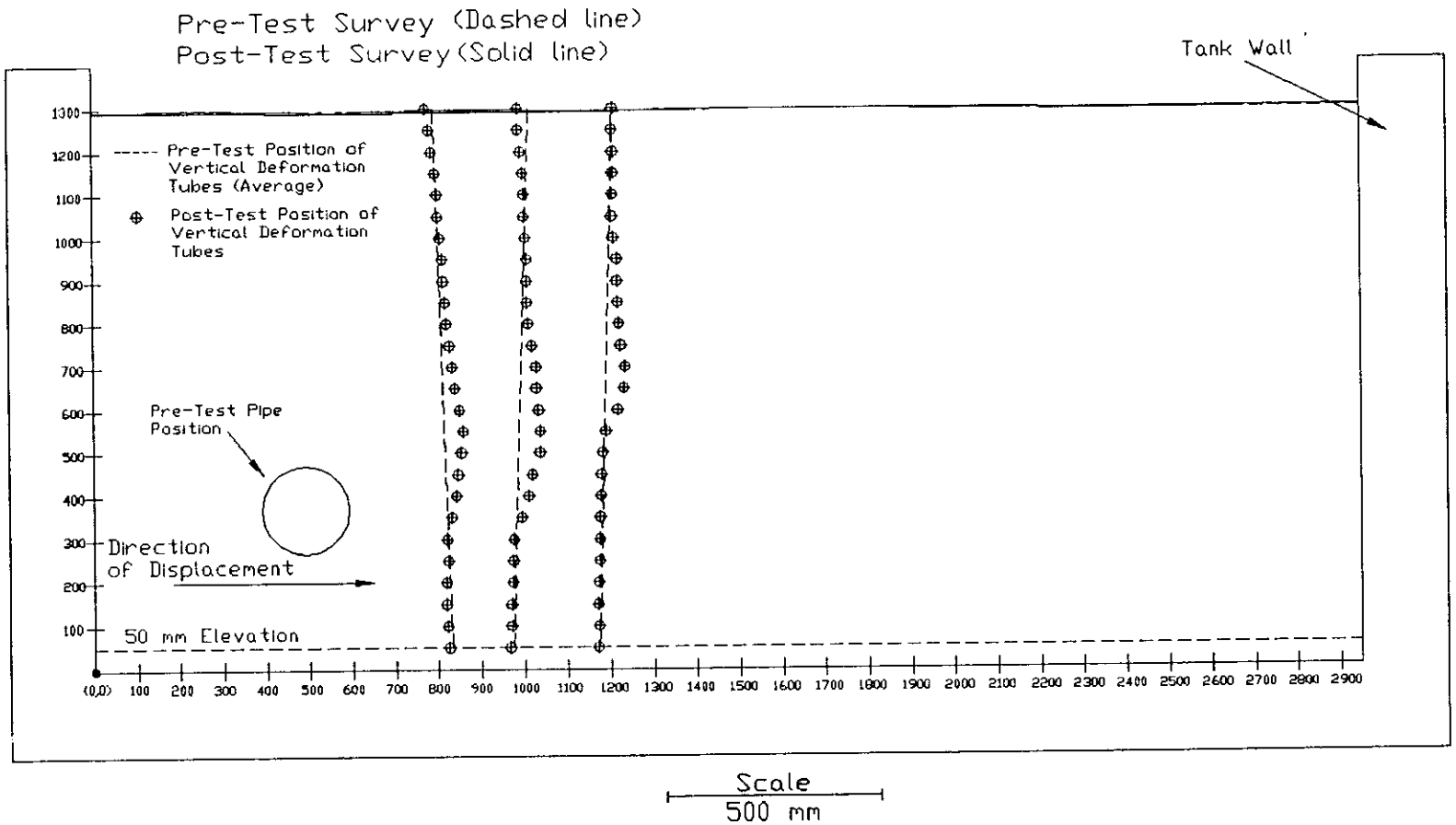

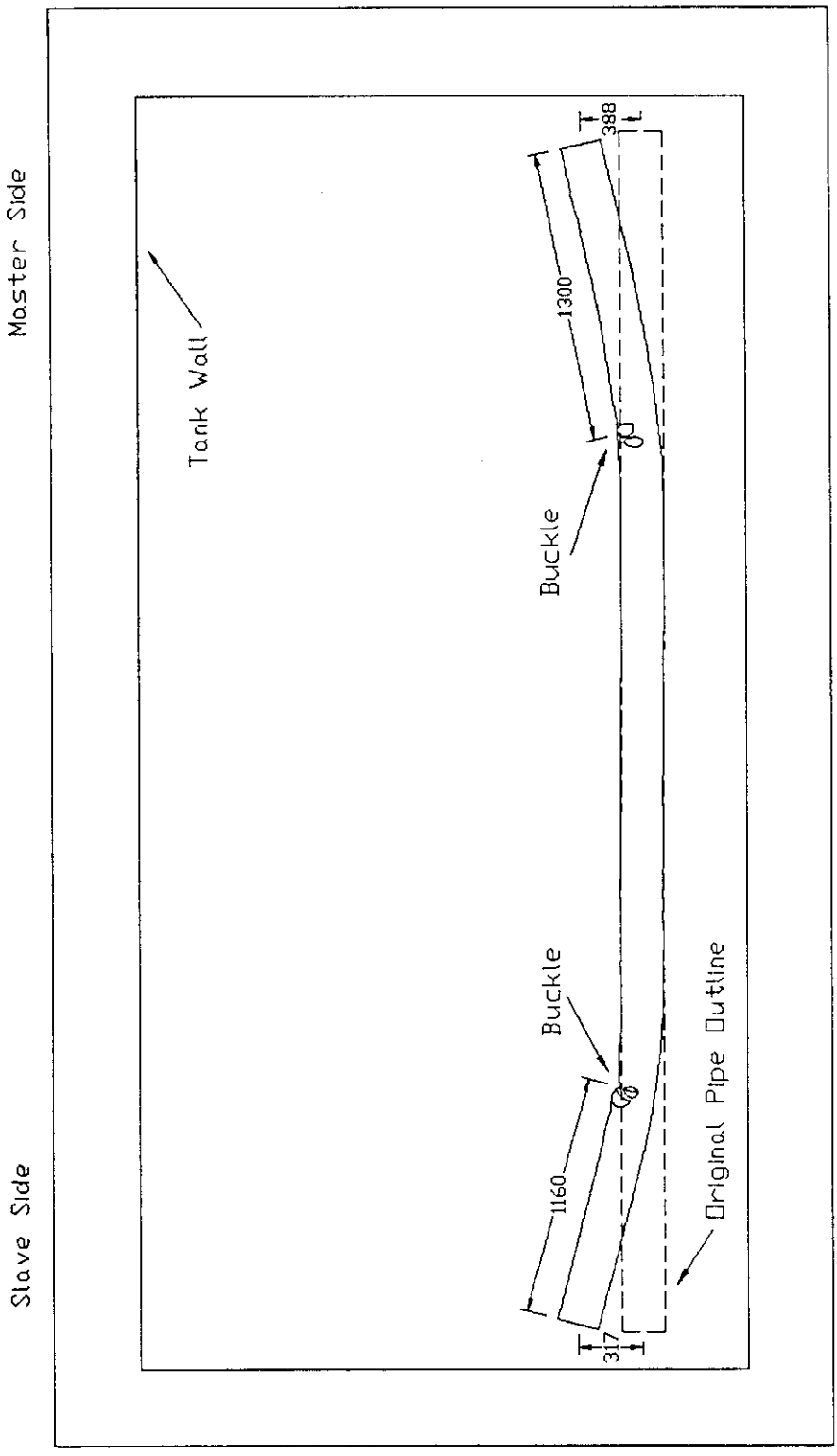
Master Side
Tank Wall
1300
388
Buckle
Buckle
1160
317
Original Pipe Outline
Slave Side

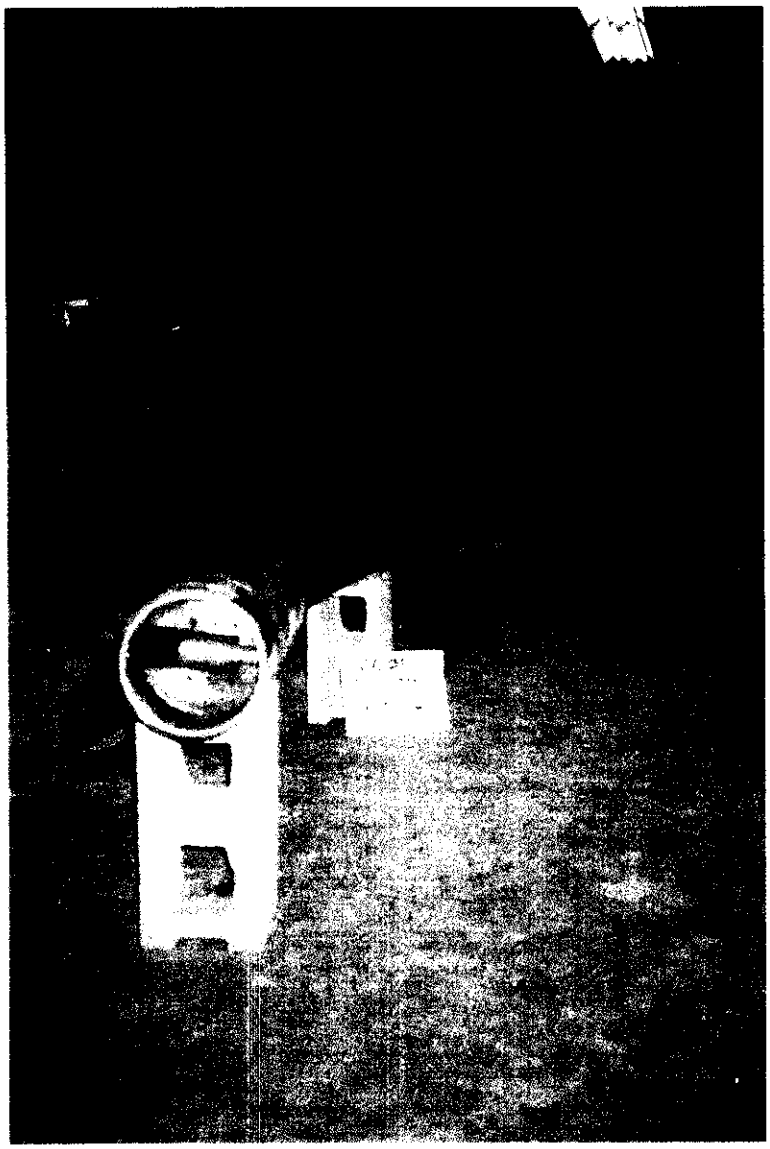

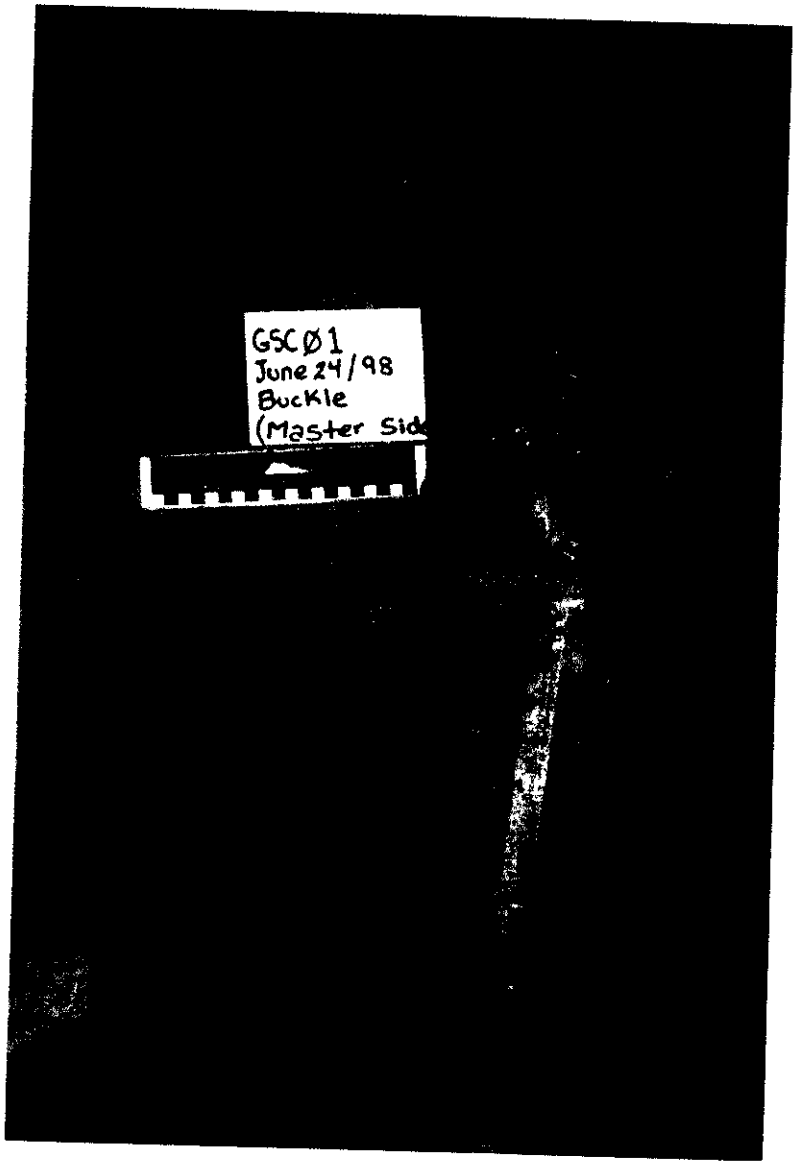
GSCØ1
June 24/98
Buckle
(Master Sid